0050454

PNL-8971
UC-903

Three-Dimensional Conceptual Model for the Hanford Site Unconfined Aquifer System, FY 1993 Status Report

4 MAR 1999
RECEIVED
EDMC

P. D. Thorne
M. A. Chamness
F. A. Spane, Jr.
V. R. Vermeul
W. D. Webber

December 1993

Prepared for the U.S. Department of Energy
under Contract DE-AC06-76RLO 1830

Pacific Northwest Laboratory
Operated for the U.S. Department of Energy
by Battelle Memorial Institute

Battelle

PNL-8971

DISCLAIMER

This report was prepared as an account of work sponsored by an agency of the United States Government. Neither the United States Government nor any agency thereof, nor Battelle Memorial Institute, nor any of their employees, makes **any warranty, expressed or implied, or assumes any legal liability or responsibility for the accuracy, completeness, or usefulness of any information, apparatus, product, or process disclosed, or represents that its use would not infringe privately owned rights.** Reference herein to any specific commercial product, process, or service by trade name, trademark, manufacturer, or otherwise does not necessarily constitute or imply its endorsement, recommendation, or favoring by the United States Government or any agency thereof, or Battelle Memorial Institute. The views and opinions of authors expressed herein do not necessarily state or reflect those of the United States Government or any agency thereof.

PACIFIC NORTHWEST LABORATORY
operated by
BATTELLE MEMORIAL INSTITUTE
for the
UNITED STATES DEPARTMENT OF ENERGY
under Contract DE-AC06-76RLO 1830

Printed in the United States of America

Available to DOE and DOE contractors from the Office of Scientific and Technical Information, P.O. Box 62, Oak Ridge, TN 37831; prices available from (615) 576-8401. FTS 626-8401.

Available to the public from the National Technical Information Service, U.S. Department of Commerce, 5285 Port Royal Rd., Springfield, VA 22161.

The contents of this report were printed on recycled paper

PNL-8971
UC-903

Three-Dimensional Conceptual Model for the Hanford Site Unconfined Aquifer System, FY 1993 Status Report

P. D. Thorne
M. A. Chamness
F. A. Spane, Jr.
V. R. Vermeul
W. D. Webber

December 1993

Prepared for
the U.S. Department of Energy
under Contract DE-AC06-76RLO

Pacific Northwest Laboratory
Richland, Washington 99352

THIS PAGE INTENTIONALLY
LEFT BLANK

Summary

The Ground-Water Surveillance Project is responsible for monitoring the movement of chemical and radioactive contaminants in ground water beneath the Hanford Site. To support this effort, a three-dimensional conceptual model of ground-water flow in the unconfined aquifer system is being developed. The conceptual model will be the basis for three-dimensional numerical modeling and will enable more accurate predictions of contaminant transport under changing site conditions.

The model region will eventually extend from the Columbia River on the east and north to the Yakima River and basalt ridges on the south and west. Development of the conceptual model began during 1991 with the region between 200-East Area and the Columbia River. During the past year, the study area was expanded south to the 300 Area, and west to basalt ridges that bound the unconfined aquifer system. The conceptual model within the earlier study area was also refined and updated.

Geologic descriptions of samples from selected wells were interpreted to determine the extent and thickness of significant hydrogeologic units composing the unconfined aquifer system. Nine units were identified above basalt. Definition of these units was based on textural differences that are expected to reflect differences in hydraulic properties. The geologic data were entered into a geographical information system and used to generate contour maps for each unit surface.

Hydraulic properties were determined by conducting field tests, and by compiling and reanalyzing the results of previous aquifer tests. A constant-rate discharge test was conducted at a multiple-well site near B Pond. The results of this test were analyzed to determine vertical anisotropy, as well as hydraulic conductivity and storativity. Single-well aquifer tests were conducted at several sampling network wells to estimate hydraulic conductivity. However, these tests were conducted using the existing sampling pumps, and, in most cases, the flow rates were too low to create an analyzable drawdown response.

The flow system boundary corresponding to the Yakima River was evaluated by long-term monitoring of river stage elevation and water levels in a well with completion intervals in both the unconfined and confined aquifer systems. The results showed that the aquifer was affected by leakage from a canal located between the monitored well and the river. Other boundary conditions are also being evaluated.

The status of the reconfiguration of two "Golder" wells is also presented. The Golder wells, many of which extend to basalt, were drilled to support an earlier investigation for a proposed nuclear power plant, and are nearly all unused at present. They provide possible sites for collecting data from the deeper unconfined aquifer system. However, many of the wells are damaged and all require reconfiguration to access the aquifer and to assure that well construction standards are met.

Contents

Summary iii

1.0 Introduction 1
1.1 Objective of Three-Dimensional Modeling 1
1.2 Scope of the Conceptual Model 3

2.0 Geology and Hydrology of the Hanford Site 5
2.1 Geologic Setting 5
2.2 Hydrologic Setting 6

3.0 Data Sources 9

4.0 Definition of Hydrogeologic Structure 13

5.0 Aquifer Hydraulic Properties 27
5.1 Results of Aquifer Testing 27
5.1.1 Multiple-Well Aquifer Test to Determine Vertical Anisotropy 28
5.1.2 Single-Well Aquifer Tests Conducted at Sampling Network Wells 28
5.2 Aquifer Test Reanalyses 31
5.3 Assignment of Hydraulic Properties to Units 31

6.0 Boundary Conditions 35
6.1 Perimeter Boundaries 35
6.2 Top and Bottom of the Unconfined Aquifer System 38
6.3 Boundary Conditions within the Flow System Boundaries 39

7.0 Hydraulic Heads 43

8.0 Contaminant Distributions 47

9.0 References 51

Appendix A - Analysis of a Constant-Rate Pumping Test Monitored with a Westbay Multiport Monitoring System A.1

Appendix B - Hydrologic Testing at Hanford Sitewide Monitoring Wells B.1

Appendix C - Reconfiguration of "Golder" Wells C.1

Figures

1.1 Location of the Hanford Site 2

3.1 Locations of Wells Used for Defining Hydrogeologic Structure 11

4.1 Stratigraphic Nomenclature of Various Authors 17

4.2 Structural Contours for the Top of Basalt 18

4.3 Structural Contours for the Top of Unit 9 19

4.4 Structural Contours for the Top of Unit 8 20

4.5 Structural Contours for the Top of Unit 7 21

4.6 Structural Contours for the Top of Unit 6 22

4.7 Structural Contours for the Top of Unit 5 23

4.8 Structural Contours for the Top of Unit 4 24

4.9 Structural Contours for the Top of Unit 3 25

4.10 Structural Contours for the Top of Unit 2 26

6.1 Map Showing Monitoring Wells Near the Yakima River and the River Stage Measurement Station 36

6.2 Yakima River Stage and Water-Level Elevations in the Unconfined and Confined Aquifers at Well 699-S24-19 37

6.3 Irrigated Areas South of the Hanford Site 41

8.1 Locations of Two Reconfigured Golder Wells and Tritium Concentration Contours for the Upper Unconfined Aquifer in 1992 49

8.2 Locations of Two Reconfigured Golder Wells and Iodine-129 Concentration Contours for the Upper Unconfined Aquifer in 1992 50

8.3 Tritium Concentration Trend During Development Pumping of the Reconfigured Golder Well 699-31-11 51

A.1 Distances Between Pumping and Observation Wells at the Constant-Rate Discharge Test Site A.2

A.2 As-Built Diagrams of Wells 699-42-42B, 699-43-42J, and 699-43-42K A.3

A.3 Equipment Configuration at Pumping Well 699-42-42B During the Constant-Rate Discharge Test A.5

A.4 Discharge Rate and Drawdown Measured at Pumping Well 699-42-42B A.7

A.5 Pre-Test Atmospheric Pressure and Pressures Recorded in Wells A.10

A.6 Example of Composite Drawdown Analysis A.14

A.7 Drawdown and Drawdown Derivative Type-Curve Analysis for Well 699-43-42K: Monitor Zone 4 . . . . . A.16

A.8 Drawdown and Drawdown Derivative Type-Curve Analysis for Well 699-43-42K: Monitor Zone 3 . . . . . A.17

A.9 Observed Drawdown and Recovery at Well 699-43-42J A.19

A.10 Full Unconfined Type-Curve Analysis of Composite Recovery-Drawdown Plot at Well 699-43-42J A.21

B.1 Log-Log Diagnostic Plot of Drawdown and Drawdown Derivative at Well 699-15-15B B.5

B.2 Log-Log Diagnostic Plot of Drawdown and Drawdown Derivative at Well 699-29-4 . . . . . B.6

B.3 Log-Log Diagnostic Plot of Drawdown and Drawdown Derivative at Well 699-55-89 . . . . . B.7

B.4 Log-Log Diagnostic Plot of Drawdown and Drawdown Derivative at Well 699-57-83A B.8

B.5 Cooper and Jacob Straight Line Analysis for Well 699-15-15B B.9

B.6 Cooper and Jacob Straight Line Analysis for Well 699-29-4 . . . . . B.10

B.7 Cooper and Jacob Straight Line Analysis for Well 699-55-89 . . . . . B.11

B.8 Cooper and Jacob Straight Line Analysis for Well 699-57-83A B.12

B.9 Simulated Theis Response at Average Discharge Rate of 8 gpm and Indicated Transmissivity B.13

C.1 As-Built Diagrams for Well 699-18-21 (Golder S-12) Before and After Reconfiguration C.3

C.2 As-Built Diagrams for Well 699-31-11 (Golder 50) Before and After Reconfiguration C.4

Tables

5.1 Results for the Constant-Rate Discharge Test at the Westbay Multiport Well Site Near B Pond 29

5.2 Results of Single-Well, Constant-Rate Discharge Tests Conducted at Sampling Network Wells 30

7.1 Well Cluster Sites and Wells with Piezometers in the Unconfined Aquifer System 44

A.1 Results of Barometric Efficiency Calculations for Monitoring Locations A.11

A.2 Hydraulic Properties Estimated from Composite Drawdown Analysis of Selected Monitoring Locations. A.13

A.3 Pertinent Well Completion and Test Information. A.15

B.1 Results from Constant-Rate Tests of Sitewide Monitoring Wells. B.4

1.0 Introduction

The ground water underlying parts of the Hanford Site (Figure 1.1) contains radioactive and chemical contaminants at concentrations exceeding regulatory standards (Dresel et al. 1993). The Hanford Site Ground-Water Surveillance Project, operated by Pacific Northwest Laboratory (PNL),[a] is responsible for monitoring the movement of these contaminants to ensure that public health and the environment are protected. To support the monitoring effort, a sitewide three-dimensional ground-water flow model is being developed. This report provides an update on the status of the conceptual model that will form the basis for constructing a numerical three-dimensional flow model for the site. Thorne and Chamness (1992) provide additional information on the initial development of the three-dimensional conceptual model.

1.1 Objective of Three-Dimensional Modeling

A sitewide three-dimensional flow model supported by detailed, three-dimensional information on geology, hydraulic properties, and hydrochemistry is needed for predicting the movement of contaminants both under present hydrologic conditions and under various conditions that may result from ground-water remediation or other activities on site. Specific objectives of the Hanford sitewide ground-water flow model are as follows:

- predict the migration pattern of the widespread contaminant plumes originating in the 200 Areas
- provide estimates of contaminant flux through ground water to the Columbia River
- predict the effects of remediation activities and changes in waste-water discharge on the flow system and on the monitoring network
- provide realistic boundary conditions for localized ground-water flow models
- improve understanding of the sitewide ground-water flow system.

(a) PNL is a multiprogram national laboratory operated for the U.S. Department of Energy by Battelle Memorial Institute under contract DE-AC06-76RLO 1830.

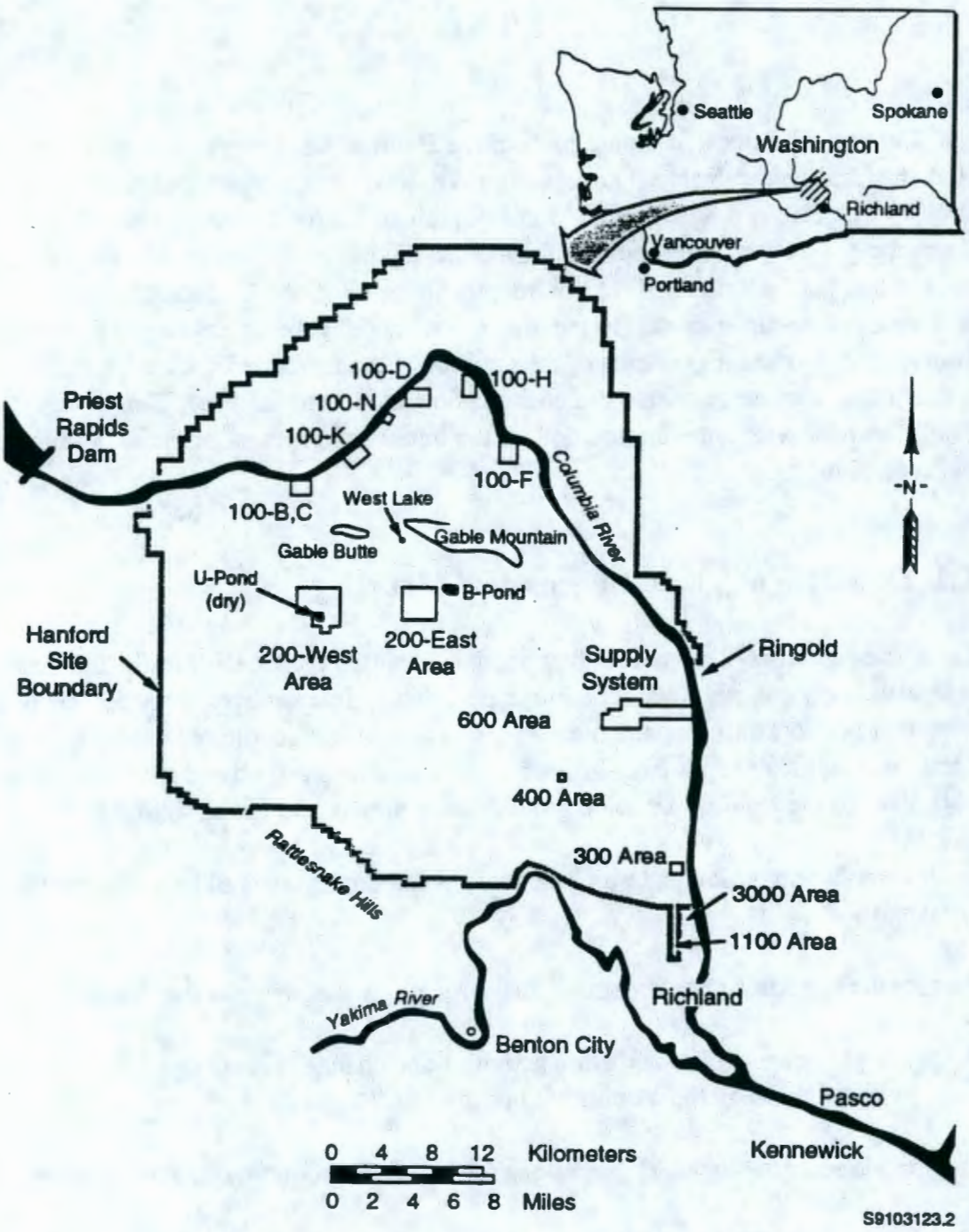

Figure 1.1. Location of the Hanford Site

Numerical models have been used for simulating ground-water flow at the Hanford Site to determine the rate and direction of contaminant movement and to predict responses to changing site conditions (Cearlock et al. 1975; Evans et al. 1988; Jacobson and Freshley 1990). However, most numerical flow models applied to the Hanford Site have been two-dimensional, assuming that hydraulic properties, hydraulic head, and contaminant concentrations do not vary vertically through the aquifer thickness. This two-dimensional approach does not realistically represent ground-water flow in the aquifer, and because higher concentrations of contaminants are found in the uppermost part of the aquifer, two-dimensional transport models have not been successful at determining the flux of contaminants through the unconfined aquifer system. A three-dimensional flow model can provide more accurate predictions of contaminant transport. However, before a numerical model can be built and used to simulate ground-water flow and contaminant transport, a conceptual model describing the flow system is needed.

1.2 Scope of the Conceptual Model

The areal extent of the Hanford Site model is defined by the Columbia River on the east and north, and by basalt outcrops and the Yakima River on the west and south. Development of a three-dimensional conceptual model for this area is a large task. Therefore, the work is being done over a period of several years. Work conducted during the 1992 fiscal year (Thorne and Chamness 1992) focused on defining the hydrogeologic structure of the unconfined aquifer in the area extending eastward from the 200-East Area to the Columbia River. Contaminants discharged to waste-water disposal facilities in the 200-East Area travel through the unconfined aquifer in this area as they move toward the Columbia River. During the past year, work on the conceptual model has concentrated on the following:

- extending the definition of hydrogeologic units to the west and south
- assigning hydraulic properties to hydrogeologic units
- defining the bottom surface of the unconfined aquifer system
- conducting a test to estimate vertical hydraulic conductivity
- collecting data to better define the boundary corresponding to the Yakima River on the southwest perimeter.

The conceptual model describes the geometry of the flow system, defines hydraulic properties throughout the model region, describes boundary conditions, and establishes initial conditions for variables such as hydraulic head and contaminant concentrations. For the three-dimensional conceptual model, describing flow system geometry involves defining the orientation and extent of hydrogeologic units that make up the unconfined aquifer system. Constant hydraulic properties may be defined for a particular unit, or a spatial distribution of properties may be assigned to the unit. Both horizontal and vertical hydraulic conductivities must be defined to support the three-dimensional model because vertical flow is important. Boundary conditions must be defined for the perimeter of the modeled region. These are usually defined as prescribed-head or prescribed-flux boundaries. Boundary conditions must also be defined for the upper and lower surface of the aquifer. Because the model describes an unconfined aquifer, the upper boundary is not fixed. The definition of the upper boundary also reflects input of water from disposal facilities, irrigation, or natural recharge. The lower boundary may be a no-flow boundary or a prescribed-flux boundary describing the exchange of ground water with the underlying confined aquifer system.

2.0 Geology and Hydrology of the Hanford Site

Hanford Site geology and hydrology have been studied extensively over the years. Thorne and Chamness (1992) give a synopsis of the geology of the Hanford Site and more detailed descriptions are provided in Myers and Price (1979), DOE (1988), and Lindsey et al. (1992). Consequently, the background geologic information is briefly summarized in this report.

2.1 Geologic Setting

The Hanford Site lies within the Pasco Basin, a structural depression that has accumulated a relatively thick sequence of fluvial, lacustrine, and glaciofluvial sediments. This structural depression and nearby anticlines and synclines are formed in the underlying Columbia River Basalt Group, a sequence of flood basalts. The most recent basalt flow underlying much of the Hanford Site is the Elephant Mountain Member of the Saddle Mountains Basalt.

Overlying the basalt are the fluvial and lacustrine sediments of the Ringold Formation. The fluvial sequences consist of coarser-grained deposits of migrating channels and the finer-grained overbank deposits of the ancestral Columbia and/or Salmon-Clearwater river systems. Several lithologic units present only in the western portion of the Pasco Basin are the Plio-Pleistocene unit, consisting of paleosol/calcrete and sidestream sediments, and the early "Palouse" soil, an eolian sand and silt deposit. The uppermost sedimentary unit covering much of the Hanford Site is the Hanford formation, a complex series of coarse- and fine-grained layers deposited by cataclysmic floods during the last ice age. For the most part, the fine-grained sediments are found near the margins of the basin and in areas protected from the main flood currents that deposited the coarse-grained sediments. Capping the Hanford formation in many areas is a thin veneer of eolian sands and/or recent fluvial deposits.

As the post-basalt sediments were being deposited, the basalt was continuing to deform structurally. The basin continued to subside, and the ridges continued to rise. This process led to the formation of sedimentary units that are thickest in the center of the basin and become thin or, in places, pinch out at the anticlines. In a few places, Hanford formation sediments directly overlie the basalt where the Ringold Formation either was never deposited or was eroded away by pre-Missoula flood rivers or by the Missoula floods.

2.2 Hydrologic Setting

An uppermost unconfined aquifer and a sequence of confined aquifers lie beneath most of the Hanford Site. The unconfined aquifer is generally located in unconsolidated to semiconsolidated sediments overlying the basalt bedrock and the confined aquifers are generally brecciated tops of basalt flows and sedimentary interbeds located within the Columbia River Basalt. In some areas, deeper parts of the suprabasalt sediments are locally confined by overlying mud units. However, because the entire suprabasalt aquifer system is interconnected on a sitewide scale, it has commonly been referred to as the "Hanford unconfined aquifer." This nomenclature is used in this report. Aquifers located within the Columbia River Basalt are referred to as the confined aquifer system.

Ground water in both the confined and unconfined aquifer systems generally flows toward the Columbia River, which acts as a drain for the ground-water flow system. However, in some places, ground water within the confined system flows under the river, apparently towards areas of higher vertical communication between the confined and unconfined aquifers (Bauer et al. 1985; Spane 1987; DOE 1988). Ground water in the confined aquifers comes mainly from infiltration of precipitation and streamflow within recharge areas along the periphery of the Pasco Basin (DOE 1988). With regard to development of a conceptual model for the unconfined aquifer, the confined aquifer system is important because there is a potential for significant ground-water leakage between the two systems, particularly in areas of increased vertical permeability such as the area northeast of the 200-East Area (Graham et al. 1984).

The unconfined aquifer at Hanford lies mainly within the Ringold and Hanford formations. Because the sand and gravel facies of the Ringold Formation are generally more consolidated, contain more silt, and are less well sorted, they are about 10 to 100 times less permeable than the sediments of the overlying Hanford formation (DOE 1988). Prior to waste-water disposal operations at the Hanford Site, the uppermost aquifer was almost entirely within the Ringold Formation and the water table extended into the Hanford formation at only a few locations near the Columbia River (Newcomb et al. 1972). However, waste-water discharges have increased the water-table elevation causing it to rise into the Hanford formation in the vicinity of the 200-East Area and in a wider area near the Columbia River.

Ground water in the unconfined aquifer at Hanford generally flows from recharge areas in the elevated region near the western boundary of the Hanford Site toward the Columbia River on the eastern and northern boundaries. The Yakima River borders the Hanford Site on the southwest and is generally regarded as a source of recharge. The Columbia River is the primary discharge area for the unconfined aquifer. Natural areal recharge from precipitation

at the Hanford Site is low, less than 1.25 cm/y over most of the site, although a few nonvegetated areas with coarse soils may reach 5 cm/y of infiltration (Gee and Heller 1985; Bauer and Vaccaro 1990). Since 1944, the artificial recharge from Hanford waste-water disposal operations has been greater than the natural recharge. As of 1989, an estimated 1,681,000,000 m^3 (444 billion gallons) of liquid were discharged to the ground through disposal ponds, trenches, and cribs (Freshley and Thorne 1992).

THIS PAGE INTENTIONALLY
LEFT BLANK

3.0 Data Sources

Data needed for developing a three-dimensional conceptual model of ground-water flow were derived from a variety of previous studies and ongoing Hanford Site investigations. Hydraulic property data were obtained from previous tests documented in reports of various Hanford Site contractors. Selected previous well tests documented in Bierschenk (1959), Kipp and Mudd (1973), and Deju (1974) are being reanalyzed. New hydraulic tests were conducted at selected Hanford sampling network wells using the existing sampling pumps. In addition, tests were conducted at a well cluster site to determine both vertical and horizontal hydraulic conductivities.

Information on the subsurface geologic framework came primarily from interpreting geologic descriptions of samples acquired during well drilling. These interpretations were based on previous work by Lindsey (1991), which redefined the Hanford suprabasalt sediments in terms of lithofacies units. Many of the wells used to define the geologic framework were drilled to basalt as part of a study for a proposed nuclear power plant (PSPL 1982). Other wells used in defining the top of basalt were drilled for the Basalt Waste Isolation Program (DOE 1988), which studied the basalts underlying Hanford for disposal of high-level nuclear waste. The number of wells used for defining hydrogeologic structure was greatly expanded from those used to generate the cross sections presented in last year's report (Thorne and Chamness 1992). Wells were added by extending out from those cross sections primarily to the west and south and to a lesser extent to the north. Figure 3.1 shows the distribution of wells used for this report. However, many of the wells shown on Figure 3.1 were used only for determining the elevation of the top of basalt, and others have been only tentatively or incompletely interpreted. Additional interpretation and refining of the hydrogeologic structure is needed within the study area. The area north of Gable Mountain is being studied by Westinghouse Hanford Company (WHC), and their information will eventually be incorporated into the hydrogeologic model. Most of the wells added this year extend down to basalt and/or have hydraulic parameters available from aquifer tests.

Liikala (1993) provided information on the ground-water flow system in the southern part of the Hanford Site. Information on the configuration of Hanford Site wells was obtained from McGhan (1989) and from the Hanford Environmental Information System (HEIS) data base.

THIS PAGE INTENTIONALLY
LEFT BLANK

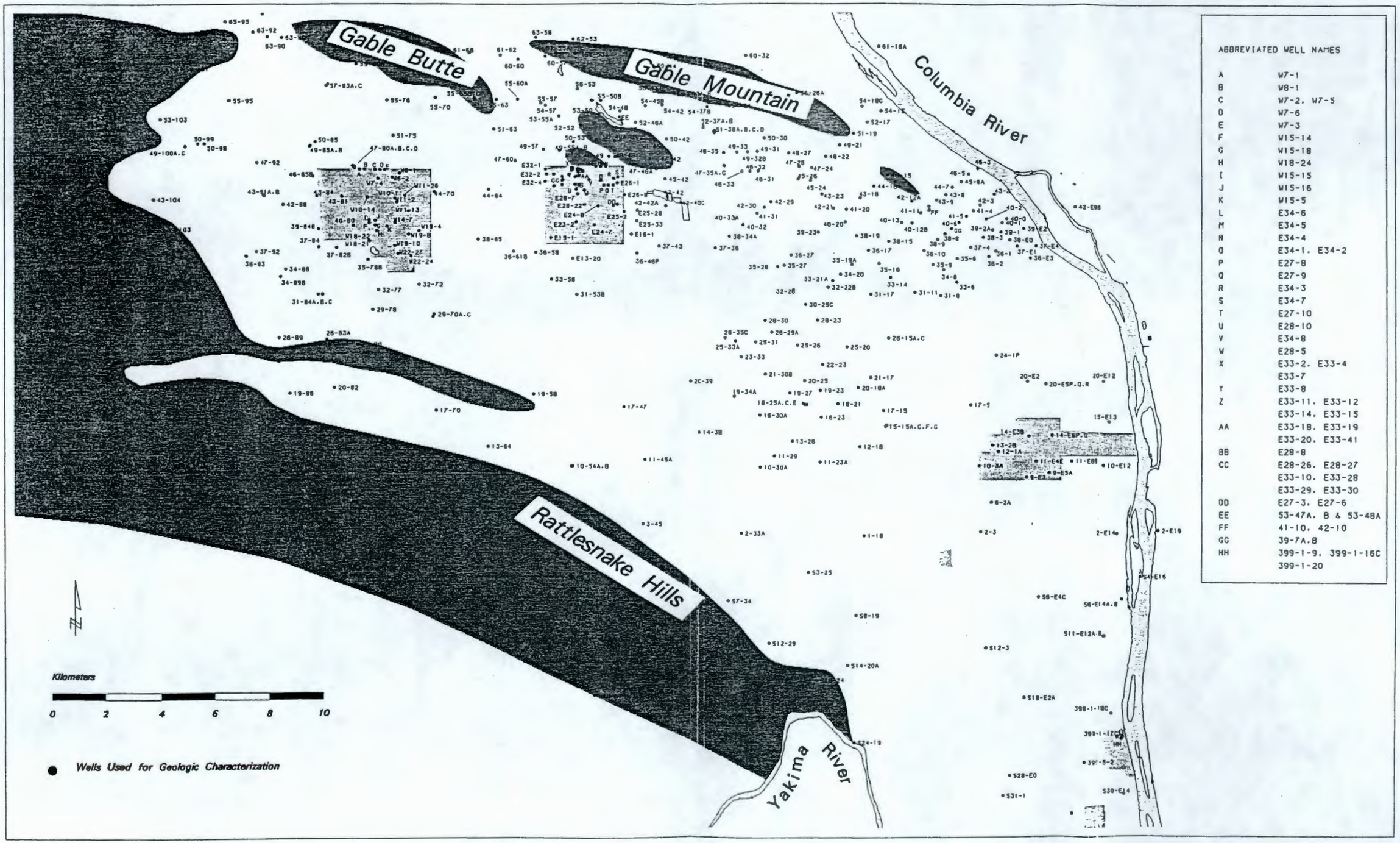

Figure 3.1. Locations of Wells Used for Defining Hydrogeologic Structure

THIS PAGE INTENTIONALLY
LEFT BLANK

4.0 Definition of Hydrogeologic Structure

The unconfined aquifer system underlying the Hanford Site is composed of a sequence of mostly discontinuous sedimentary deposits with differing hydraulic properties that are related to the texture, degree of sorting, and cementation of the sediments. One component in developing the conceptual model is describing the three-dimensional geologic structure of the aquifer in enough detail to reflect important changes in hydraulic characteristics. The status of the developing conceptual model of three-dimensional aquifer structure is described in this section and figures showing contours for the top of each unit within the current study area are shown. Because of the large number of figures presented in this section, they are placed at the end.

The hydrogeologic framework of the three-dimensional model needs to be accurate, but relatively simplistic, for two reasons. First, lateral and vertical variation are quite high in the primarily fluvial depositional environment of the Hanford Site and cannot be completely described with the distribution of boreholes and wells available for subsurface data. Second, the computer simulations would be very complex and difficult to run with a multitude of discrete sedimentary lenses. Therefore, the unconfined aquifer system has been divided into relatively extensive lithofacies units. Areally limited lenses within a unit are not recognized as separate layers in the conceptual model. It should be noted that the definition of hydrogeologic units presented in this report is not definitive, because examination of data from additional wells is continuing. Most units probably extend beyond the boundaries shown in the figures and into areas outside the current study area.

Work on the hydrogeologic model began last year by interpreting the geology along four cross sections in the central and eastern portions of the Hanford Site (Thorne and Chamness 1992). Classification of the sediments into lithofacies units was based on work by Lindsey (1991; Lindsey et al. 1992), calcium carbonate and particle size data, and the available geologist's and driller's logs. In some areas, geophysical logs were also used to assist in correlation. The textural facies were often grouped into larger units based on an assumed similarity in hydraulic parameters. Consequently, sands were generally grouped with sandy gravels, and silt was grouped with clay. This resulted in the generation of 9 units above the top of the basalt, which are shown in the stratigraphic column presented in Figure 4.1. Because these units are not correlated in all cases to the revised stratigraphic column in Lindsey et al. (1992), they are numbered sequentially from top to bottom as Unit 1, 2, and so on in this report. More work needs to be done to better correlate these units to Lindsey's lithofacies units.

The sedimentary section of interest for this model is underlain by basalt, generally the Elephant Mountain member of the Saddle Mountains Basalt. The Ice Harbor member is found in the southeastern part of the site. The top-of-basalt contour map shown in Figure 4.2 was generated from the top-of-basalt map for the Hanford Site, which is currently under revision. Top-of-basalt data are based on geologist's/driller's logs or geophysical logs, where available. Overlying the basalt near the middle of the synclines and in the structural depressions is a sand and/or gravel unit, Unit 9 (Figure 4.3). This is the lowest unit in the sedimentary sequence of Hanford and corresponds to Lindsey's Ringold Unit A. Unit 9 tends to be basalt-rich in comparison to later Ringold gravels. Along the edges of the synclines and structural depressions, Unit 9 pinches out and the clay or mud to sandy mud of overlying Unit 8 is in contact with the basalt (Figure 4.4). Unit 8 corresponds to the finer-grained portion of Lindsey's Lower Mud Sequence. This unit often contains a layer of white volcanic ash and one or more paleosols. Where it lies directly on top of the basalt, it often includes weathered basalt fragments and basalt altered to clay. The calcium carbonate content increases in this unit in places due to the paleosols, and there are color changes as well. Lower portions of Unit 8 often have a blue-green color, while the upper part may be yellow, tan, or blue-green.

Unit 7 is a coarse-grained unit that consists of sand to muddy, sandy, basalt-poor gravel occurring primarily in the central and eastern portions of the basin (Figure 4.5). Some of the sandy portions of this unit correlate to parts of Lindsey's Lower Mud Sequence, which includes fluvial sands (Lindsey et al. 1992). The sands have been grouped with the gravelly portions of Unit 7 because their hydraulic properties are probably more similar to those of the muddy, sandy, gravel in Unit 7 than the clay and silt in Unit 8.

Overlying Unit 7 through much of the central portion of the basin (Figure 4.6) is Unit 6, a mud and clay layer. Unit 6 is only tentatively identified in this report. There are a number of mud layers that extend for only a few kilometers across the site. Reidel et al. (1992) identify several mud layers between their gravel units B, C, and D. However, it is very difficult to distinguish one mud layer from another over any distance. Consequently, Unit 6 as identified here may actually incorporate parts of these different mud layers. Further work is needed to distinguish more clearly between these different mud layers.

The sand to muddy, sandy, gravel of Unit 5 overlies Unit 6 and generally corresponds to Lindsey's Unit E. This unit is widespread across the basin (Figure 4.7) and contains a relatively low percentage of basalt gravels. This unit cannot be distinguished readily from Unit 7, and if there is no fine-grained layer separating the two, they have been grouped together as Unit 5. In many areas, Unit 5 forms the top Ringold unit, except where it is overlain by Unit 4. Unit 4 corresponds to the fine-grained portions of Lindsey's Upper Ringold Unit. In this report, Unit 4 is restricted to silt and clay deposits. Sand layers

included in Lindsey's Upper Ringold Unit have been grouped with coarser-grained sediments either underlying or overlying Unit 4, as appropriate. Unit 4 occurs in the western and east central portions of the Hanford Site and forms the extensive White Bluffs on the east side of the Columbia River (Figure 4.8). It has been eroded from a relatively narrow band running northeast-southwest in the 200-West Area and from the east side of the 200-West Area to east of B Pond. Erosion probably occurred during the hiatus when the Plio-Pleistocene and early "Palouse" soil units were deposited. The Plio-Pleistocene unit (Unit 3) developed during a depositional hiatus as a calcite and/or basaltic side-stream gravel deposit. Unit 3 has been identified only in the western portion of the Pasco Basin (Figure 4.9) where it developed and/or was deposited on the eroded surface of Unit 4 (Upper Ringold) or Unit 5 (Lindsey's Unit E). The extent and thickness of early "Palouse" soil (Unit 2) is undergoing evaluation. Some of what has been called early "Palouse" soil in the past is probably "sand-dominated" Hanford formation sediments. An effort has been made to incorporate this re-evaluation of the early "Palouse" soil into the data set (Figure 4.10), but there will undoubtedly be more modifications to the extent and thickness of this unit in the future.

Overlying all of the Ringold Formation on the Hanford Site, and in a few places resting on top of the basalt, is Unit 1, the glaciofluvial, generally basalt-rich Hanford formation. This unit consists of three lateral facies: 1) a gravel-dominated facies known as the Pasco gravels, 2) a sand-dominated facies, and 3) a mud-dominated facies known as the slackwater deposits of the Hanford formation. The coarseness of the sediments in the Hanford formation is related to their proximity to the main flood channels; i.e., the areas closest to the main channels in the center of the Hanford Site received primarily the gravel facies, while the edges of the Pasco Basin received only the mud-dominated sediments. The sand-dominated facies lie between these two extremes. The water table is below the Hanford formation over approximately the western half of the Hanford Site. Where the aquifer extends up into the Hanford formation in the study area, it is dominated primarily by the Pasco gravels. The slackwater deposits are generally not found below the water table within the study area. Consequently, the individual facies of the Hanford formation have not been distinguished in this report. Because of the relatively high permeability of the Pasco gravels, this unit plays an important role in ground-water flow in those areas where it makes up the uppermost part of the unconfined aquifer.

Lying beneath gravels of the Hanford formation in the central portion of the Hanford Site are the sand and gravel deposits commonly called the "pre-Missoula gravels" (PSPL 1982). These sediments have been grouped with the Hanford formation for the following reasons: 1) the pre-Missoula gravels cannot be readily distinguished from the Hanford formation in most driller's or geologist's logs, 2) there are no known hydraulic property data for the pre-Missoula gravels, although its properties probably lie between the younger Hanford gravel-dominated facies and older Unit 5 gravel and sand unit of the Ringold Formation, and 3) the

pre-Missoula gravels are above the water table except in some areas near the Hanford Townsite and near the solid waste landfill in the center of the Hanford Site. Therefore, they do not present a primary pathway for ground-water movement. The surficial eolian sediments have an insignificant effect on ground-water movement and have also been grouped with the Hanford formation. A structural contour map of the top of the Hanford formation has not been provided because it would simply reflect the surface topography of the Pasco Basin.

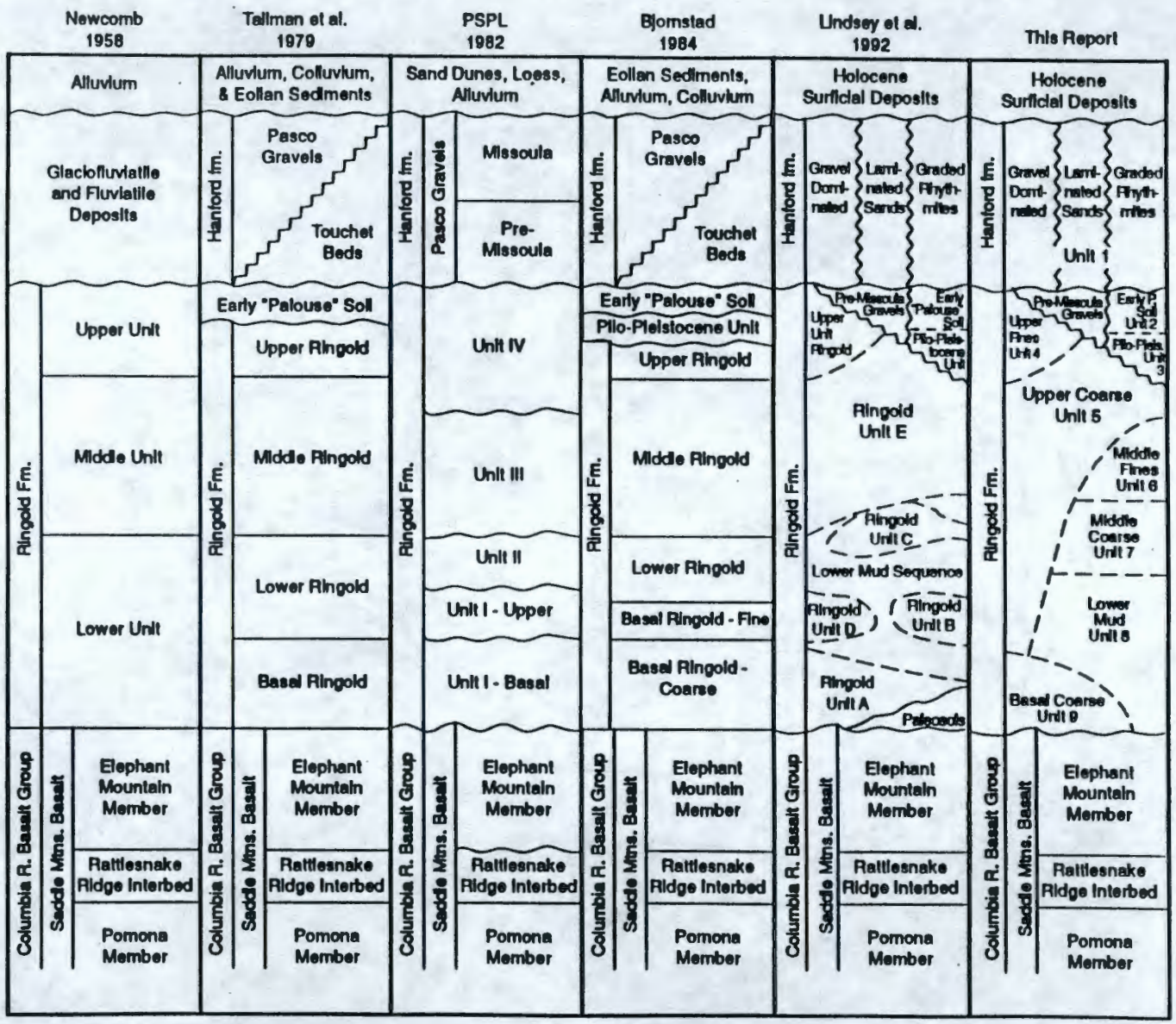

Figure 4.1. Stratigraphic Nomenclature of Various Authors

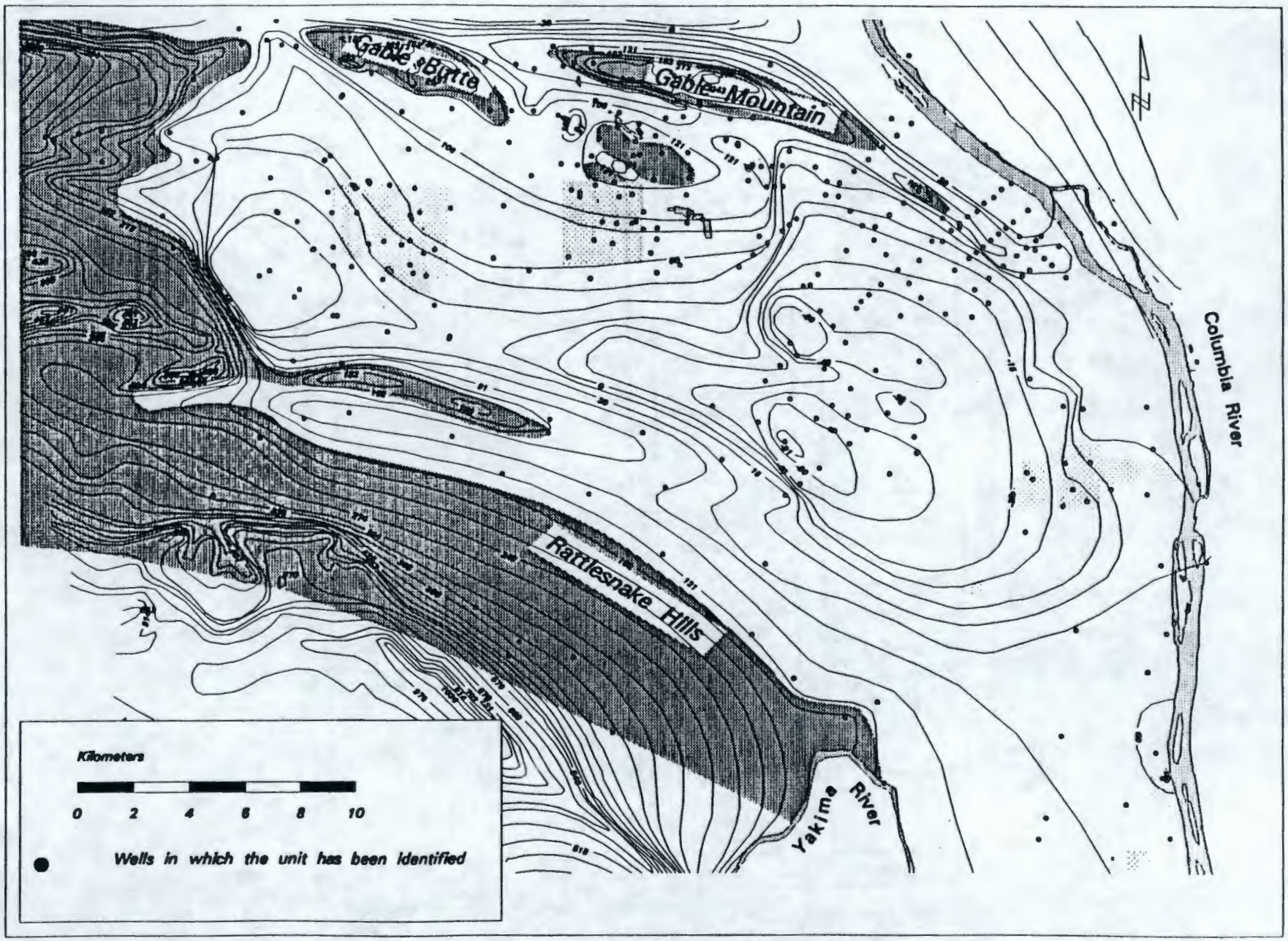

Figure 4.2. Structural Contours for the Top of Basalt

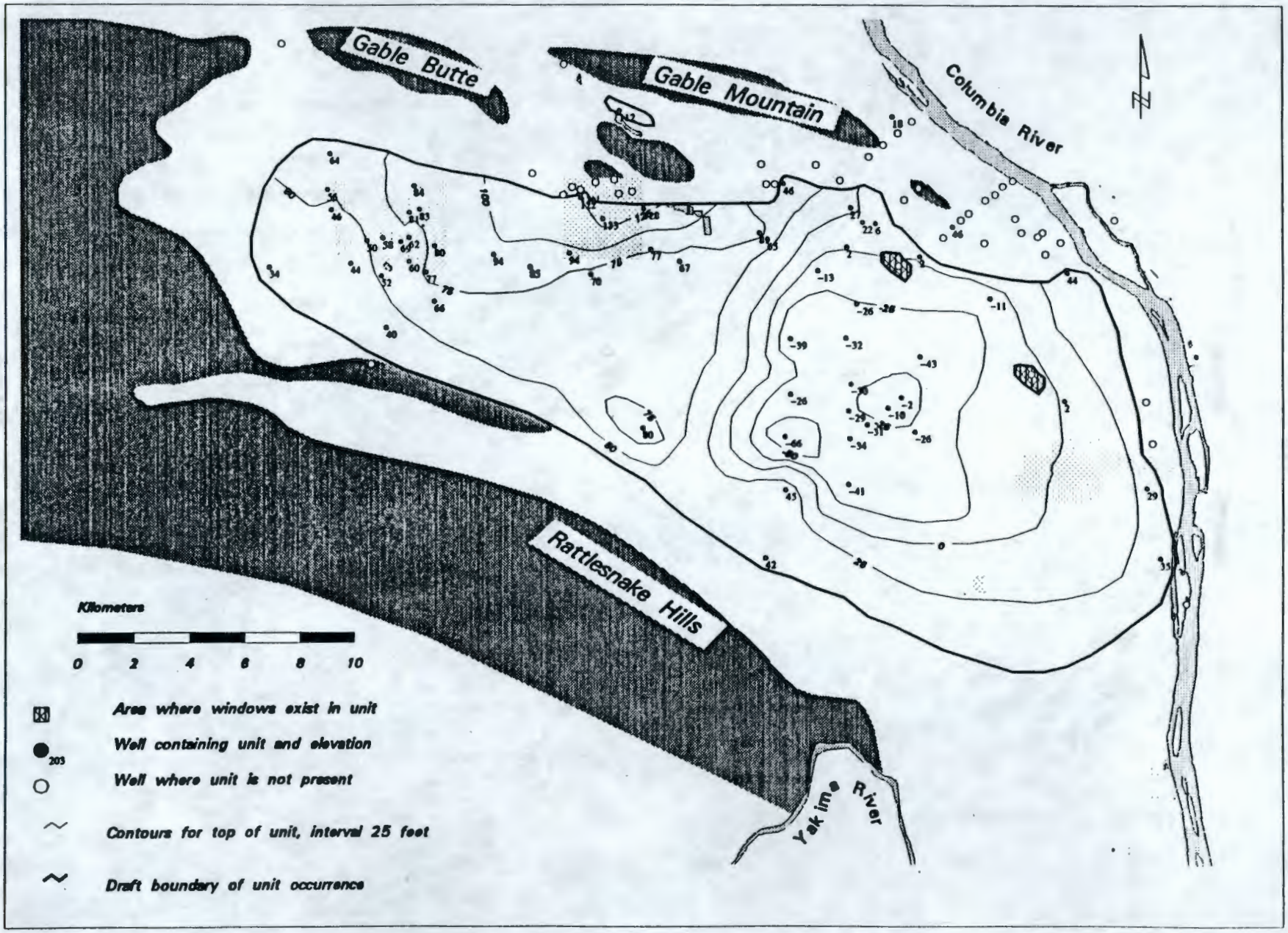

Figure 4.3. Structural Contours for the Top of Unit 9

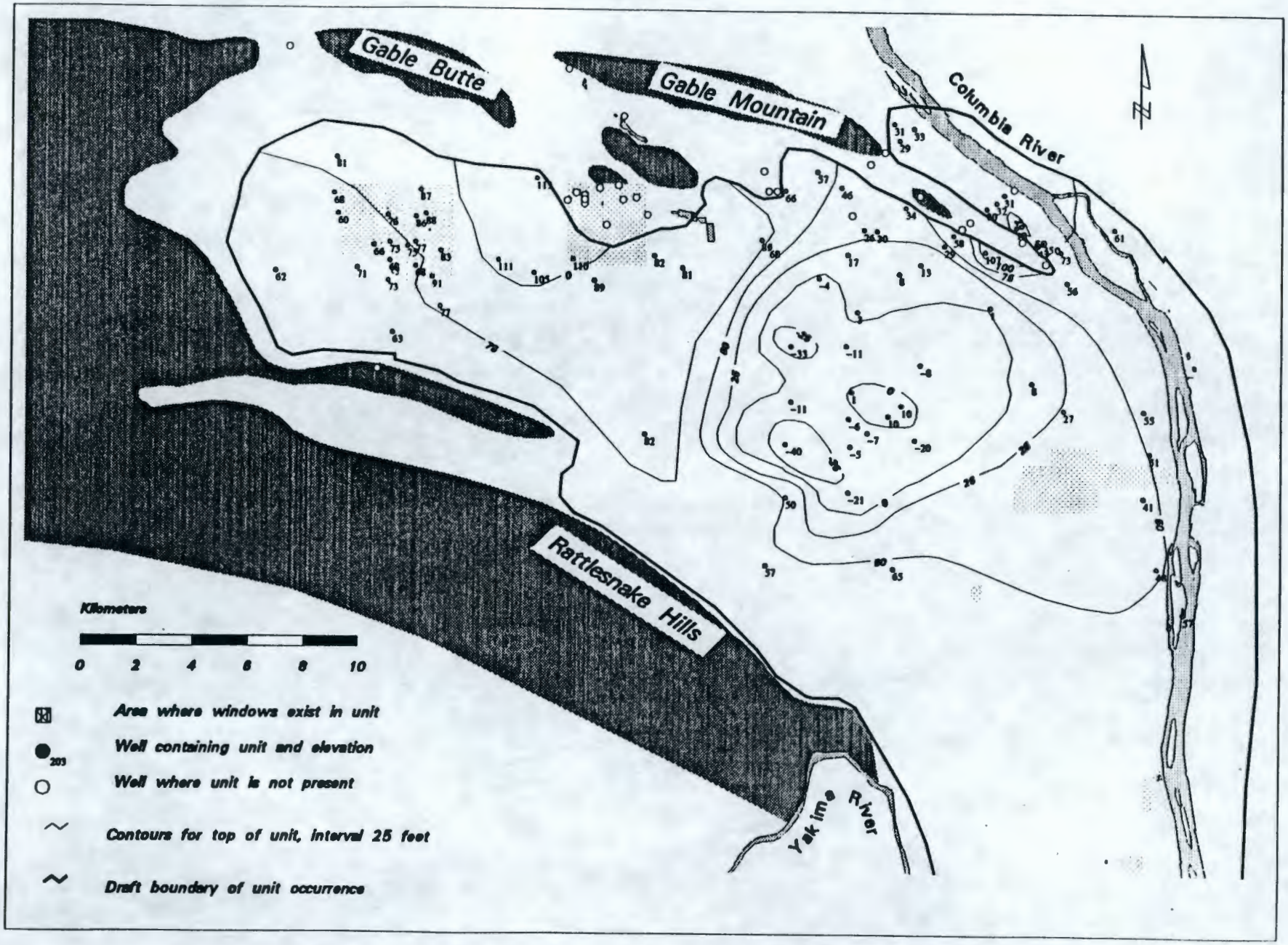

Figure 4.4. Structural Contours for the Top of Unit 8

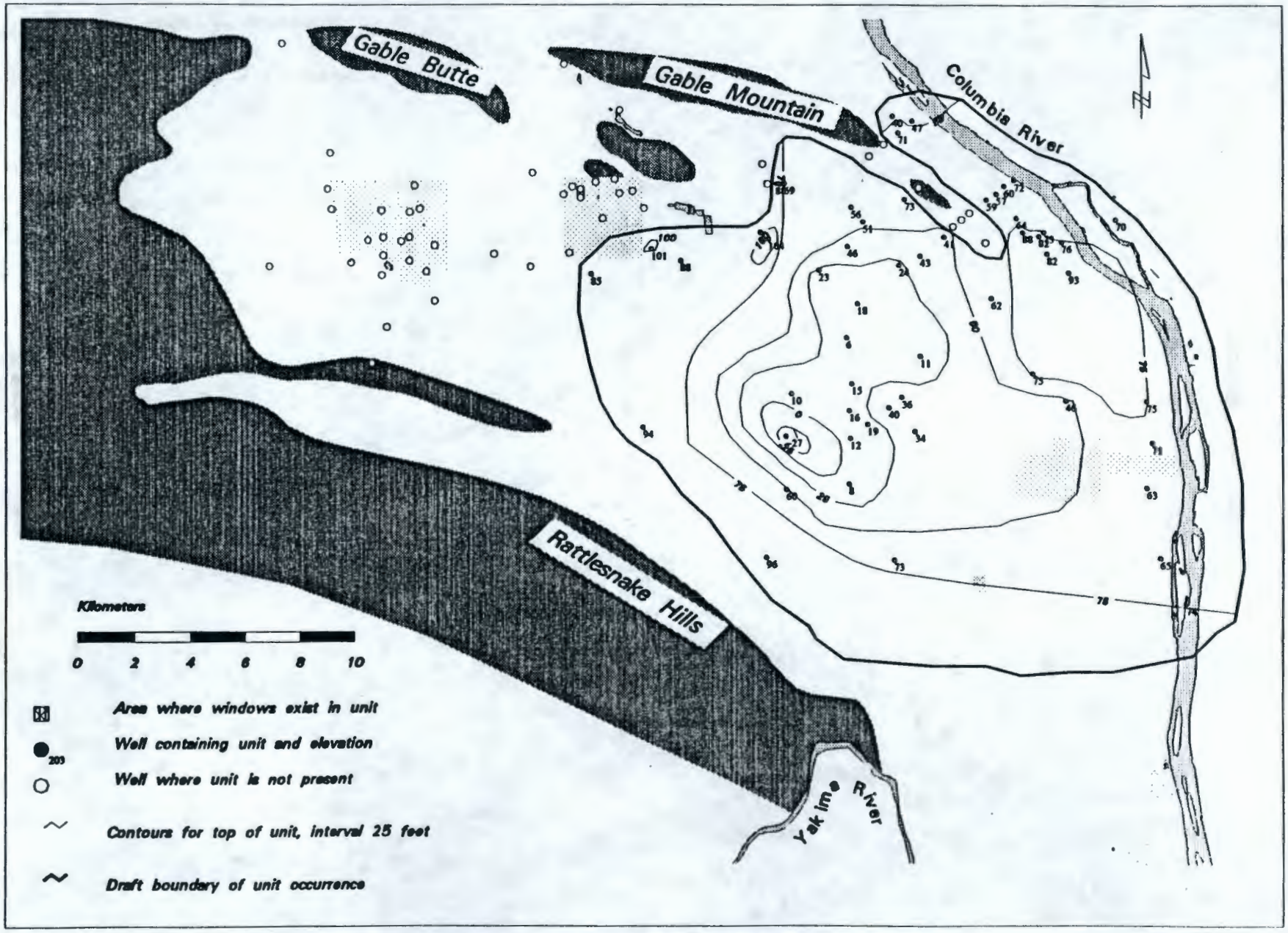

Figure 4.5. Structural Contours for the Top of Unit 7

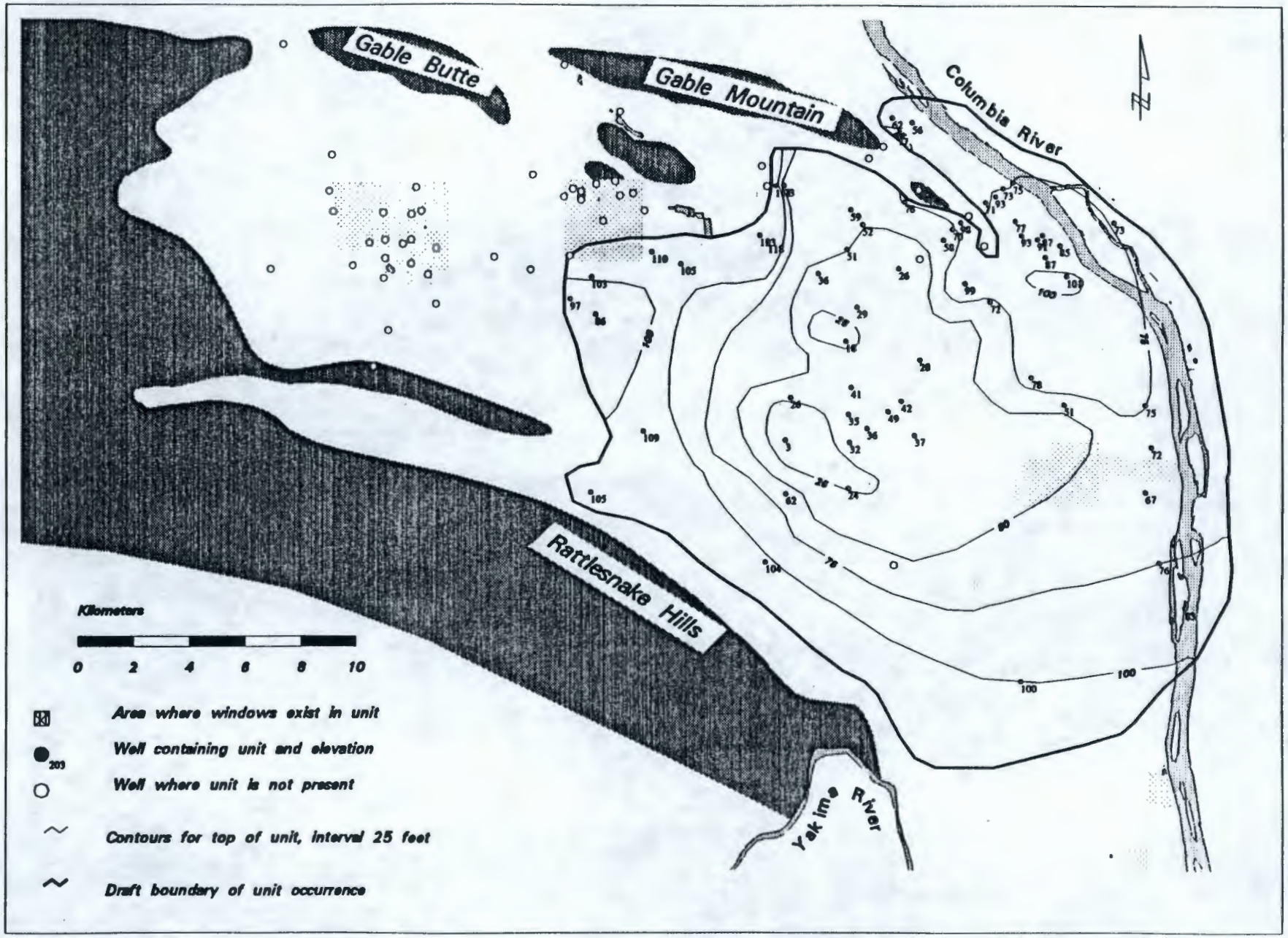

Figure 4.6. Structural Contours for the Top of Unit 6

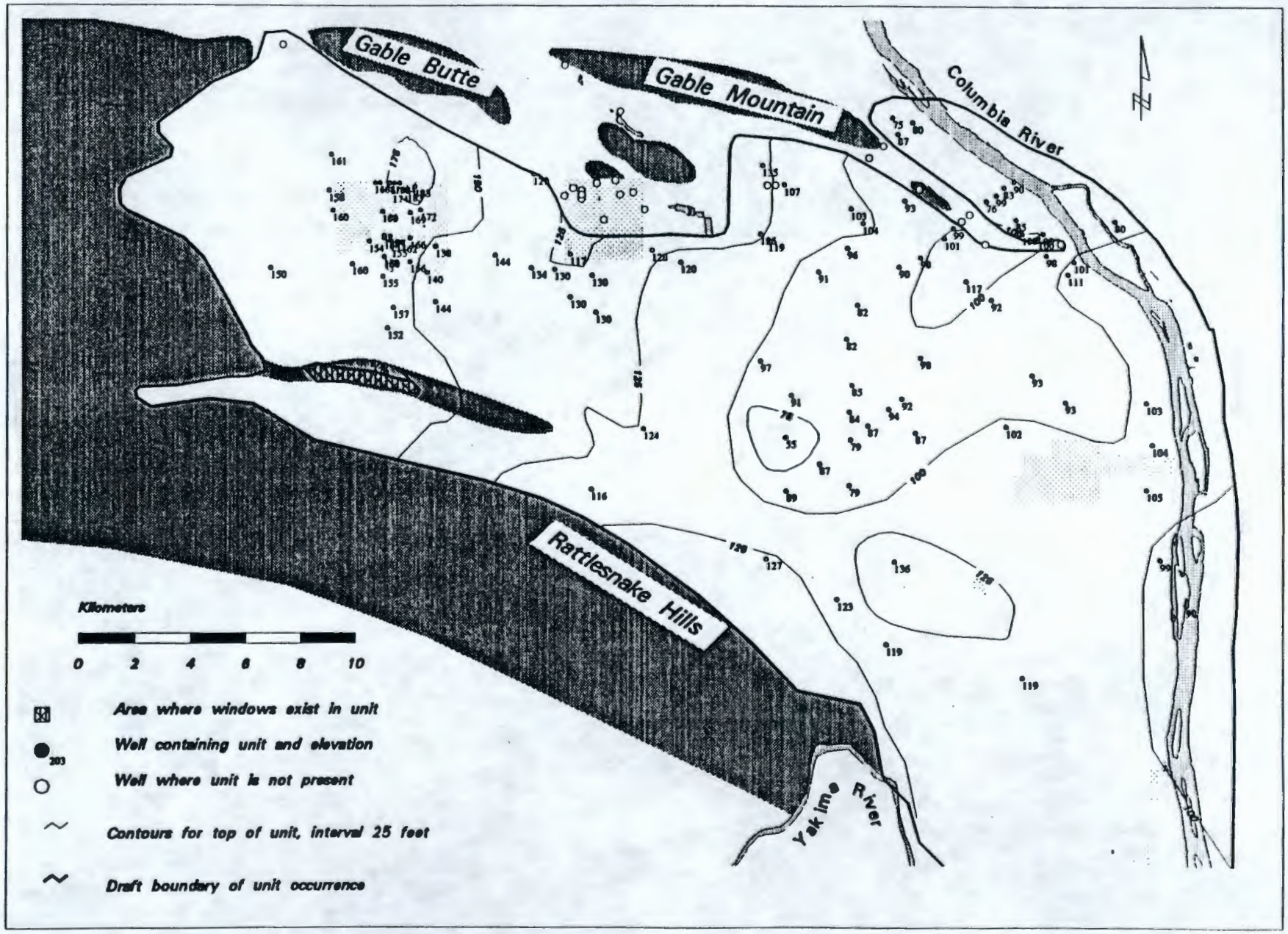

Figure 4.7. Structural Contours for the Top of Unit 5

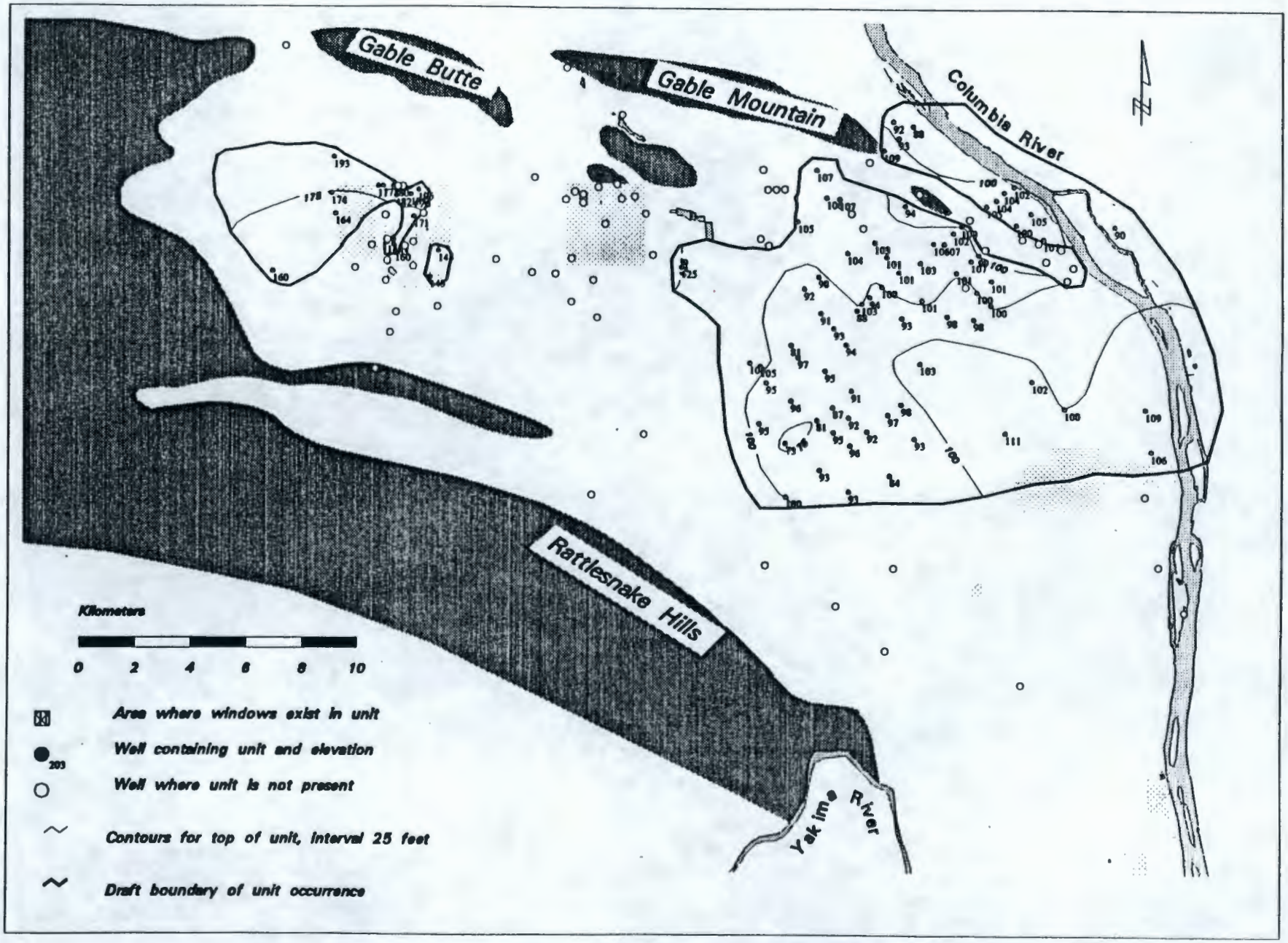

Figure 4.8. Structural Contours for the Top of Unit 4

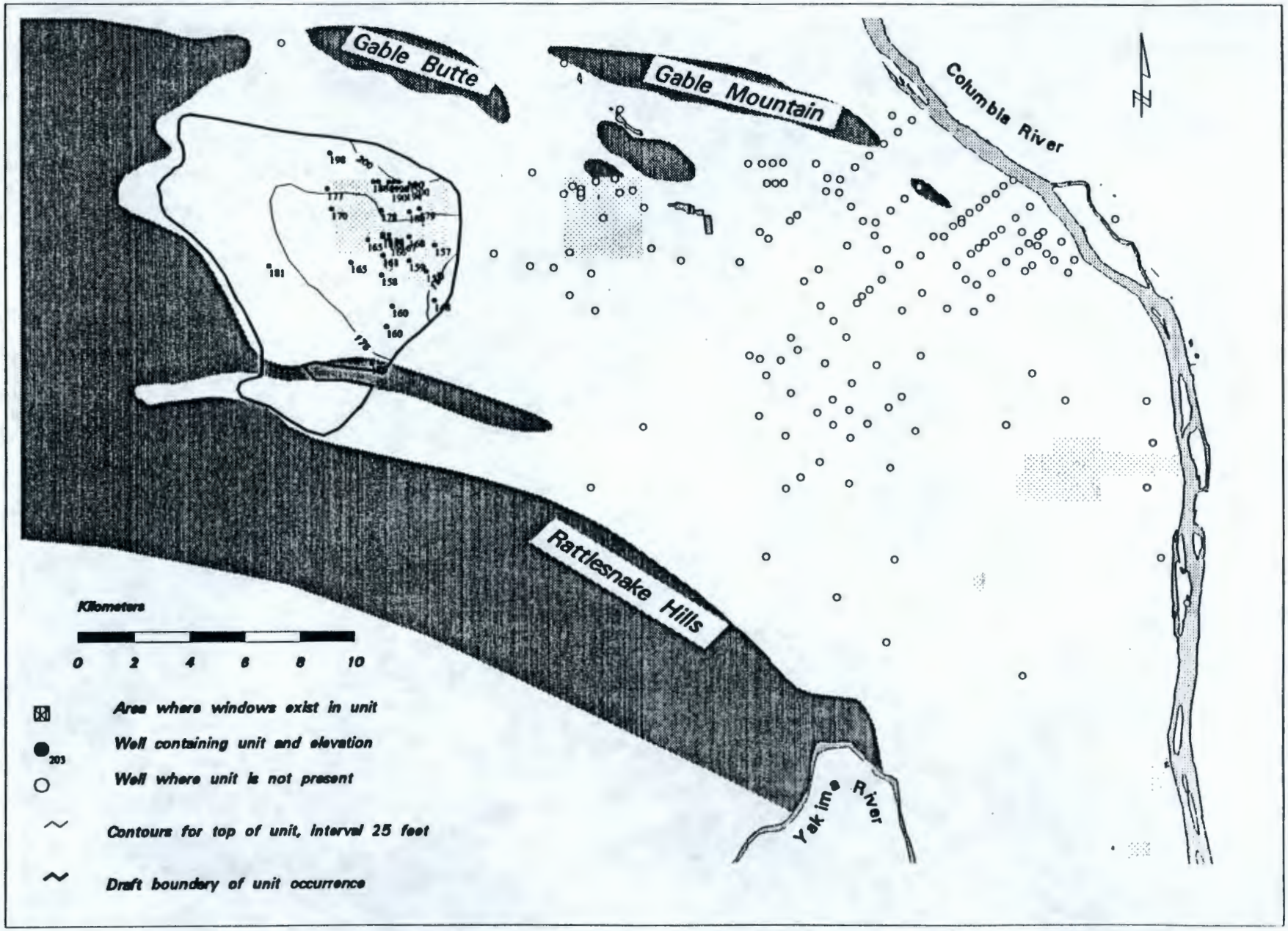

Figure 4.9. Structural Contours for the Top of Unit 3

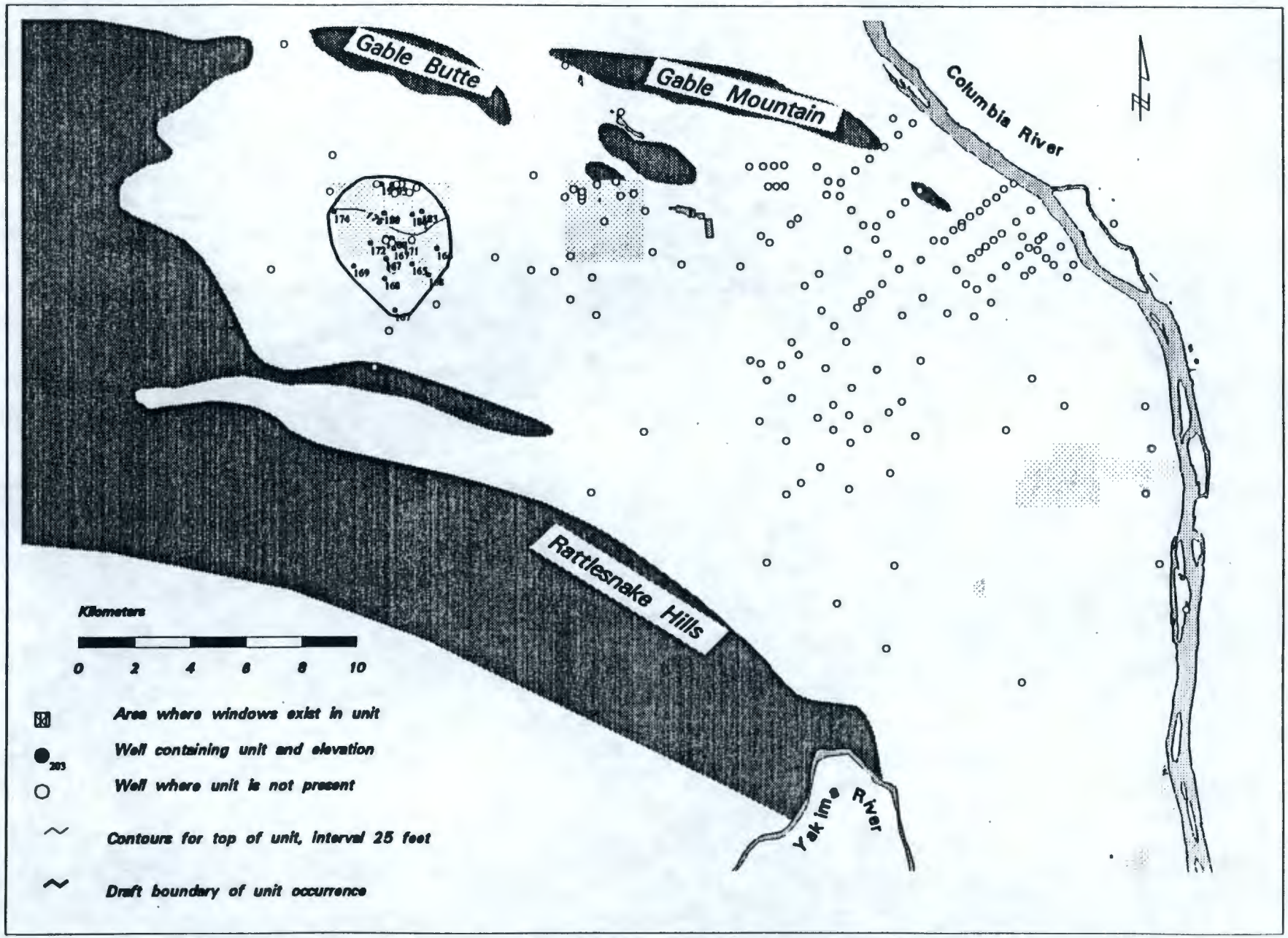

Figure 4.10. Structural Contours for the Top of Unit 2

5.0 Aquifer Hydraulic Properties

Hydraulic properties must be assigned to each unit in the three-dimensional numerical model. In addition to unit thickness, these properties include horizontal hydraulic conductivity (K), vertical hydraulic conductivity (K_v), storativity (S), and specific yield (S_y). Additional parameters, such as dispersion coefficients and retardation factors, may also be required for transport modeling. Hydraulic properties are usually determined from aquifer tests conducted on wells. They may also be estimated from laboratory testing of samples removed from boreholes or inferred from geologic information such as grain size distribution and geophysical logging results. Aquifer tests have the advantages of directly measuring flow properties in situ and of being influenced by a larger area of the aquifer than the other methods. Well tests have, therefore, been the principal method of determining hydraulic properties of more permeable hydrogeologic units within the Hanford Site flow system.

During the past year, aquifer tests have been conducted at selected wells, and previously conducted tests have been reanalyzed using improved diagnostic techniques. These results and other hydraulic property data available for selected wells on the Hanford Site are being correlated with hydrogeologic units by examining geologic logs and information on well completion. The results of hydraulic testing, findings of test reanalyses, and assignment of hydraulic property values to hydrogeologic units are discussed in this section.

5.1 Results of Aquifer Testing

Constant-rate pumping tests were conducted at 16 wells to support development of the three-dimensional conceptual model. One of the tests was conducted at a multiple-well site near B Pond that included a well (699-43-42K) equipped with a Westbay Instruments, Inc., multiport monitoring system. The system installed in this well and additional pressure monitoring equipment provided by Westbay Instruments, Inc., allowed for the simultaneous monitoring of pressure responses at four discrete depth intervals within the aquifer. The data have been analyzed to provide information on hydraulic properties, and particularly vertical anisotropy (K_v/K), at the test site. The other 15 constant-rate pumping tests were conducted on wells used for routine hydrochemical sampling of the unconfined aquifer. These tests were all conducted at single wells and utilized the existing sampling pump to remove water from the aquifer.

5.1.1 Multiple-Well Aquifer Test to Determine Vertical Anisotropy

A series of aquifer hydraulic tests were conducted at a well cluster site near B Pond in the central part of the Hanford Site. Well 699-42-42B was utilized as the stress well, and test responses were monitored at wells 699-43-42J and 699-43-42K. The Westbay multiport system was installed in Well 699-43-42K. This well was also instrumented with a Westbay Modular Subsurface Data Acquisition (MOSDAX) system with the capability of simultaneously monitoring pressure at four ports located at different depths. The stress well was completed in silty sandy gravels of the Hanford formation (Unit 1). The test site is located near the area through which most of the contaminant transport from the 200-East Area to the Columbia River takes place. However, the ground-water mound created by B Pond forces the main contaminant plume to follow a path to the south of the test site.

Slug-interference tests, sinusoidal-pulse tests, and a constant-rate pumping test were performed. The main objective of the tests was to determine hydraulic properties including K, K_v, S, and S_y for the upper unconfined aquifer at the test site. A secondary objective was to evaluate the slug-interference and sinusoidal-pulse test methods for measuring these parameters.

Results of the constant-rate pumping test are presented in Table 5.1. Details of the analysis of this test are presented in Appendix A. The constant-rate pumping test indicated a transmissivity in the range of 18 to 25 m^2/d, which corresponds to a K range of 1.4 to 2.1 m/d. Vertical anisotropy results (K_v/K) ranged from 0.01 to 0.06, and correspond to a K_v range of 0.02 to 0.08 m/d. However, the multiple-well composite analysis is believed to provide the most reliable indication of vertical anisotropy. This analysis method resulted in $K_v/K = 0.01$, which corresponds to a K_v range of 0.014 to 0.021 m/d.

Analysis of the slug-interference and sinusoidal-pulse tests is ongoing and will be presented in a later report. The analysis of these additional tests is not expected to change the results presented in this report for the constant-rate discharge test.

5.1.2 Single-Well Aquifer Tests Conducted at Sampling Network Wells

Approximately 500 wells on the Hanford Site are routinely sampled at least once each year. Most of these wells are equipped with dedicated submersible sampling pumps. Therefore, it was relatively efficient and inexpensive to conduct aquifer tests at sampling network wells using existing sampling pumps. Most of the sampling wells are completed in the upper 10 m of the unconfined aquifer, where the majority of contaminant transport takes place. Fifteen wells with sampling pumps were identified in areas where additional hydraulic

Table 5.1. Results for the Constant-Rate Discharge Test at the Westbay Multiport Well Site Near B Pond

	T (m^2/d)	S	S/S_y	K_v/K
Qualitative Composite Analyses:	27 - 32	0.0001 - 0.0003	0.018 - 0.044	0.009 - 0.01
Quantitative Analyses				
699-43-42K Zone 3:	23.5	0.0001	0.045	0.04
699-43-42K Zone 4:	18.0	0.0001	0.030	0.06
699-43-42J:	24.4	0.0002	0.023	0.01

property information is needed and tests were conducted on these wells. Results of the single-well, constant-rate discharge tests performed on sampling network wells are shown in Table 5.2. The test analyses are described in detail in Appendix B.

Some disadvantages of using the sampling pumps for aquifer testing include a maximum flow rate of about 30 L/min, which limits the maximum transmissivity that can be measured, and the lack of a check valve in the pump column, which makes it impossible to obtain analyzable recovery data and sometimes affects the early drawdown response. In spite of these difficulties, K values were determined for four wells where discernible drawdown was produced. These four tests were analyzed using confined aquifer methods and assuming that the well fully penetrates the aquifer (see Appendix B). The actual hydraulic conductivity may be lower than the calculated value if the analyzed portion of the test response was significantly affected by vertical flow within the aquifer. Because of the many non-ideal test conditions including partial penetration, unconfined aquifer conditions, anisotropy, a lack of observation wells, and a lack of recovery data, the test results should be regarded as order-of-magnitude estimates.

The flow rate was not high enough to produce a discernible drawdown at the remaining 11 wells. However, as discussed in Appendix B, a minimum value for transmissivity was estimated corresponding to the magnitude of the minimum drawdown that could be detected. The transmissivity at these wells is assumed to be greater than 100 m^2/d, or a discernible drawdown would have been observed. It should be noted that the actual transmissivity of the entire aquifer thickness may be much higher than this minimum bounding value.

Table 5.2. Results of Single-Well, Constant-Rate Discharge Tests Conducted at Sampling Network Wells

Hanford Well Number	Tested Interval Below Ground Surface (m)	Interval Length (m)	Hydraulic Conductivity (m/d)
699-S8-19	31.7-40.2	8.5	ND
699-S6-E4D	17.1-35.4	18.3	ND
699-S19-11	28.7-35.1	6.4	ND
699-4-E6	21.0-26.5	5.5	ND
699-8-17	37.2-48.2	11.0	ND
699-8-25	32.9-51.2	18.3	ND
699-15-15B	46.0-49.1	3.1	27
699-19-88	39.0-51.8	12.8	ND
699-20-E5A	29.0-30.5	1.5	ND
699-25-70	55.5-56.4	0.9	ND
699-29-4	31.1-34.1	3.0	40
699-29-78	56.4-91.4	35.1	ND
699-35-9	34.1-41.2	7.0	ND
699-55-89	48.8-64.0	15.2	6.7
699-57-83A	44.2-59.4	15.2	4.3

ND = No drawdown detected at average flow rate of 30 L/min, the transmissivity is assumed to be greater than 100 m^2/d.

5.2 Aquifer Test Reanalyses

Aquifer tests including slug tests and constant-rate discharge tests have been conducted at hundreds of wells on the Hanford Site. Of these methods, constant-rate discharge tests are generally considered to be the most accurate method for determining aquifer hydraulic properties, especially for higher-permeability units. However, constant-rate discharge tests can be affected by nonideal wellbore and aquifer conditions that make the analysis results ambiguous. These nonideal conditions include the following:

- flow-rate variations during the test
- head loss in the pumping well caused by friction effects
- a region of decreased or increased permeability surrounding the pumping well (skin effects)
- unconfined aquifer (delayed yield) conditions
- partial penetration of the aquifer by the pumping well
- flow boundaries or other heterogeneity in the aquifer
- leakage from underlying or overlying hydrogeologic units.

Because of these problems, the accuracy of many of the reported values of hydraulic properties for the Hanford unconfined aquifer system is uncertain. Recently developed techniques that utilize plots of the derivative of water-level change for well test diagnosis make it easier to detect nonideal conditions and identify data that can be used in determining aquifer properties (Bourdet et al. 1989; Spane 1993). Therefore, data from several earlier aquifer tests are being reanalyzed using derivative methods. Reanalyses of eight tests were reported in Thorne and Newcomer (1992). Additional test reanalyses are continuing and will be presented in a future document.

5.3 Assignment of Hydraulic Properties to Units

In the numerical model, an average "best estimate" of the hydraulic properties for a particular unit may be assigned to the entire unit, or an areal distribution of hydraulic properties may be defined for the unit. The vast majority of contaminant transport takes place

within the upper coarse-grained units of the aquifer. This part of the aquifer is generally composed of the gravels and sands of the Hanford formation, where this unit exists above the water table, and the muddy gravels to sands of Ringold Unit 5 in areas where the water table is below the Hanford formation. The current conceptual model approach is to assign an areal distribution of K to permeable units that form the upper part of the unconfined aquifer system. Single values of K will be assigned to mud units and to deeper permeable units. Because limited information is available on S and S_y, single values of these properties will probably be defined for each unit. An areal distribution of K_v values can be assigned to the upper permeable unit by defining a relationship between vertical anisotropy (K_v/K) and K. This relationship would assume that less permeable sediments generally are more anisotropic. Single values of K_v can be assigned to other units. Uncertainty in the hydraulic properties assigned to each unit results from a lack of hydraulic tests in some units, potential errors in test analyses, and the spatial heterogeneity of the sedimentary layers. Therefore, adjustments to the assigned hydraulic properties may be made during the model calibration process.

Hydraulic conductivity data from aquifer testing and from reanalysis of previous tests are being compiled to provide estimates for numerical modeling. Uncertainty in test results is also being estimated. Vertical and horizontal hydraulic conductivity at a location within the Hanford formation (Unit 1) was determined from the multiple-well test near B Pond (Appendix A). The results indicated a K of about 2 m/d and a K_v of about 0.02 m/d at this site. Estimates of vertical hydraulic conductivity within the Ringold Formation are available from tests at two sites near the 300 Area (Swanson 1992) and from a test conducted at the Nonradioactive Dangerous Waste (NRDW) Landfill southeast of the 200-East Area (Weekes et al. 1987). The test at the NRDW landfill was conducted across a relatively low-permeability, muddy zone within Ringold Unit 5. The K_v estimated from this test was about 0.01 m/d. K values of about 40 to 60 m/d and 0.3 to 15 m/d, respectively, were determined for the higher-permeability and muddy zones within Unit 5. A test of the overlying Hanford formation (Unit 1) at this site indicated horizontal K values of 500 to 1500 m/d. K_v was not estimated for the Hanford formation at the NRDW site. The 300 Area tests were conducted in gravels of Ringold Unit 5 and yielded K_v values of 2.1 and 5.5 m/d. The values of K determined from these tests were 36.6 and 49.1 m/d, respectively.

It is interesting to note that although the Hanford formation generally displays higher hydraulic conductivity than units within the Ringold Formation, a comparison of the test near B Pond and the tests conducted near the 300 Area shows the opposite relationship. The test near B Pond was in Hanford formation sediments that happen to contain a relatively high percentage of fines, whereas the 300 Area tests were conducted in a part of Ringold Unit 5 that is composed of unindurated gravels with minor mud content (Swanson 1992). This

illustrates the heterogeneity within each hydrogeologic unit and the need to define distributions of hydraulic conductivity for at least the uppermost units of the aquifer.

Measurements of hydraulic property data generally are not available for the mud-dominated units. However, the values assigned to these low-permeability units will not have a large effect on the flow system as long as the conductivity values are orders of magnitude less than those of the permeable units. A value of 10^{-9} m/d is indicated in Davis (1969) as a reasonable estimate for hydraulic conductivity of mud to sandy mud units.

The effective porosity of permeable sediments at Hanford has often been assumed at 0.1 for modeling studies. This assumption may be adequate for flow modeling but should be refined for transport modeling, which is more sensitive to porosity.

THIS PAGE INTENTIONALLY
LEFT BLANK

6.0 Boundary Conditions

Boundary conditions must be defined for the sitewide ground-water flow model. Nearly all the model boundaries represent physical boundaries of the flow system. Perimeter boundaries define the edges of the flow system corresponding to the Columbia River on the north and east and the Yakima River and basalt ridges on the south and west. Boundary conditions are also needed for the top and bottom of the aquifer system. Local recharge and discharge areas are represented by boundary conditions defined for elements within the model.

6.1 Perimeter Boundaries

The boundary condition corresponding to the Columbia River was discussed in Thorne and Chamness (1992). In summary, the current approach is to represent the river as a prescribed-head boundary over the depth of the river and as a no-flow boundary from the bottom of the river to the bottom of the aquifer. It is unlikely that ground water in the unconfined aquifer system flows across this boundary, although it is possible if a locally confined permeable unit extends beneath the river and is affected by stresses such as pumping. For a general sitewide model, daily and seasonal changes in the river stage resulting from releases from upstream dams can be ignored, and a time-averaged river stage can be used for the prescribed-head value at the river. The prescribed-head values along the Columbia River can be interpolated between points where river stage is routinely measured.

In past numerical models, the Yakima River has been represented by a prescribed-head boundary (Jacobson and Freshley 1990). To help define aquifer behavior in the vicinity of the Yakima River, river-stage monitoring was conducted at a point just below Horn Rapids Dam, and ground-water levels were continuously monitored at Well 699-S24-19 beginning in November 1992. Well 699-S24-19 is open to both the unconfined aquifer system and the confined system. The two aquifers were isolated at the start of the monitoring period by setting an inflatable packer between the two open intervals in the well. A canal called the "Horn Rapids ditch" is located between Well 699-S24-19 and the river (Figure 6.1). This canal receives water from the Yakima River at Horn Rapids Dam and carries it to a point about 6 km downstream where the water flows into the Yakima flood plain, which is a marshy area on the east side of the river. Water was not present in the canal from about December 20, 1992, until May 28, 1993. Hydrographs showing the measured water levels in the two monitoring wells and in the river are shown in Figure 6.2. As shown, hydraulic head in the unconfined aquifer at well 699-S24-19 increased by more than 1.6 m when water was introduced to the canal in May. The elevation of water in the canal adjacent to the well is

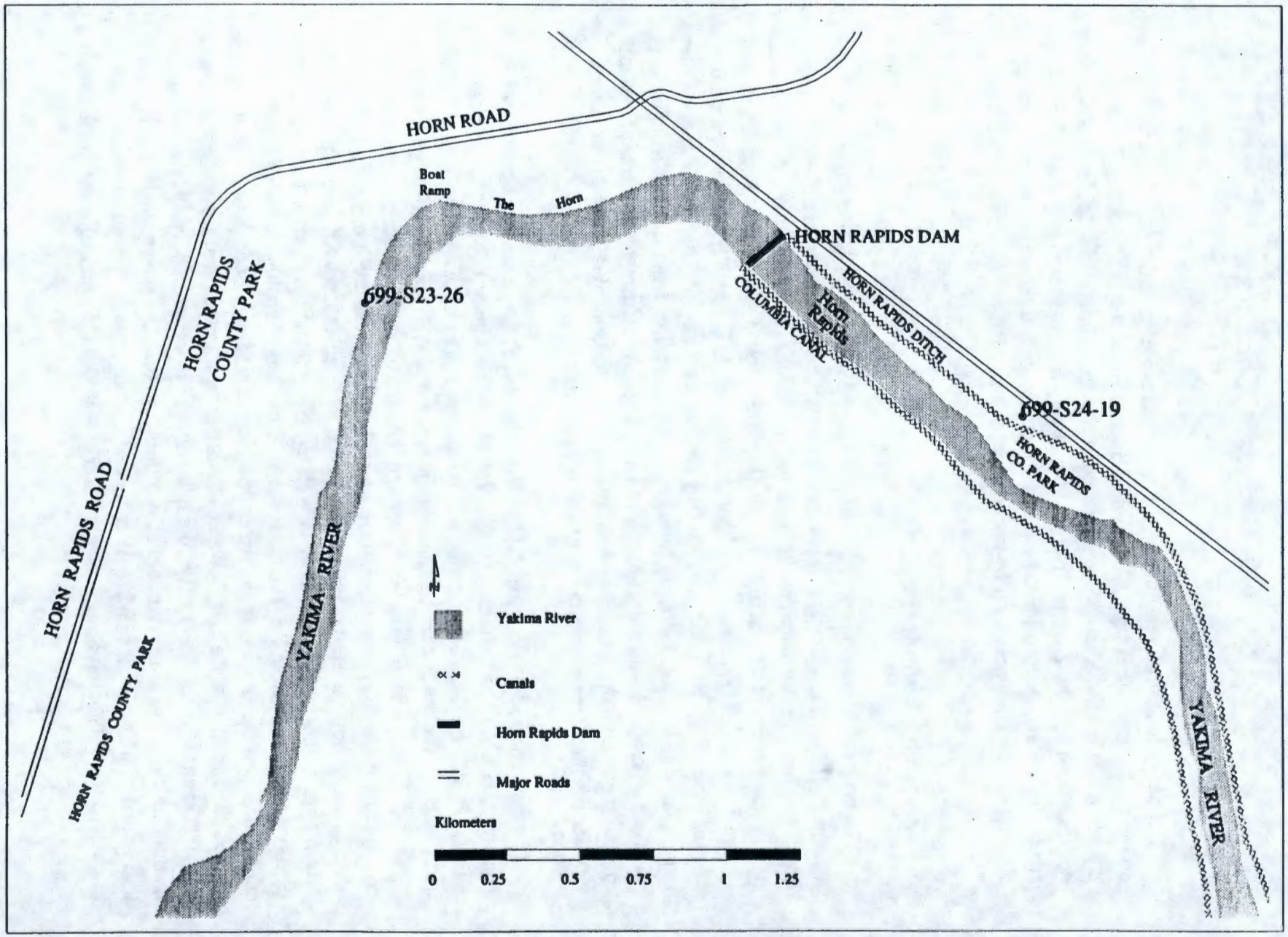

Figure 6.1. Map Showing Monitoring Wells Near the Yakima River and the River Stage Measurement Station

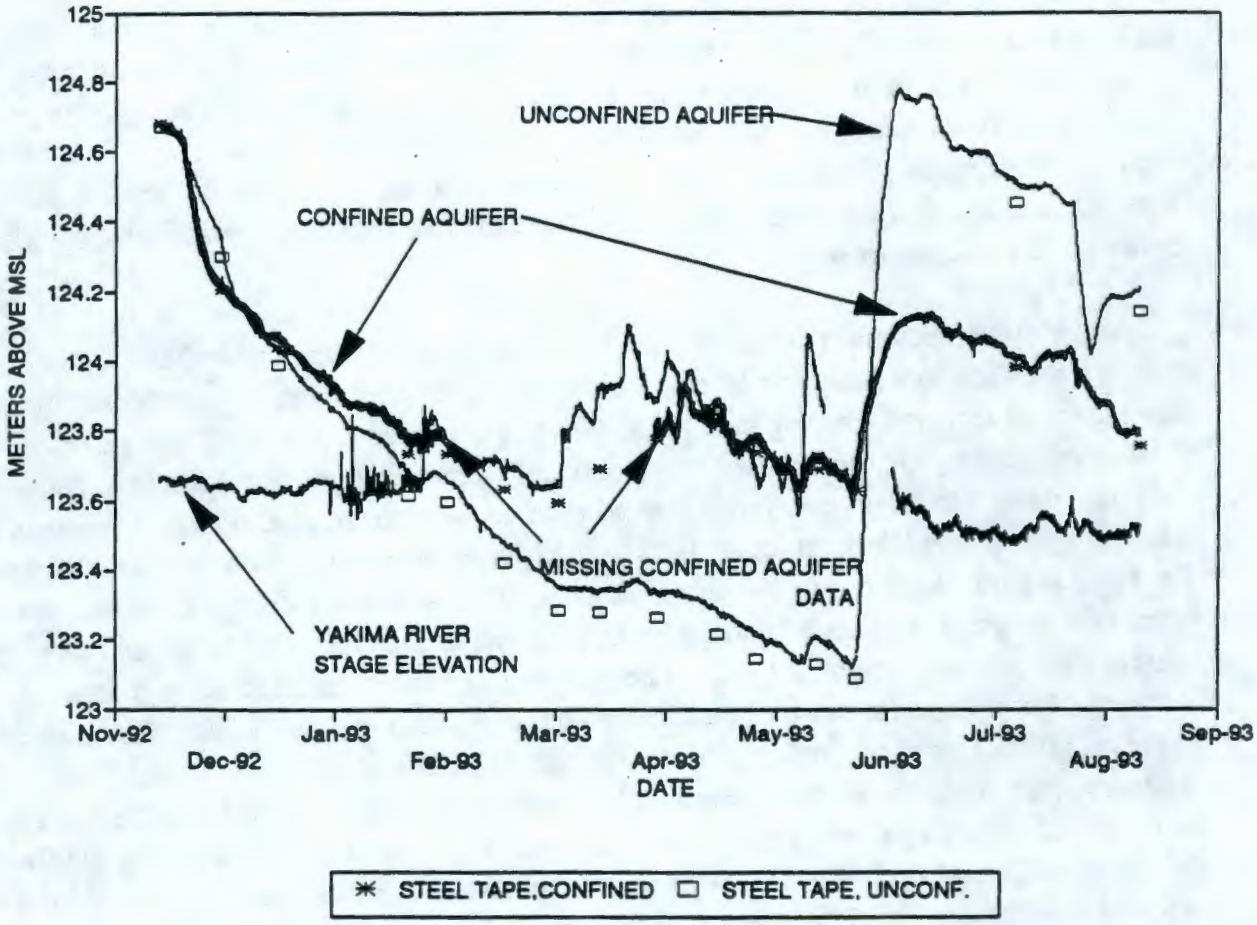

Figure 6.2. Yakima River Stage and Water-Level Elevations in the Unconfined and Confined Aquifers at Well 699-S24-19

about 127 m above msl. The data indicate that during those months when water is present in the canal, the flow system boundary between Horn Rapids Dam and the canal discharge point may be more accurately represented by a prescribed-head boundary condition equal to the elevation of water in the canal, which is higher than the river stage elevation. The hydraulic head in the aquifer rose above the river stage and above the head in the underlying confined aquifer when water was introduced to the canal. After the canal water was shut off, the hydraulic head slowly returned to a level slightly below the river stage and lower than the hydraulic head in the confined aquifer. The data confirm that the Yakima River and canal together act as a prescribed-head boundary and apparently contribute significant recharge to the unconfined aquifer. This situation probably contributes to eastward ground-water flow across the southern part of the Hanford Site, which may limit the potential for contaminants to migrate southward into the Richland area (Dresel et al. 1993).

It should be noted that Well 699-S24-19 was open to both the confined and unconfined aquifers for a period of several years prior to the monitoring period. This information explains why heads in the two intervals were equal at the beginning of the monitoring period. The isolation of these two intervals has been questioned because of uncertainties in the well construction (Liikala 1993). However, the eventual separation of measured heads in the two intervals indicates that they were effectively isolated after a packer was placed in the well between the two open intervals.

A flow-system boundary is also formed by basalt outcrops along the western edge of the flow system. This boundary can be considered no-flow or prescribed-flux depending on the importance of recharge entering the flow system at a particular location. This western perimeter boundary crosses the Dry Creek and Cold Creek valleys, which are regarded as recharge areas. Boundary conditions defined at these locations in past models have usually been prescribed-flux (Cearlock et al. 1975). Rattlesnake Mountain also supplies recharge to the aquifer, particularly during the winter months. The estimated recharge from Rattlesnake Mountain has previously been included in the recharge assigned to Cold Creek and Dry Creek valleys (Jacobson and Freshley 1990). The defined flux should reflect actual recharge volumes. However, a lack of data on recharge has resulted in the flux across these boundaries being set by the model calibration process. In past two-dimensional flow models, flux at recharge areas along the western perimeter has been set at 9116 m^3/d for Cold Creek Valley and 1331 m^3/d for Dry Creek Valley (Cearlock et al. 1975; Jacobson and Freshley 1990). Jacobson and Freshley (1990) found that use of these values in an inverse calibration model resulted in unreasonably high heads in the vicinity of Cold Creek Valley. They achieved better results by defining the Cold Creek Valley as a prescribed-head boundary, which forces heads near the boundary to mimic the observed values. The flow system is more realistically represented by defining these boundaries as prescribed-flux. Elevated heads calculated by the model may indicate inaccuracies in the transmissivity distribution.

6.2 Top and Bottom of the Unconfined Aquifer System

The top of the unconfined aquifer is represented by the water-table surface and, therefore, is not fixed in space. The resulting variations in aquifer thickness must be handled by the numerical model. A prescribed-flux term may also be associated with the upper aquifer boundary to represent the input of water from natural or artificial recharge. Natural recharge on the Hanford Site is thought to vary from about 0 to 8 cm/yr depending on soil type and vegetation (Gee and Heller 1985; Bauer and Vaccaro 1990). As discussed in Thorne and Chamness (1992), the natural recharge distribution determined by Bauer and Vaccaro (1990) can be assumed for initial model runs. However, during the past 40 years, artificial recharge

from waste-water disposal operations has been much greater than natural recharge across the site and has had a greater impact on the ground-water flow system. Boundary conditions that account for the input of artificial recharge are discussed in the next report section.

The boundary condition for the bottom of the aquifer could be no-flow or prescribed-flux depending on whether leakage between the unconfined and confined aquifer systems is considered significant, as discussed in Thorne and Chamness (1992).

6.3 Boundary Conditions within the Flow System Boundaries

Other areas where boundary conditions must be defined include the following: 1) sources of artificial recharge, such as ponds and cribs; 2) points of discharge, such as production wells; and 3) "islands" within the flow system where relatively impermeable basalt rises above the water table. Whether a specific recharge or discharge boundary condition has a significant effect on results of the numerical model may depend on the objectives of the simulation. For example, pumping at Well 399-4-12 in the 300 Area, which supplies water to trout research ponds, has a negligible effect on most of the sitewide ground-water flow system. However, continuous water-level monitoring in the 300 Area has shown that pumping of this well affects water levels and ground-water flow directions within and around the 300 Area. Therefore, it would be important to accurately define the discharge boundary condition at this well if the model were being used to predict ground-water or contaminant movement in the 300 Area.

During the past 40 years, the volume of artificial recharge caused by waste water discharged to disposal facilities on the Hanford Site has been greater than natural recharge and has significantly affected the ground-water flow system. The volume of artificial recharge is currently decreasing (Dresel et al. 1993). However, it is expected to be significant for several more years. Artificial recharge can be represented by defining prescribed-flux boundary conditions at disposal facilities such as cribs and ponds. B Pond is currently the largest source of artificial recharge on the Hanford Site. However, until it was taken out of service, Gable Mountain Pond received a larger volume of discharge. Major ground-water mounds, which have affected sitewide flow patterns have occurred beneath B Pond, Gable Mountain Pond, and U Pond (Bierschenk 1959). U Pond and Gable Mountain Pond have been decommissioned and are now dry. Although a small volume of waste water has been discharged to a ditch near the U Pond, the ground-water mound in this area is declining (Dresel et al. 1993). Other smaller-volume recharge sources exist in the 100, 200, and 300 Areas and may affect ground-water flow on a local scale. These sources could be important in simulations of contaminant transport if they are near, or coincident with, contaminant sources.

The City of Richland infiltration ponds, agricultural and lawn irrigation, and ground disposal of waste water at a potato-processing plant are other sources of artificial recharge that may affect ground-water flow in the North Richland area and in the southern part of the Hanford Site (Liikala 1993). The City of Richland pumps water from the Columbia River into infiltration ponds to provide recharge for a well field used as a secondary source of water for the city. The volume of water pumped into the ponds is consistently higher than the amount removed from the surrounding well field. The resulting net recharge to the unconfined aquifer during the period June 1989 to May 1990 was estimated at 16,790 m^3/d (Liikala 1993). Agricultural irrigation on lands just south of the Hanford Site has increased in the past 5 years. Figure 6.3 shows the locations of irrigation circles in this area during the 1991 growing season. Most of the water applied to these fields comes from the Columbia River, where supply pumps are reported to have a combined capacity of 27,257 m^3/d (Liikala 1993). However, the actual volumes of irrigation water applied to the fields are unknown, and the net recharge after accounting for evaporation and crop use is expected to be a small percentage of the total applied volume. Approximately 1680 acres (6,800,000 m^2) are currently irrigated in this area. In order to make a rough approximation of the yearly recharge volume, it was estimated that 10% of the water applied to the fields recharged the aquifer and that 1.52 m/yr was applied. The resulting recharge volume is 1,036,320 m^3/yr, which is about 17% of the net recharge estimated for the Richland well field. This estimate should be regarded as an order-of-magnitude estimate because of the uncertainty in application rates and evapotranspiration.

Areas within the boundaries of the unconfined aquifer system where relatively impermeable basalt rises above the water table can generally be represented by no-flow boundaries. Aquifer recharge at these structures is small enough to be negligible. Gable Mountain and Gable Butte are the largest of these impermeable "islands" within the flow system. Smaller subcrops exist at the northern edge of the 200-East Area and to the east of Gable Mountain. Accurate definition of the extent these features may have a significant effect on the ground-water flow model.

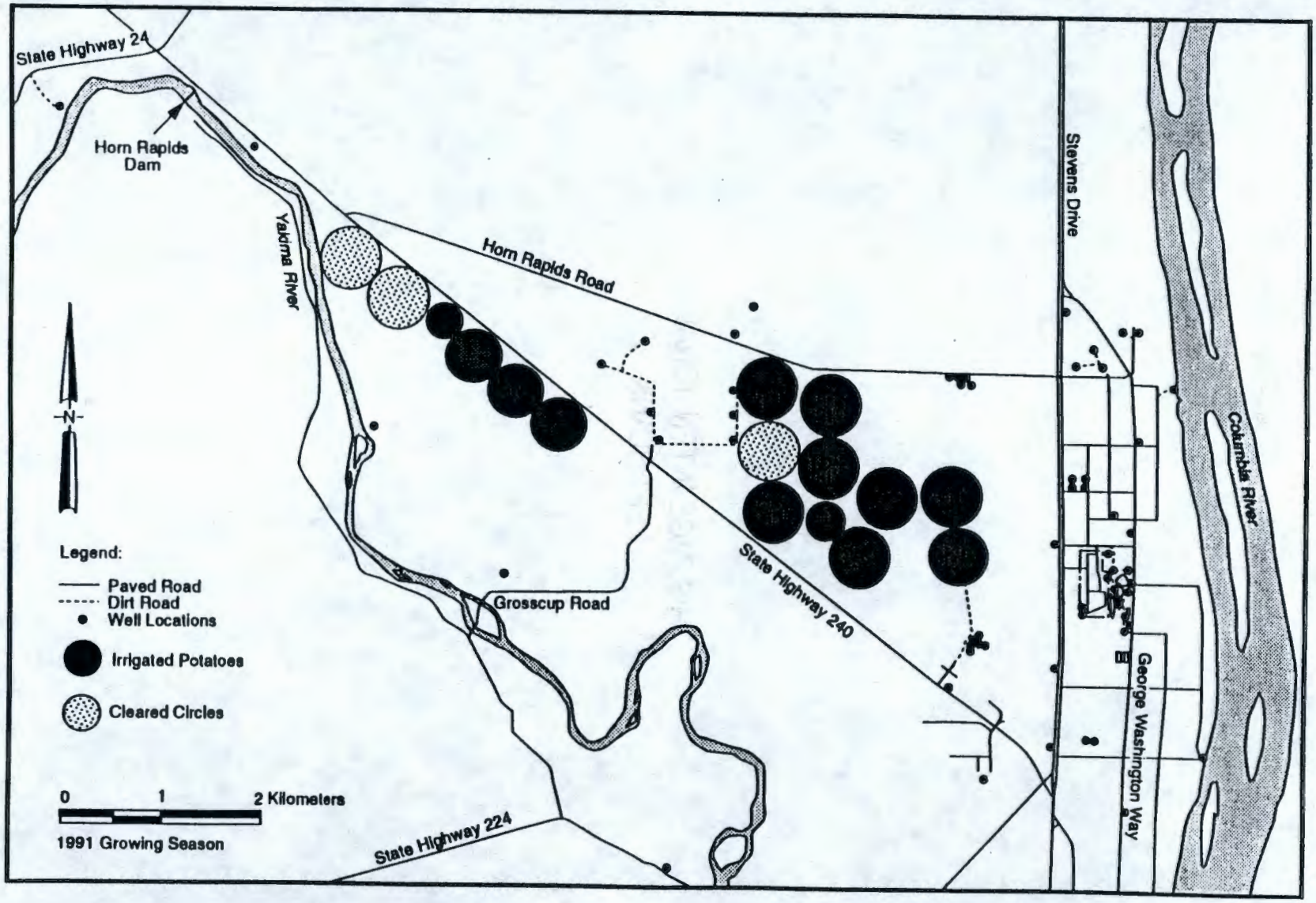

Figure 6.3. Irrigated Areas South of the Hanford Site (after Liikala 1993)

THIS PAGE INTENTIONALLY
LEFT BLANK

7.0 Hydraulic Heads

The hydraulic head distribution for the unconfined aquifer on the Hanford Site and the surrounding area is determined each year by measuring water levels at hundreds of wells. Results of the measurements made in 1992 are presented in Dresel et al. (1993). Additional water-level data for the North Richland area are provided in Liikala (1993). The annual water-level measurements provide an extensive data base that can be used to define initial head conditions for numerical modeling and for a comparison of modeling runs with historical data.

Most of the wells in the current unconfined aquifer monitoring network are completed in the upper part of the aquifer, within 7 m of the water table. Three-dimensional modeling will require more extensive information on the vertical distribution of hydraulic head. Therefore, clusters of individual wells completed at different depths and wells with individual piezometers open to different depth intervals are being identified. A preliminary list of these wells is given in Table 7.1. Additional well clusters exist in the 100, 200, 300, and 1100 Areas.

Additional information on hydraulic heads within deeper permeable units of the unconfined aquifer system, as well as hydraulic properties and hydrochemistry data, can be obtained by reconfiguration of some existing unused boreholes. Several relatively deep wells were drilled on the Hanford Site in 1979-1982 as part of the studies for a proposed Skagit-Hanford Power Plant (PSPL 1982). These wells are commonly known as "Golder" wells because Golder Associates, Inc., supervised the well installation. The Golder wells, many of which extend to basalt, have been used extensively in defining the hydrogeologic structure of the unconfined aquifer system. However, they generally have casing or liners to the bottom depth and do not have screens or perforations. In many cases, the liner has been damaged or the borehole is partially filled, and the integrity of the casing and/or liner is in doubt. The wells also do not meet minimum Washington State well-construction standards for surface seals. Reconfiguration and remediation of the wells are, therefore, required to obtain reliable data. Two of these wells, 699-18-21 and 699-31-11, were reconfigured during the past year. These two wells were selected for reconfiguration because they are located in areas where additional information on the vertical distribution of hydraulic properties, hydraulic heads, and contaminant concentrations is needed. They are also located along the travel path of the major contaminant plumes originating in the 200-East Area. Details concerning the reconfiguration of these wells are presented in Appendix C.

Table 7.1. Well Cluster Sites and Wells with Piezometers in the Unconfined Aquifer System

Well	Well Diameter (in.)	Original Interval (ft bls)	Current Interval 1 (ft bls)	Current Interval 2 (ft bls)	Current Interval 3 (ft bls)	Current Interval 4 (ft bls)	Current Interval 5 (ft bls)	Notes
699-S41-E13A	4	47-57						screen
699-S41-E13B	4	77-87						screen
699-S36-E12A	8	?						
699-S36-E12B	8	?						
699-S36-E13A	8	52-72						screen
699-S36-E13B	8	?						
699-S18-E2A	8	70-260	?	P 250-260				
699-S18-E2B	8	60-100						
699-S14-20A	8	89-159	93-138					screen, plug at 138
699-S14-20B	12	?						
699-S12-29	8	83-175	83-115?	Q 150-155	P 185-190			
699-2-33A	8	130-405	130-180					plug at 180
699-2-33B	8	?-450	?-170	Q 335-340	P 440-445			plug at 270
699-10-E12	8	60-340	Q 95-100	P 360-365				
699-14-38	8	110-409	110-165?	Q 175-180	P 415-420			annulus interval 110-165?
699-15-15A	8	140-635	140-190	P 205-218				plug at 190
699-15-15B	6	141-161						
699-17-26B	?	?	R 120-125	Q 156-161	P 268-288			condition unknown
699-17-26C	?	?	R 120-125	Q 155-160	P 186-189			condition unknown
699-19-26B	?	?	Q 131-136	P 189-194				condition unknown
699-20-E12	8	65-344	O 80-100	S 113-138	R 178-198	Q 228-253	P 320-345	P in basalt
699-20-39	8	130-632	130-490	P 608-618				plug at 490, P in basalt
699-24-1	?	?						P in basalt
699-25-33A	4	191-200						screen
699-25-33B	8	?	Q 188-193	P 215-220				screens
699-26-35A	5	120-140	120-140					
699-26-35C	4	193-203	193-203					
699-26-35D	8	?	Q 195-200	P 223-338				condition unknown
699-28-40	8	150-465	?	Q 340-350	P 452-462			annulus open 150-320? plug at 320
699-31-31	8	135-540	135-270	Q 360-370	P 590-600			plug at 270, P in basalt, seals ?
699-31-53A	12	301-423	228-340					plug at 340
699-31-53B	12	306-430	O 300-320	P 410-430				

Table 7.1. (contd)

Well	Well Diameter (in.)	Original Interval (ft bls)	Current Interval 1 (ft bls)	Current Interval 2 (ft bls)	Current Interval 3 (ft bls)	Current Interval 4 (ft bls)	Current Interval 5 (ft bls)	Notes
699-31-65	8	240-450	O 240-260	R 310-330	Q 370-390	P 410-430		condition unknown
699-32-62	8	275-500	275-340	Q 365-375	P 490-500			plug at 340
699-32-72	8	210-485	210-415	P 465-470				plug at 415
699-36-46	?	?	S 300-310	R 370-380	Q 400-450	P 510-520		separate wells, Q and P in basalt
699-37-82A	?	221-408						condition unknown
699-37-82B	8	163-590	O 165-185	S 230-250	R 310-330	Q 390-410	P 540-560	condition unknown
699-37-82C	8	165-279						condition unknown
699-37-82D	?	155-190						condition unknown
699-38-65	8	220-536	220-440	P 460-536				plug at 420-440
699-42-12A	8	120-320	120-180					plug at 180
699-42-12B	12	140-240						
699-42-12C	6	?						condition unknown
699-51-75	8	190-370	190-235	P 245-382				plug at 235-245
699-53-55A	8	160-455	165-270	P 310-455				perf. 160-190 & 255-275, P in basalt
699-54-37A	8	?	?-132					condition unknown
699-54-37?	6	?	?					condition unknown
699-55-50A	8	40-100	Q 64-78	P 96-98				condition unknown
699-55-50C	8	35-59	35-56					plug at 56
699-55-50D	8	33-90	33-90					
699-55-60A	12	190-230						
699-55-60B	24	230-285						
699-55-60C	?	?						
699-55-70	8	136-202	136-180	P 190-195				cement plug at 180
699-65-59A	8	100-125						
699-65-59B	12	100-190						
699-65-59C	6	100-140						
699-67-51	8	100-250	100-170	Q 184-194	P 230-235			plug at 170
699-69-45	8	80-300	O 153-178	R 153-178	Q 210-235	P 255-277		condition unknown
699-80-43	?	?	S 30-50	R 116-140	Q 212-230	P 437-447		
699-84-35	8	10-355	O 10 -?	S 127-153	R 191-217	Q 255-281	P 325-351	
699-96-49	8	28-96	28-60	P 70-96				plug at 60-70

NOTE: Original well logs use english units. To convert inches to centimeters, multiply by 2.54. To convert feet to meters, multiply by 0.3048.

THIS PAGE INTENTIONALLY
LEFT BLANK

8.0 Contaminant Distributions

Information on the distributions of contaminants within the unconfined aquifer is needed for setting initial conditions and for calibration of a numerical transport model. Contaminants also act as tracers that provide clues to the movement of ground water within the flow system.

The concentrations of both chemical and radiological contaminants are measured in hundreds of Hanford Site wells each year, and plume maps are constructed that show the contaminant distributions. Contaminant distributions measured during 1992 and information on sampling and analysis techniques are provided in Dresel et al. (1993). Like the hydraulic-head measurement network, the sampling network is composed mainly of wells completed in the upper part of the unconfined aquifer system, generally less than 7 m below the water table. A limited number of wells completed in the upper confined (interbasalt) aquifers are sampled each year (Evans et al. 1992).

Distributions of tritium, nitrate, and iodine-129 provide the most useful information concerning ground-water flow on a sitewide scale. All three of these contaminants were discharged to liquid waste disposal facilities in the 200 Areas and are mobile in ground water. Tritium replaces hydrogen in a water molecule and moves at the same rate as water through the aquifer. However, tritium has a relatively short half-life (12.3 yr) and eventually becomes undetectable. This trait limits its usefulness as a tracer in the deeper aquifer system where concentrations are lower and ground water moves more slowly. Nitrate and iodine-129 are also very mobile under the ground-water chemistry conditions at the Hanford Site. The nitrate distribution is similar, but not identical, to the tritium distribution (Dresel et al. 1993). The variations reflect differences in sources and the radioactive decay that affects tritium. Offsite agricultural sources of nitrate in the Cold Creek Valley to the west of the Hanford Site have impacted ground water on the site (Evans et al. 1992). There is also a potential for natural sources or pre-Hanford agricultural sources of nitrate to exist on the site. These other sources may complicate the interpretation of nitrate distribution on the Hanford Site. Iodine-129 has a long half-life (16 million years) that makes it of particular concern as a contaminant. It has a distribution in the upper unconfined aquifer similar to that of tritium (Dresel et al. 1993). Iodine-129 has been found in the upper confined aquifer system (Evans et al. 1992) and may prove to be useful as a tracer for vertical movement of ground water in the unconfined aquifer. However, the analyses required for detecting activity concentrations less than 1 pCi/L are difficult and expensive to perform.

Eddy et al. (1978) investigated the vertical distribution of contaminants in the unconfined aquifer and found that contaminant concentrations were highest near the top of the aquifer.

This finding was attributed, in part, to an upward hydraulic gradient. Relatively low vertical permeability may also limit the downward migration of contaminants. Following the investigation of Eddy et al. (1978), many of the sitewide sampling network wells were reconfigured so they were open to only the upper part of the aquifer, less than 7 m below the water table. Remediation of the wells improved contaminant monitoring because water containing the highest concentrations was sampled and dilution with relatively uncontaminated water from deeper in the aquifer was avoided. Remediation of the sampling wells also eliminated the potential for enhanced vertical migration of contaminants through the well casing.

Relatively few of the wells on the Hanford Site are currently open to the deeper parts of the unconfined aquifer system. Some of these are listed in the compilation of well cluster sites and piezometer wells (Table 7.1). Sampling of these and other wells in the deeper unconfined aquifer will provide additional information on the vertical distribution of contaminants. The unused Golder wells are also potentially useful for hydrochemical characterization. However, reconfiguration of the wells is required to gain access to hydrostratigraphic intervals that are of interest. Appendix C contains details on the reconfiguration of two of these wells, 699-18-21 and 699-31-11, conducted during the past year. Locations of these wells and the concentration contours for tritium and iodine-129 plumes in the upper unconfined aquifer are shown in Figures 8.1 and 8.2, respectively.

Samples were collected from one of the reconfigured Golder wells, 699-31-11, and were analyzed for tritium and iodine-129. Development pumping and sampling have not yet been conducted at well 699-18-21. The results at well 699-31-11, which is open to a depth interval 19.2 to 26.3 m below the current water table, were about 180,000 pCi/L for tritium and 2 pCi/L for iodine-129. These concentrations are approximately the same as those found in nearby sampling network wells completed at the top of the aquifer (see Figures 8.1 and 8.2). Well 31-11 is completed at the top of Unit 5, an areally extensive muddy sand and gravel unit, and just below Unit 4, a mud unit that is about 12 m thick at this well. Nearby sampling network wells are completed in the Hanford formation (Unit 1) directly overlying Unit 4. The sampling results show that these contaminants are evenly distributed in the upper 50 m of the unconfined aquifer system, which has a total thickness of about 130 m at this location.

One objective of the sampling was to determine if contaminated water could migrate vertically downward along the existing well casing during pumping, resulting in false indications of contaminants at depth. Therefore, samples for tritium were taken three times during development pumping. A plot of the tritium results in relation to pumped volume is shown in Figure 8.3. An increasing trend would indicate the possibility of vertical leakage along the casing. The results, however, indicated a slight decline in tritium concentration.

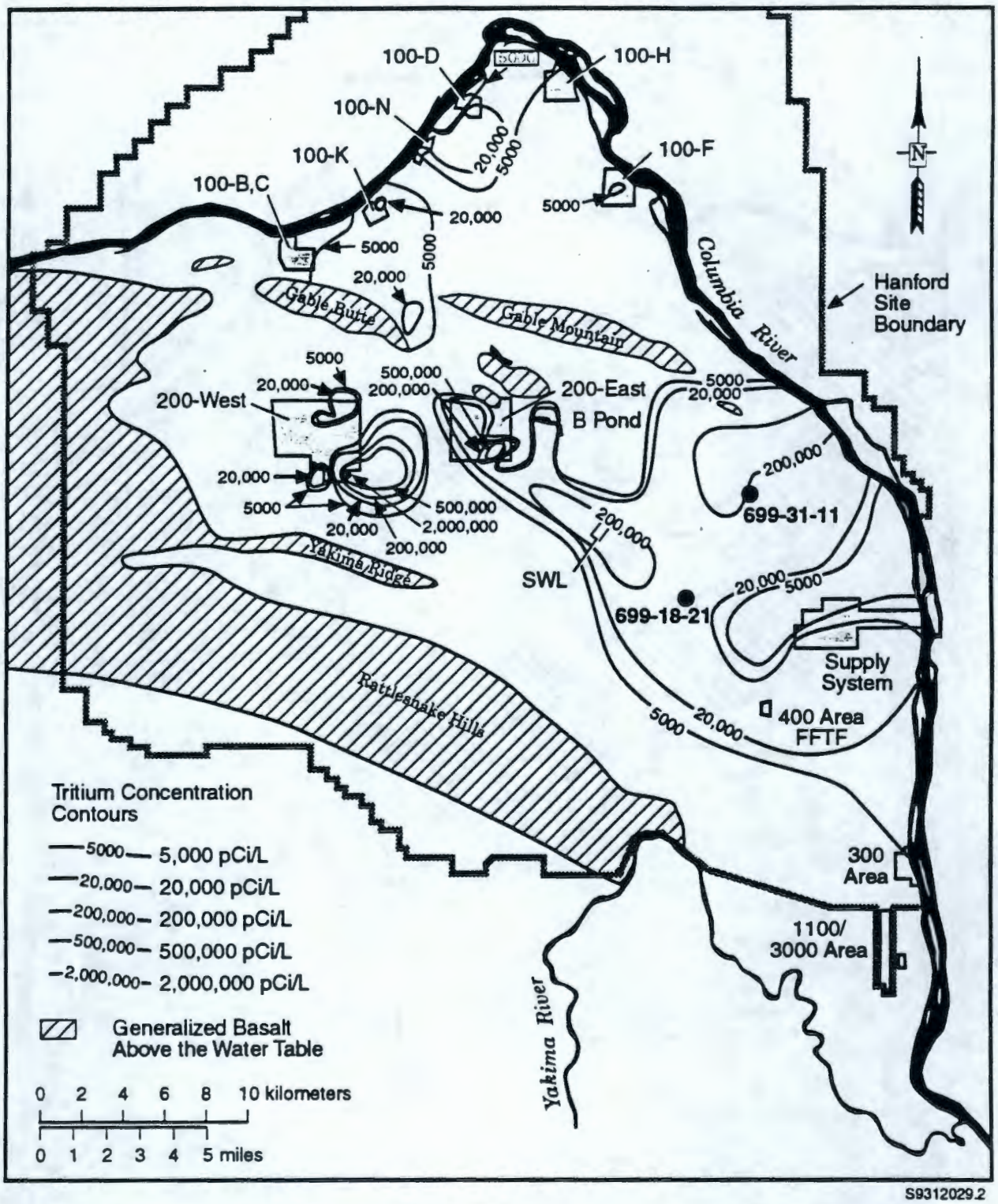

Figure 8.1. Locations of Two Reconfigured Golder Wells and Tritium Concentration Contours for the Upper Unconfined Aquifer in 1992 (modified from Woodruff et al. 1993)

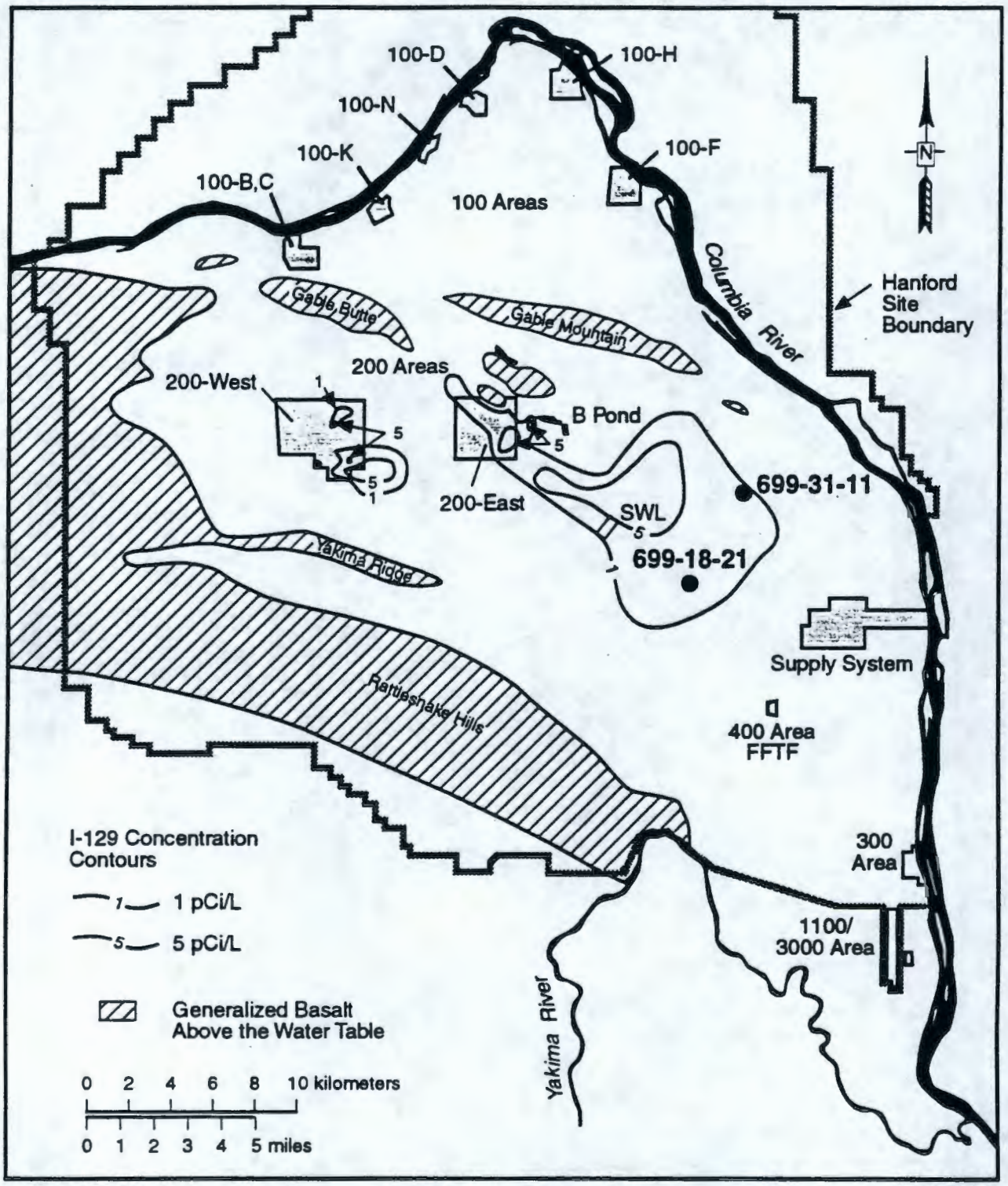

Figure 8.2. Locations of Two Reconfigured Golder Wells and Iodine-129 Concentration Contours for the Upper Unconfined Aquifer in 1992 (modified from Woodruff et al. 1993)

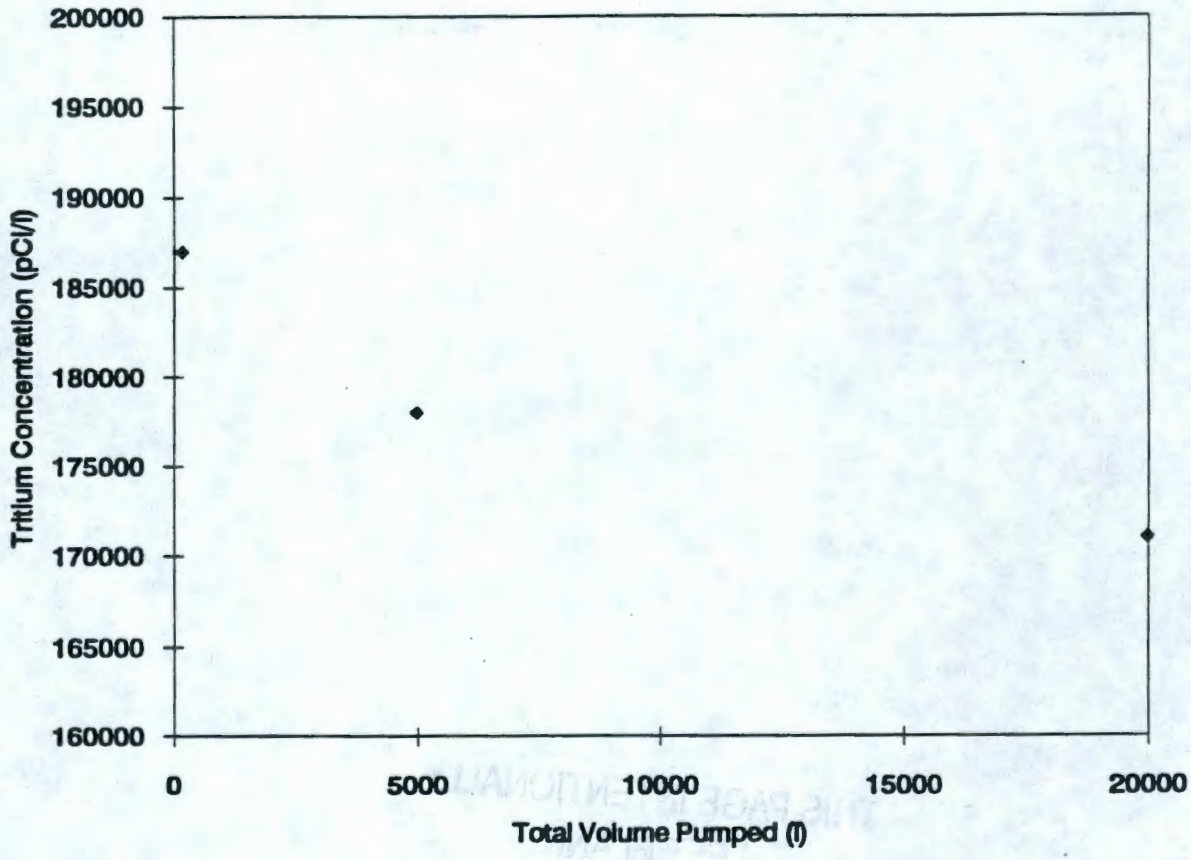

Figure 8.3. Tritium Concentration Trend During Development Pumping of the Reconfigured Golder Well 699-31-11

Although the decrease was less than the potential error in the tritium analyses, vertical migration of contaminants along the casing during pumping is not indicated.

Examination of the hydrogeologic structure shows that Unit 4 extends over a large area between 200-East Area and the Columbia River. However, Unit 4 is not found directly beneath the 200-East Area, where the contaminant plumes originate. It is, therefore, not surprising that contaminants are found below this unit. The ground-water mound in the vicinity of B Pond also may create a downward gradient, causing vertical mixing of contaminants.

THIS PAGE INTENTIONALLY
LEFT BLANK

9.0 References

Bauer, H. H., and J. J. Vaccaro. 1990. *Estimates of Ground-Water Recharge to the Columbia Plateau Regional Aquifer System, Washington, Oregon, and Idaho for Predevelopment and Current Land Use Conditions*. Water Resources Investigation Report 88-4108, U.S. Geological Survey, Tacoma, Washington.

Bauer, H. H., J. J. Vaccaro, and R. C. Lane. 1985. *Maps Showing Ground-Water Levels in the Columbia River Basalt and Overlying Materials, Spring 1983, Southeastern Washington*. Water Resources Investigation Report 84-4360, U.S. Geological Survey, Tacoma, Washington.

Bierschenk, W. H. 1959. *Aquifer Characteristics and Ground-Water Movement at Hanford*. HW-60601, General Electric Company, Hanford Atomic Products Operation, Richland, Washington.

Bjornstad, B. N. 1984. *Suprabasalt Stratigraphy Within and Adjacent to the Reference Repository Location*. SD-BWI-DP-039, Rockwell Hanford Operations, Richland, Washington.

Bourdet, D., J. A. Ayoub, and Y. M. Pirard. 1989. "Use of Pressure Derivative in Well Test Interpretation." *SPE Formation Evaluation* (June 1989), pp. 293-302.

Cearlock, D. B., K. L. Kipp, and D. R. Friedrichs. 1975. *The Transmissivity Iterative Calculation Routine - Theory and Numerical Implementation*. BNWL-1706, Pacific Northwest Laboratory, Richland, Washington.

Davis, S. N. 1969. "Porosity and Permeability of Natural Materials." In *Flow Through Porous Media*, ed. R.J.M. DeWiest, pp. 54-89. Academic Press, New York.

Deju, R. A. 1974. *The Hanford Field Testing Program*. ARHC-00004-201, Atlantic Richfield Hanford Company, Richland, Washington.

DOE (see U.S. Department of Energy)

Dresel, P. E., D. R. Newcomer, J. C. Evans, W. D. Webber, F. A. Spane, Jr., R. G. Raymond, and B. E. Opitz. 1993. *Hanford Site Ground-Water Monitoring for 1992*. PNL-8716, Pacific Northwest Laboratory, Richland, Washington.

Eddy, P. A., D. A. Myers, and J. R. Raymond. 1978. *Vertical Contamination in the Unconfined Ground Water at the Hanford Site, Washington*. PNL-2724, Pacific Northwest Laboratory, Richland, Washington.

Evans, J. C., D. I. Dennison, R. W. Bryce, P. J. Mitchell, D. R. Sherwood, K. M. Krupka, N. W. Hinman, E. A. Jacobson, and M. D. Freshley. 1988. *Hanford Site Ground-Water Monitoring for July Through December 1989*. PNL-6315, Vol. 2, Pacific Northwest Laboratory, Richland, Washington.

Evans, J. C., R. W. Bryce, and D. J. Bates. 1992. *Hanford Site Ground-Water Monitoring for 1991*. PNL-8284, Pacific Northwest Laboratory, Richland, Washington.

Freshley, M. D., and P. D. Thorne. 1992. *Ground-Water Contribution to Dose from Past Hanford Operations*. PNWD-1974 HEDR, Battelle, Pacific Northwest Laboratories, Richland, Washington.

Gee, G. W., and P. R. Heller. 1985. *Unsaturated Water Flow at the Hanford Site: A Review of Literature and Annotated Bibliography*. PNL-5428, Pacific Northwest Laboratory, Richland, Washington.

Graham, M. J., G. V. Last, and K. R. Fecht. 1984. *An Assessment of Aquifer Intercommunication in the B Pond, Gable Mountain Pond Area*. RHO-RE-ST-12P, Rockwell Hanford Operations, Richland, Washington.

Jacobson, E. A., and M. D. Freshley. 1990. *An Initial Inverse Calibration of the Ground-Water Flow Model for the Hanford Unconfined Aquifer*. PNL-7144, Pacific Northwest Laboratory, Richland, Washington.

Kipp, K. L., and R. D. Mudd. 1973. *Collection and Analysis of Pump Test Data for Transmissivity Values*. BNWL-1709, Pacific Northwest Laboratory, Richland, Washington.

Liikala, T. L. 1993. *Hydrogeology Along the Southern Boundary of the Hanford Site Between the Yakima and Columbia Rivers, Washington*. Unpublished M.S. Thesis, Washington State University, Pullman, Washington.

Lindsey, K. A. 1991. *Revised Stratigraphy for the Ringold Formation, Hanford Site, South-Central Washington*. WHC-SD-EN-EE-004, Westinghouse Hanford Company, Richland, Washington.

Lindsey, K. A., B. N. Bjornstad, J. W. Lindberg, and K. M. Hoffman. 1992. *Geologic Setting of the 200-East Area: An Update*. WHC-SD-EN-TI-012, Westinghouse Hanford Company, Richland, Washington.

McGhan, V. L. 1989. *Hanford Wells*. PNL-6907, Pacific Northwest Laboratory, Richland, Washington.

Myers, C. W., and S. M. Price. 1979. *Geological Studies of the Columbia Plateau - A Status Report*. RHO-BWI-ST-4, Rockwell Hanford Operations, Richland, Washington.

Newcomb, R. C. 1958. "Ringold Formation of Pleistocene Age in Type Locality, The White Bluffs, Washington." *American Journal of Science* 256:328-340.

Newcomb, R. C., J. R. Strand, and F. J. Frank. 1972. *Geology and Ground-Water Characteristics of the Hanford Reservation of the U.S. Atomic Energy Commission, Washington*. Prof. Paper 717, U.S. Geological Survey, Washington, D.C.

Puget Sound Power and Light (PSPL). 1982. *Skagit/Hanford Nuclear Project, Preliminary Safety Analysis Report*. Appendix 20, Amendment 23, Puget Sound Power and Light Company, Bellevue, Washington.

Reidel, S. P., K. A. Lindsey, and K. R. Fecht. 1992. *Field Trip Guide to the Hanford Site*. WHC-MR-0391, Westinghouse Hanford Company, Richland, Washington.

Spane, F. A., Jr. 1987. *Fresh-Water Potentiometric Map and Inferred Flow Direction of Ground Water Within the Mabton Interbed, Hanford Site, Washington State - January 1987*. SD-BWI-TI-335, Rockwell Hanford Operations, Richland, Washington.

Spane, F. A., Jr. 1993. *Selected Hydraulic Test Analysis Techniques for Constant-Rate Discharge Tests*. PNL-8539, Pacific Northwest Laboratory, Richland, Washington.

Swanson, L. C. 1992. *Phase 1 Hydrogeologic Summary of the 300-FF-5 Operable Unit, 300 Area*. WHC-SD-EN-TI-052, Westinghouse Hanford Company, Richland, Washington.

Tallman, A. M., K. R. Fecht, M. C. Marratt, and G. V. Last. 1979. *Geology of the Separations Areas, Hanford Site, South-Central Washington*. RHO-ST-23, Rockwell Hanford Operations, Richland, Washington.

Thorne, P. D., and M. A. Chamness. 1992. *Status Report on the Development of a Three-Dimensional Conceptual Model for the Hanford Site Unconfined Aquifer System*. PNL-8332, Pacific Northwest Laboratory, Richland, Washington.

Thorne, P. D., and D. R. Newcomer. 1992. *Summary and Evaluation of Available Hydraulic Property Data for the Hanford Site Unconfined Aquifer System*. PNL-8337, Pacific Northwest Laboratory, Richland, Washington.

U.S. Department of Energy (DOE). 1988. *Consultation Draft, Site Characterization Plan, Reference Repository Location, Hanford Site, Washington*. DOE/RW-0164, Vol. 1 and 2, U.S. Department of Energy, Richland, Washington.

Weekes, D. C., S. P. Luttrell, and M. R. Fuchs. 1987. *Interim Hydrogeologic Characterization Report and Groundwater Monitoring System for the Nonradioactive Dangerous Waste Landfill, Hanford Site, Washington.* WHC-EP-0021, Westinghouse Hanford Company, Richland, Washington.

Woodruff, R. K., R. W. Hanf, and R. E. Lundgren, eds. 1993. *Hanford Site Environmental Report for Calendar Year 1992.* PNL-8682, Pacific Northwest Laboratory, Richland, Washington.

Appendix A

Analysis of a Constant-Rate Pumping Test Monitored with a Westbay Multiport Monitoring System

THIS PAGE INTENTIONALLY
LEFT BLANK

Appendix A

Analysis of a Constant-Rate Pumping Test Monitored with a Westbay Multiport Monitoring System

A series of hydraulic tests were conducted at a well cluster site near B Pond that included a well equipped with a Westbay Instruments, Inc., multiport monitoring system. The tests included slug-interference tests, sinusoidal-pulse tests, and a constant-rate pumping test. The main objective of the tests was to determine hydraulic properties including both horizontal and vertical hydraulic conductivity, storativity and specific yield of the unconfined aquifer. A secondary objective was to evaluate slug-interference and sinusoidal-pulse tests for measuring these parameters.

Analysis of the constant-rate pumping test conducted at the cluster site is presented in this appendix. Slug-interference and sinusoidal-pulse test analyses are ongoing and will be presented in a later report. Analysis of these tests is not expected to change the results presented in this report for the constant-rate discharge test.

Test Site and Test Equipment

The tests were conducted at a cluster of three wells located near B Pond in the central part of the Hanford Site. Well 699-42-42B was the stress well and responses were monitored at wells 699-43-42J and 699-43-42K. The approximate distances between the wells are shown in Figure A.1. Depth to water at the test site under static hydraulic conditions was approximately 49 m below land surface (bls). Construction as-built diagrams for each of the wells are presented in Figure A.2. Well 699-42-42B, the stress well, is screened with a 4-in. ID, 10-slot stainless steel screen between the depths of 59 and 62 m bls and is cased to the surface with 4-in. ID stainless steel casing. Well 699-43-42J is screened with a 4-in. ID, 5-slot stainless steel screen between the depths of 48 and 54 m bls and is cased to the surface with 4-in. ID stainless steel casing.

The Westbay multiport system at well 699-43-42K is constructed of 1.5-in. ID PVC pipe installed in a 10-in. borehole (Gilmore 1989). It has four operable pressure monitoring ports located at depths of 49, 53, 57, and 61 m bls. Four additional ports, located at greater depths, can not be accessed because of a bend in the casing.

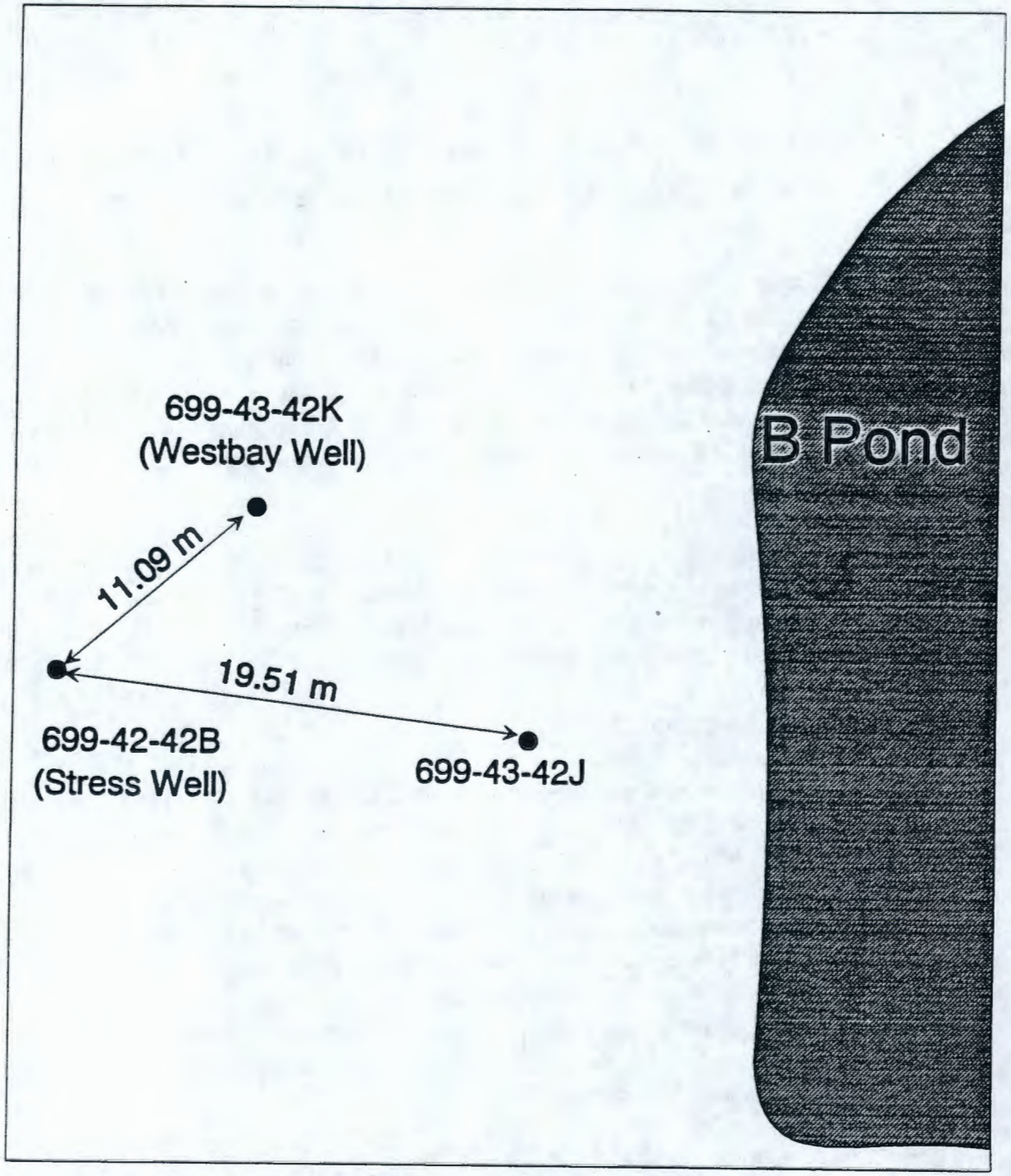

Figure A.1. Distances Between Pumping and Observation Wells at the Constant-Rate Discharge Test Site

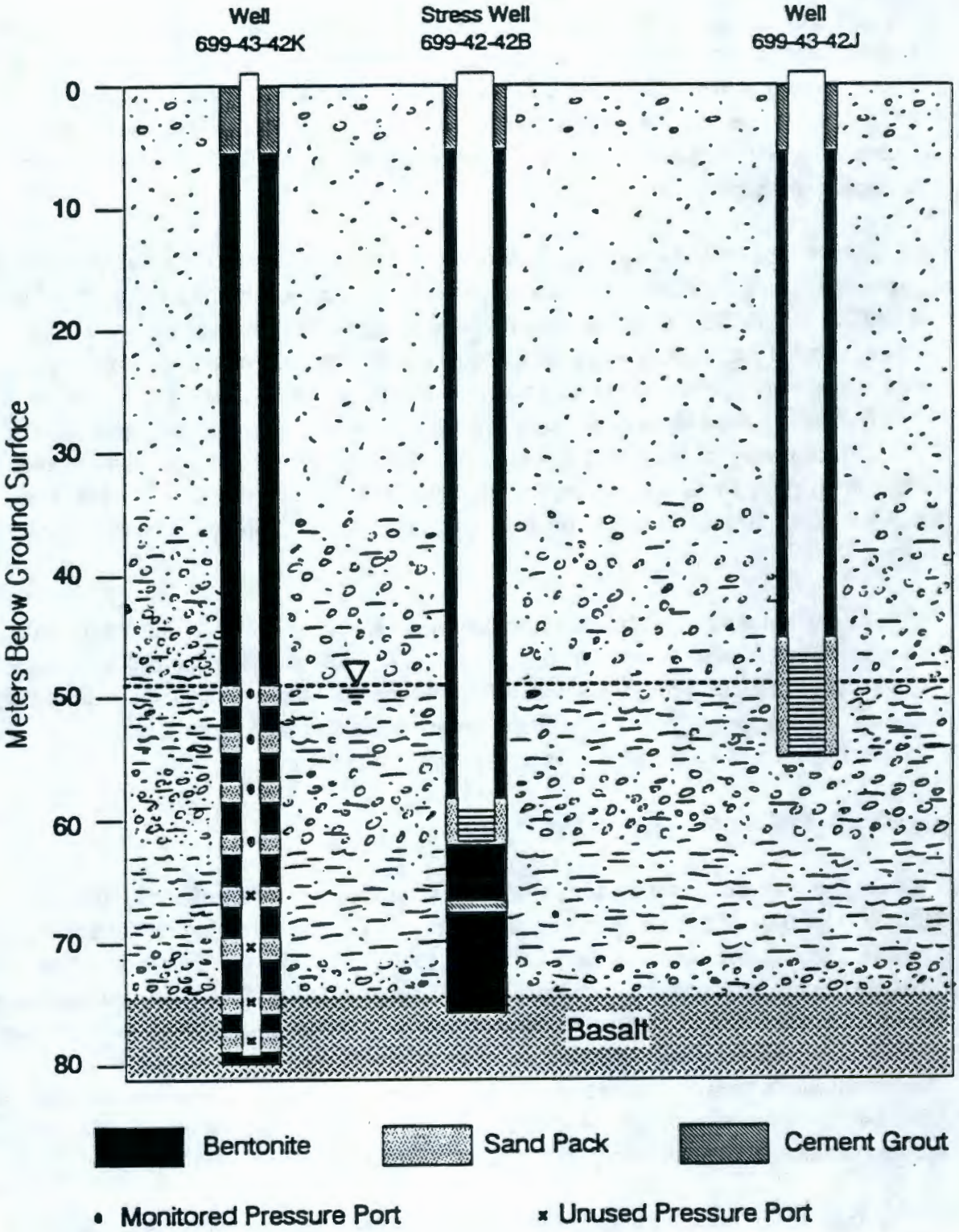

Figure A.2. As-Built Diagrams of Wells 699-42-42B, 699-43-42J, and 699-43-42K

However, this problem did not adversely affect the testing. Each port provides access to a discrete depth interval where the annular space between the borehole wall and the Westbay casing is filled with size 20-40 sand. The sand pack intervals are approximately 2 m long and are isolated with bentonite annular seals. A probe can be lowered from the surface and connected to any Westbay system port for measurement of hydraulic pressure, or for collection of samples.

For the tests, Westbay provided a Modular Subsurface Data Acquisition (MOSDAX) system with the capability of monitoring pressure simultaneously at all the ports in Well 699-43-42K. The MOSDAX system consisted of a string of four pressure probes that were attached to the four upper ports in the Westbay well. Pressure data measured by the downhole probes were multiplexed and transmitted to a surface computer over a single-conductor wireline cable. An additional Westbay pressure probe was placed in the pumping well and was also connected to the MOSDAX system. A separate pressure transducer and data acquisition system was used to monitor the water level in Well 699-43-42J. This consisted of a Druck, Inc., 10-psi (68.9 kPa) pressure transducer and a Campbell Scientific, Inc., data logger.

The configuration of equipment installed in the stress well (699-42-42B) during the constant-rate discharge test is shown in Figure A.3. Flow rate was controlled with a gate valve and continuously measured with a "Paddlewheel Flosensor" manufactured by Signet Scientific Company. Flow rate readings were periodically checked by measuring the time required to fill a 19-L (5-gal) bucket to a known volume mark.

Description of Tests

The constant-rate pumping test, with associated recovery measurements, was the primary test conducted to determine hydraulic properties. In addition, slug-interference tests and sinusoidal-pulse tests were conducted to evaluate these methods for use in unconfined aquifers. The slug-interference test involves conducting a slug test in the stress well and monitoring pressure responses in one or more observation wells. The sinusoidal-pulse test is conducted by repeatedly applying and releasing a stress to the well for equal time intervals. Superposition of the responses to each pulse creates a trend in the pressure peaks and troughs that can be analyzed to determine hydraulic properties. For this report, only the analysis and results of the constant-rate pumping test are presented.

During the drawdown phase of the constant-rate pumping test, Well 699-42-42B was pumped at a constant rate of approximately 18.5 L/min for 24 h. Drawdown responses were measured in each of the four zones at well 699-43-42K using the MOSDAX

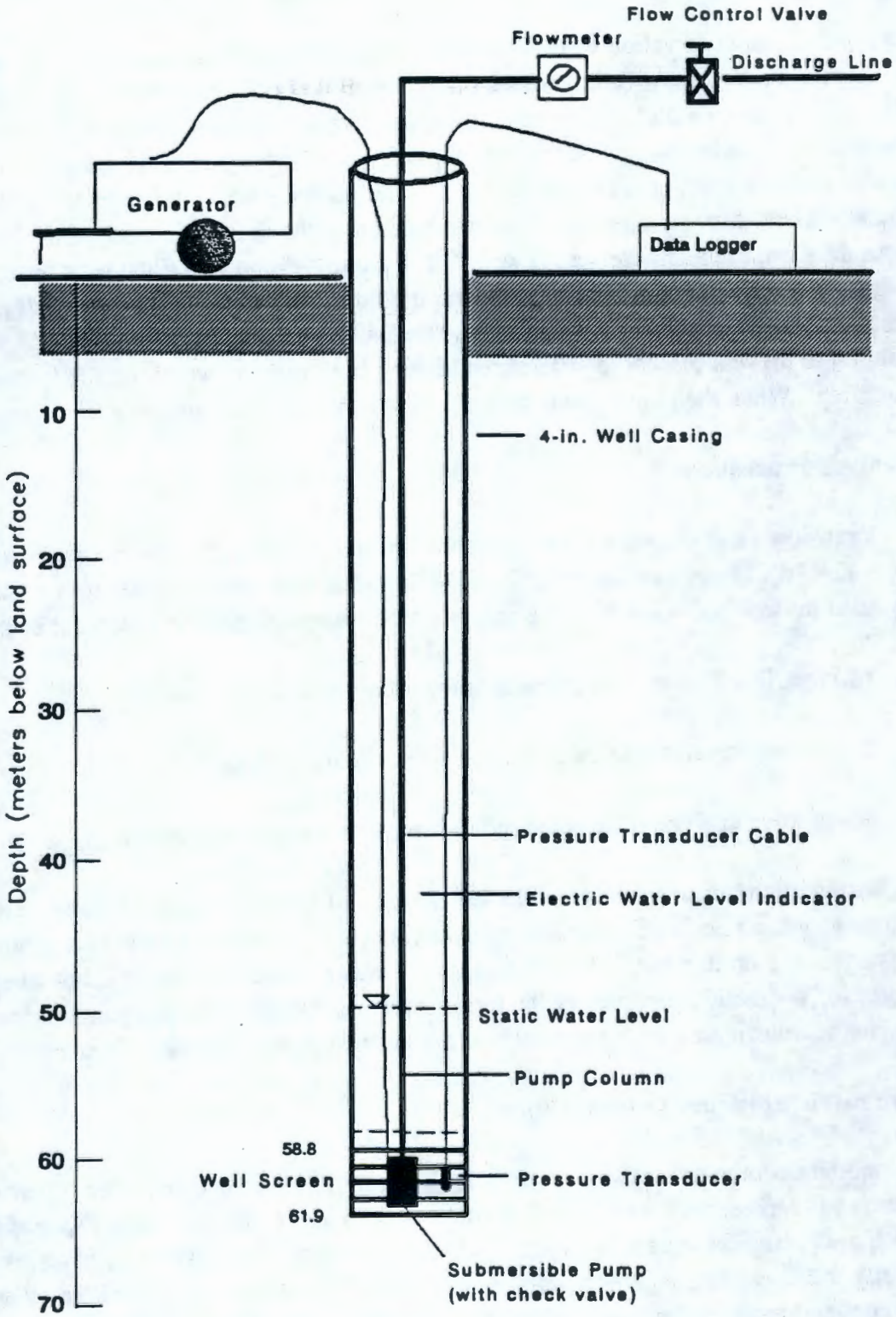

Figure A.3. Equipment Configuration at Pumping Well 699-42-42B During the Constant-Rate Discharge Test

system, and in observation well 699-43-42J using a pressure transducer. Drawdown was also monitored in the stress well to ensure that the well was not dewatered to the pump intake. Figure A.4 shows a plot of flow rate and drawdown measured at the pumping well. The flow rate had to be adjusted several times in the early part of the pumping period (<30 min) to obtain the maximum possible drawdown without allowing the water level to reach the pump intake. These flow-rate perturbations can be seen in the drawdown early drawdown data at both the pumping and observation wells. The pump column was filled with water before beginning the test to eliminate a high pumping rate at the start of pumping. All joints in the discharge column pipe were sealed and a check-valve was used at the bottom of the pump column to prevent discharge water from leaking back into the well after the termination of pumping. When the pump was turned off, recovery was monitored in each of the wells.

Analysis Procedures

Drawdown and recovery data were collected during the test at the pumped well (699-42-42B), at observation well 699-43-42J, and at four Westbay monitoring zones within observation well 699-43-42K. The analysis procedure included the following elements:

1. barometric efficiency determinations for each monitoring location

2. composite drawdown analysis for multiple monitoring locations

3. quantitative analysis of selected individual monitoring locations.

Barometric efficiencies were evaluated for each of the monitoring locations and were used to remove atmospheric effects from test data collected during and immediately following the constant-rate pumping test. Composite analysis was utilized to obtain qualitative estimate ranges for hydraulic properties of the tested interval. Detailed test analysis was performed for selected monitoring zones for quantitative determination of hydraulic properties.

Barometric Efficiency Determination

Aquifers commonly respond to variations in atmospheric pressure. These barometric fluctuations represent an areal, blanket stress applied at the land surface. The manner in which a well/aquifer system responds to changes in atmospheric pressure, however, is related directly to the existing aquifer conditions (i.e., whether the aquifer is confined or unconfined). For confined aquifers the transmission of atmospheric pressure effect is instantaneous, with the magnitude of formation pressure change at any particular locality being a function of the degree of aquifer confinement, rigidity of the aquifer matrix, and the specific weight of

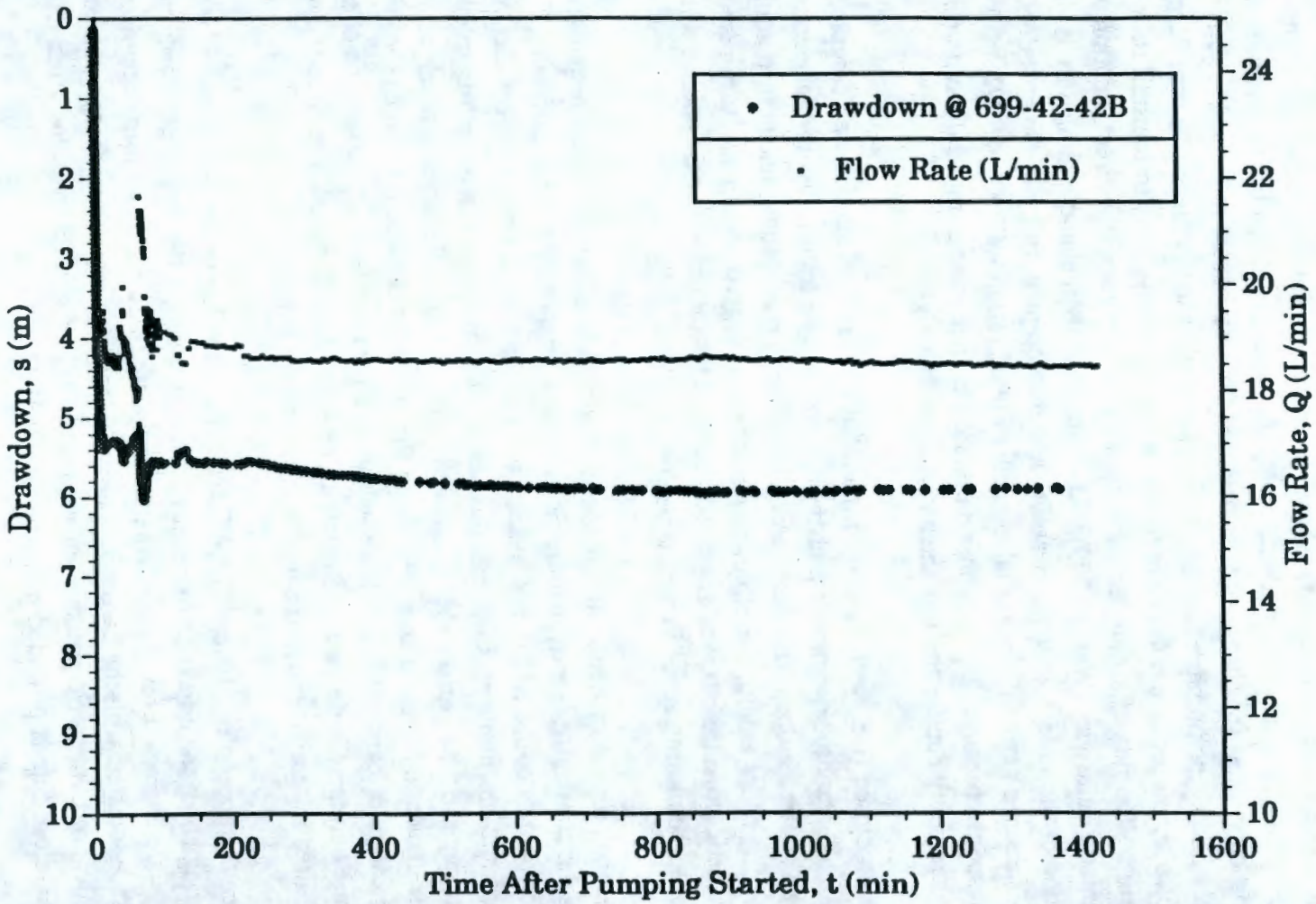

Figure A.4. Discharge Rate and Drawdown Measured at Pumping Well 699-42-42B

ground water. For unconfined aquifers different mechanisms are involved. As noted by Weeks (1979), unconfined aquifer response to barometric fluctuations is a function of the aquifer's depth below land surface, and the vertical pneumatic diffusivity of the overlying vadose zone. For an open, unconfined aquifer well completed below the water table, atmospheric pressure changes are transmitted instantaneously to the water surface within the well, whereas the pressure change at the water-table surface displays a time-lagged response because air must move into or out of the overlying vadose zone to transmit the change in pressure. The rate of air movement within the vadose zone is a direct function of its vertical pneumatic diffusivity (Weeks 1979). The vadose zone pneumatic diffusivity is, in turn, a function of the vadose zone permeability and the compressibility of the contained gas. Open wells screened across the water table, such as observation well 699-43-42J, may not display this response because the atmospheric pressure change is transmitted directly to the surface of the surrounding aquifer through the air in the well casing.

For a closed (i.e., with a packer installation) unconfined aquifer well completed below the water table, atmospheric pressure changes would not be transmitted instantaneously to water in the well as for the open well case. For a closed well completion, unconfined aquifer monitoring zones would, therefore, display the time-lagged aquifer pressure response to atmospheric pressure changes described above. This closed-well case applies to the Westbay multiport monitoring zones in well 699-43-43K.

For the purpose of removing extraneous barometric effects from test responses monitored during the constant-rate test, barometric efficiency relationships were calculated from baseline monitoring data collected prior to the initiation of the test. Baseline atmospheric pressure readings and downhole pressure measurements were recorded at a recording frequency of 30 min, during the time period May 28 through June 1, 1993. Barometric efficiencies for each monitoring location were determined using the method described by Clark (1967) for determination of barometric efficiency within confined aquifers. To assess the effects of time lag in the barometric efficiency calculation, pressure data observed at each monitoring location were shifted in time to match the barometric pressure pattern.

Once the appropriate barometric efficiency and time lag values were determined for each monitoring zone, the effects of barometric pressure changes that occurred during the course of the test were corrected for by removing the calculated water-level or formation pressure response associated with the barometric pressure change from the test data. An example of the removal of barometric pressure effects from confined aquifer hydrologic test data for wells on the Hanford Site is provided in Spane (1992; 1993).

Figure A.5 shows a comparison of atmospheric pressure fluctuations and associated pressure responses recorded in monitoring zones 2 and 4 at well 699-43-42K and in well 699-43-42J. Table A.1 provides a summary of the barometric efficiency and time-lag results for the pumping well and monitoring locations. For the pumping well (699-42-42B) and multiple monitoring zones at well 699-43-42K, closed well completion conditions existed. For observation well 699-43-42J, an open well completion is indicated. However, for this monitoring location, the well screen extends above the water table, enabling atmospheric pressure changes to be transmitted directly to the water table via the open well. For this reason, a barometric efficiency relationship was not calculated for monitoring well 699-43-42J.

As shown in Table A.1, barometric efficiencies ranging between 0.2 and 0.35, for time lags ranging between approximately 15 to 17 min, and between 0.24 and 0.29 for time lags ranging between 1.75 and 2.75 hr were calculated. The cause of the apparent high correlations for both short-period (i.e., 15 to 17 min) and longer-period (i.e, 1.75 to 2.75 hr) time lags is not readily apparent. Weeks (1979), however, notes that in addition to barometric fluctuations other daily cyclical stresses (earth tides) can also affect aquifer pressure response. The apparent multiple time-lag correlations may be attributed to these various external stresses. An extended base-line period, with higher recording frequencies (e.g., 10 min), would be required to establish cause and effect relationships of the various external stress factors.

Since the objective of the barometric efficiency analysis is to remove of extraneous stress components from the test records, (and not for quantitative hydraulic property analysis) monitored test responses were corrected for barometric effects using the barometric efficiencies associated with the short-period time lags. It should also be noted that Monitor Zone 1 at well 699-43-42K exhibited no similar high barometric efficiency correlation for a long-period time lag. The cause for this divergence from the behavior observed at other zones is not readily apparent. However, it should be noted that the Monitor Zone 1 monitoring interval encompasses the water-table surface, and is not fully saturated. Capillary effects within the monitoring zone, therefore, may be responsible for the divergent behavior.

Multiple-Well Composite Analysis

To obtain preliminary, qualitative estimate ranges for hydraulic properties, drawdown data recorded during the constant-rate pumping test for Monitoring Zones 1 through 4 at well 699-43-42K and for well 699-43-42J were analyzed compositely. The composite diagnostic analysis involved collectively matching the drawdown responses observed at each of the monitoring wells, with predicted drawdown responses for various anisotropy values (i.e.,

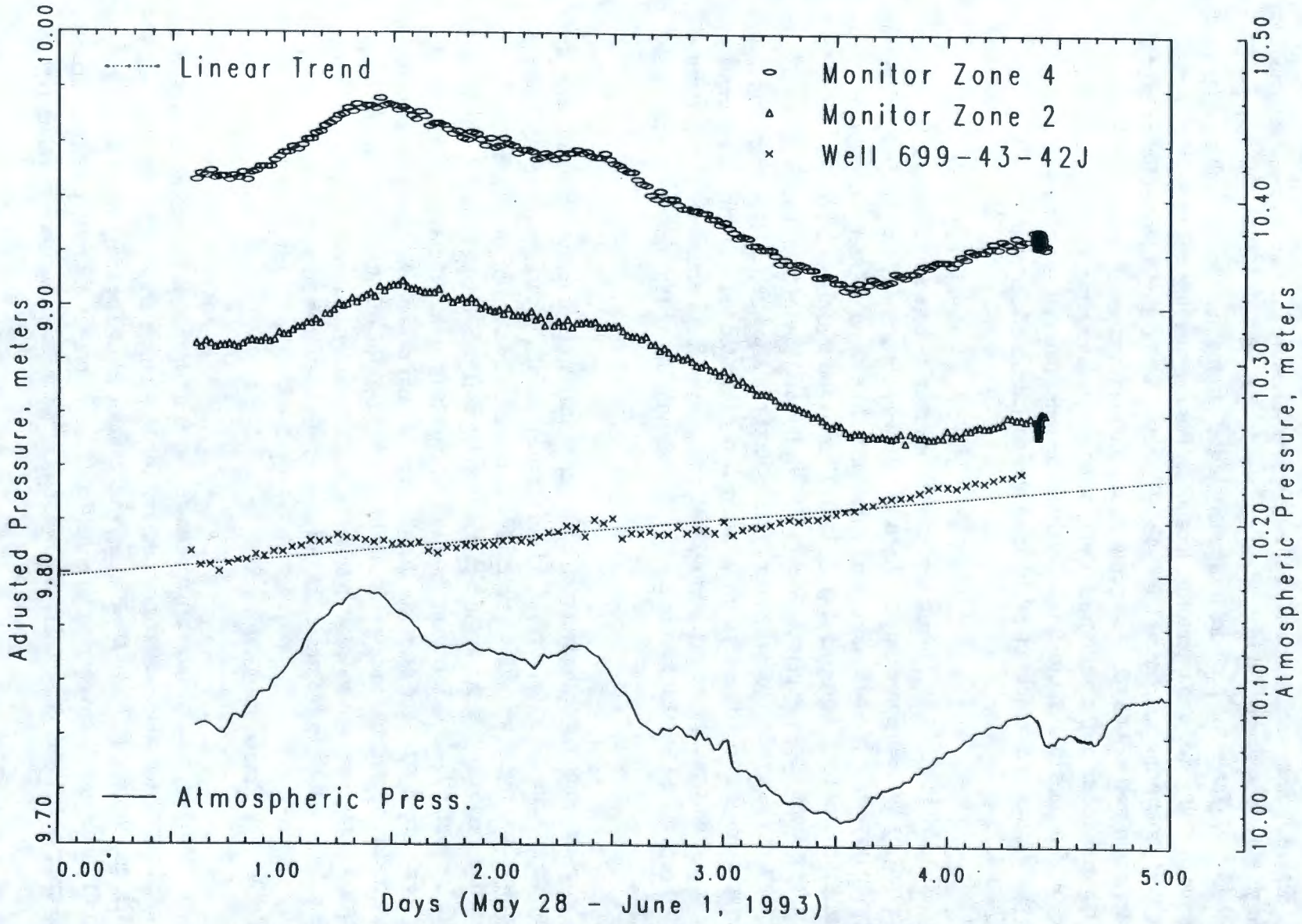

Figure A.5. Pre-Test Atmospheric Pressure and Pressures Recorded in Wells

Table A.1. Results of Barometric Efficiency Calculations for Monitoring Locations

Monitoring Well Facility	Barometric Efficiency %	Time Lag	Correlation Coefficient	Standard Error of Estimate
699-42-42B	13	23 min	0.979	0.0041
699-43-42J				
Monitor Zone 1	20	17 min	0.989	0.0049
Monitor Zone 2	19	15 min	0.987	0.0053
Monitor Zone 3	25	17 min	0.993	0.0050
Monitor Zone 4	35	17 min	0.991	0.0077
Monitor Zone 2	25	1.75 hr	0.992	0.0052
Monitor Zone 3	25	2.75 hr	0.995	0.0042
Monitor Zone 4	29	2.4 hr	0.996	0.0047

K_v/K_h), storativity/specific yield ratios, and aquifer transmissivities. Test data used in the composite analysis reflected delayed yield unconfined aquifer test conditions [i.e., segment 2 or the intermediate unconfined test response described in Neuman (1972)]. Test data reflective of early-time (segment 1) test response were not utilized in this analysis procedure because these data are typically influenced by wellbore storage effects, which are not accounted for with the composite analysis type curves utilized in this analysis procedure. Predicted drawdown responses were calculated for each monitoring location for the given distance to the pumping well, aquifer thickness, and partial penetration condition, and for various hydraulic property combinations using the DELAY 2 computer program described in Neuman (1975). The composite drawdown response for the four monitoring zones at well 699-43-42K and the monitoring zone at well 699-43-42J were then visually matched with the DELAY2 predicted drawdown patterns to find the best match and the corresponding hydraulic properties.

As a means of refining the preliminary hydraulic property ranges obtained from the composite drawdown analysis, various well drawdown combinations were analyzed with a commercially available, automatic type-curve matching program, ANIAQX, which is

described in Hydralogic (1989). The Neuman gravity drainage option was utilized, which describes complete unconfined aquifer test response (i.e., all 3 segments).

Table A.2 presents a summary of the composite analysis results. As indicated, for selected observation well combinations, fairly close agreement in hydraulic properties were indicated using the automated type-curve matching program. The relative uniformity of estimated hydraulic properties suggests that the aquifer is homogeneous over the region investigated by the test.

Based on the composite analysis, the following ranges for aquifer hydraulic properties within the test area are indicated:

Transmissivity: 27 - 32 m^2/d

Storativity: 1×10^{-4} to 2.7×10^{-4}

Storativity/Specific Yield: 0.018 to 0.044

Anisotropy (K_v/K_h): 0.009 to 0.01

It should be noted that drawdown data for the pumped well (well 699-42-42B) was not utilized in the multiple-well composite analysis. This is because of non-formational drawdown components (e.g., skin effects and well inefficiency) that occur at the pumped well. A discussion of these non-formational effects during constant-rate discharge tests is presented in Spane (1993).

Figure A.6 shows an example of a typical composite type-curve/drawdown match for all monitoring zones at well 699-43-42K and for drawdown at well 699-43-42J. As indicated, relatively good matches were obtained using the hydraulic property relationships shown in the figure.

Quantitative Test Analysis

Detailed quantitative analyses were performed on constant-rate test responses observed at well 699-43-42J and at Monitor Zones 3 and 4 within well 699-43-42K. Monitor zones 1 and 2 at well 699-43-42K were not analyzed because the magnitude of the test response was not adequate to provide a definitive, detailed analysis. Detailed analysis was also not performed for the pumped well (699-42-42B), because of non-formational test responses noted previously.

Table A.2. Hydraulic Properties Estimated from Composite Drawdown Analysis of Selected Monitoring Locations

Well 699-43-42K				Well				
Zone 1	Zone 2	Zone 3	Zone 4	699-43-42J	T m^2/d	S x 10^{-4}	S/Sy	Kv/Kh
X	X	X	X	X	29	1.2	0.019	0.01
X	X	X	X		29	1.5	0.020	0.01
	X	X	X		31	1.0	0.038	0.009
		X	X	X	32	1.0	0.033	0.009
X		X	X		31	1.1	0.020	0.009
X	X			X	27	2.7	0.044	0.009
X		X	X	X	30	1.2	0.018	0.01

The quantitative analysis procedure for each monitoring location included a diagnostic derivative analysis of drawdown or recovery data, and type-curve matching of the observed drawdown or recovery response. Drawdown and recovery data were converted to derivative format using the DERIV program described in Spane and Wurstner (1992). The derivative plots were then examined diagnostically to indicate the type of test behavior (i.e., presence of wellbore storage, delayed-yield response). Results of the diagnostic analysis indicated that Type A unconfined aquifer behavior (i.e., elastic and delayed-yield, unconfined aquifer response) was indicated at all the monitoring locations analyzed. In addition, wellbore storage effects of the pumping well were also evident within the early-time, observation well data.

Type A unconfined aquifer type curves utilized in the analysis were calculated with a computer program (Model Number 15) presented in Dawson and Istok (1991). This program accounts for partial penetration, aquifer anisotropy, and pumping well wellbore storage effects on the Type A type-curve response. Because of the closed well installation utilized for monitoring zones at well 699-43-42K, no observation well wellbore storage effects were expected for these monitoring locations. Observation wellbore storage effects, however, were expected at well 699-43-42J, and were accounted for using a procedure described in Spane (1993). Pertinent distance relationships from the pumping well and well completion information used in the test analysis are summarized in Table A.3.

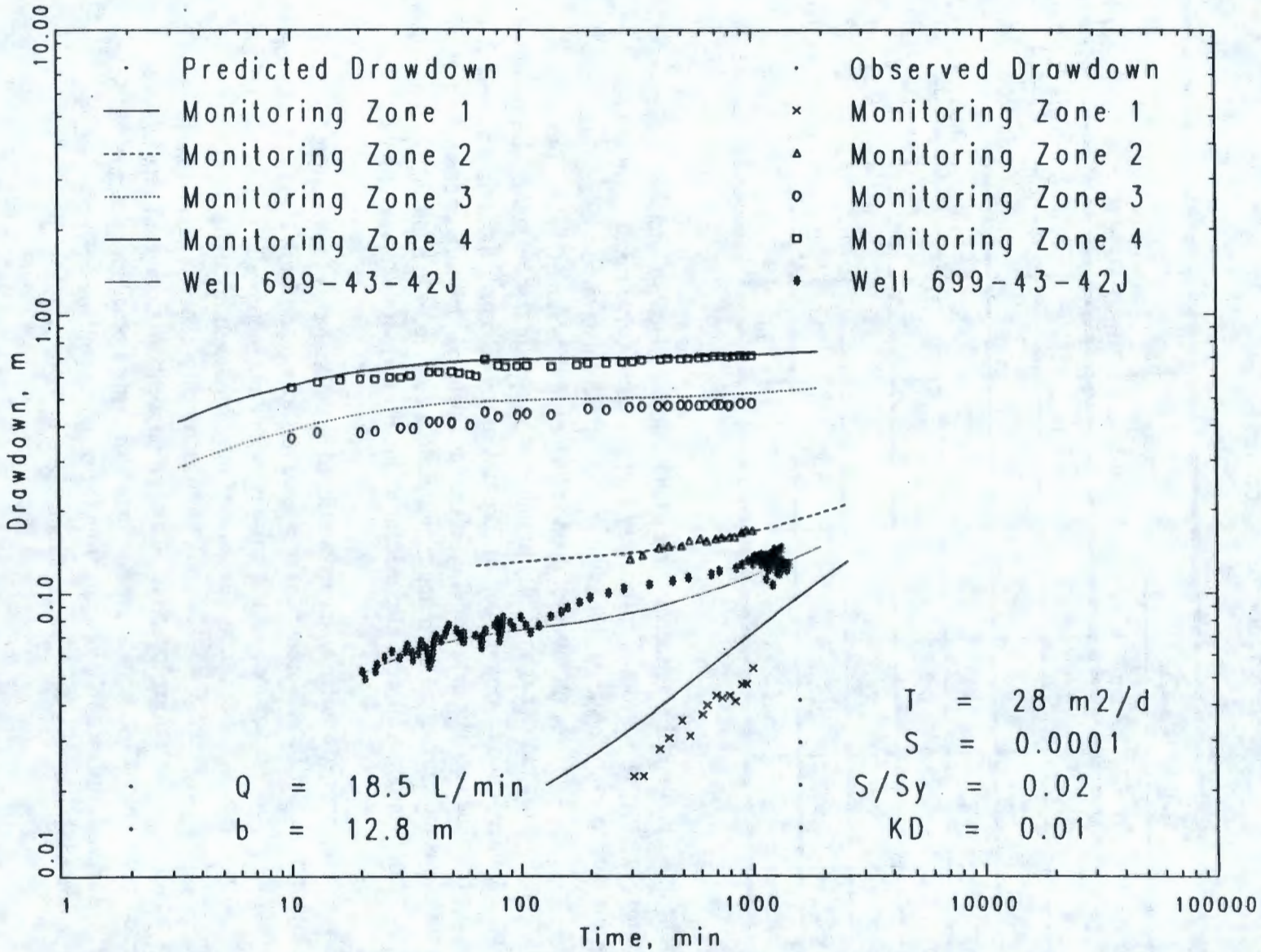

Figure A.6. Example of Composite Drawdown Analysis

Table A.3. Pertinent Well Completion and Test Information

Interval Depths and Distance Relationships				
Monitoring Locations	Depth Below Water Table		Distance from Pumping Well (m)	Well Radius (m)
	Top of Screen (m)	Bottom of Screen (m)		
699-43-42K				
Zone 4	10.97	12.80	11.09	0.051
Zone 3	6.71	8.83	11.09	0.051
Zone 2	2.74	4.88	11.09	0.051
699-43-42J	0.0	4.70	19.51	0.051
699-42-42B[a]	7.02	12.80	-	0.051
(a) Pumping Well.				
Test Information - Discharge Rate: 18.5 L/min Test Duration: 1440 min Aquifer Thickness: 12.8 m				

Well 699-43-42K: Monitor Zone 4. The drawdown data and derivative pattern for Monitor Zone 4 are shown in Figure A.7. The diagnostic plot of the drawdown data and data derivative indicate a characteristic Type A unconfined aquifer test response. For type-curve matching, drawdown data obtained during the first 30 min of the test were used. This test data set (i.e., 0 to 30 min) was selected to ensure that only Type A unconfined aquifer behavior was analyzed and to avoid the effects of small variations in the test discharge rate that occurred later in the test. Small variations in discharge rate cause minor drawdown fluctuations that are accentuated in the data derivative plot.

As indicated in Figure A.7, a wellbore storage affected Type A curve corresponding to a beta value of 0.045 provided a good curve match to the drawdown and drawdown derivative data. Transmissivity and storativity estimates obtained from the type-curve analysis match points are 18.0 m^2/d and 0.0001, respectively. An estimated value for vertical anisotropy

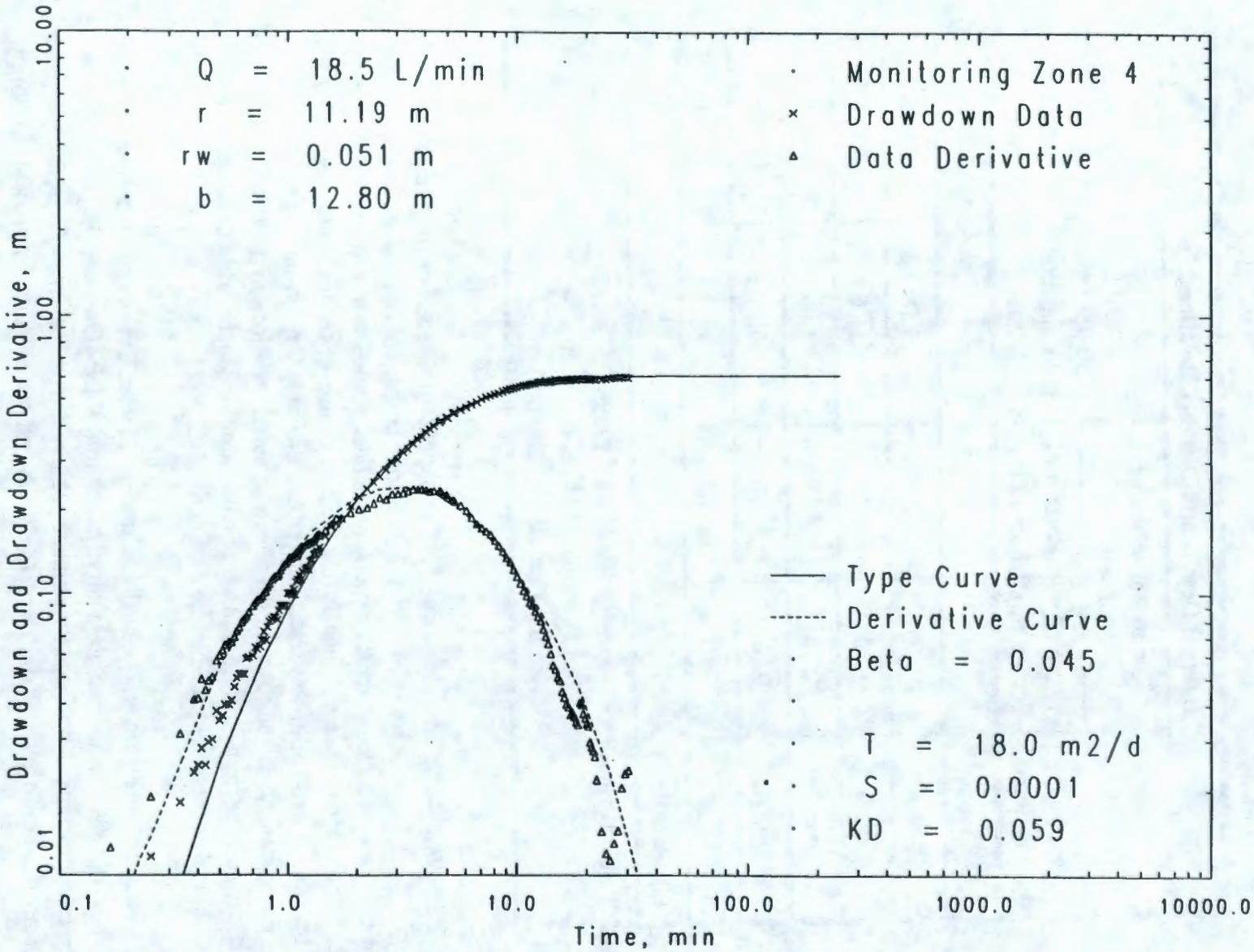

Figure A.7. Drawdown and Drawdown Derivative Type-Curve Analysis for Well 699-43-42K: Monitor Zone 4

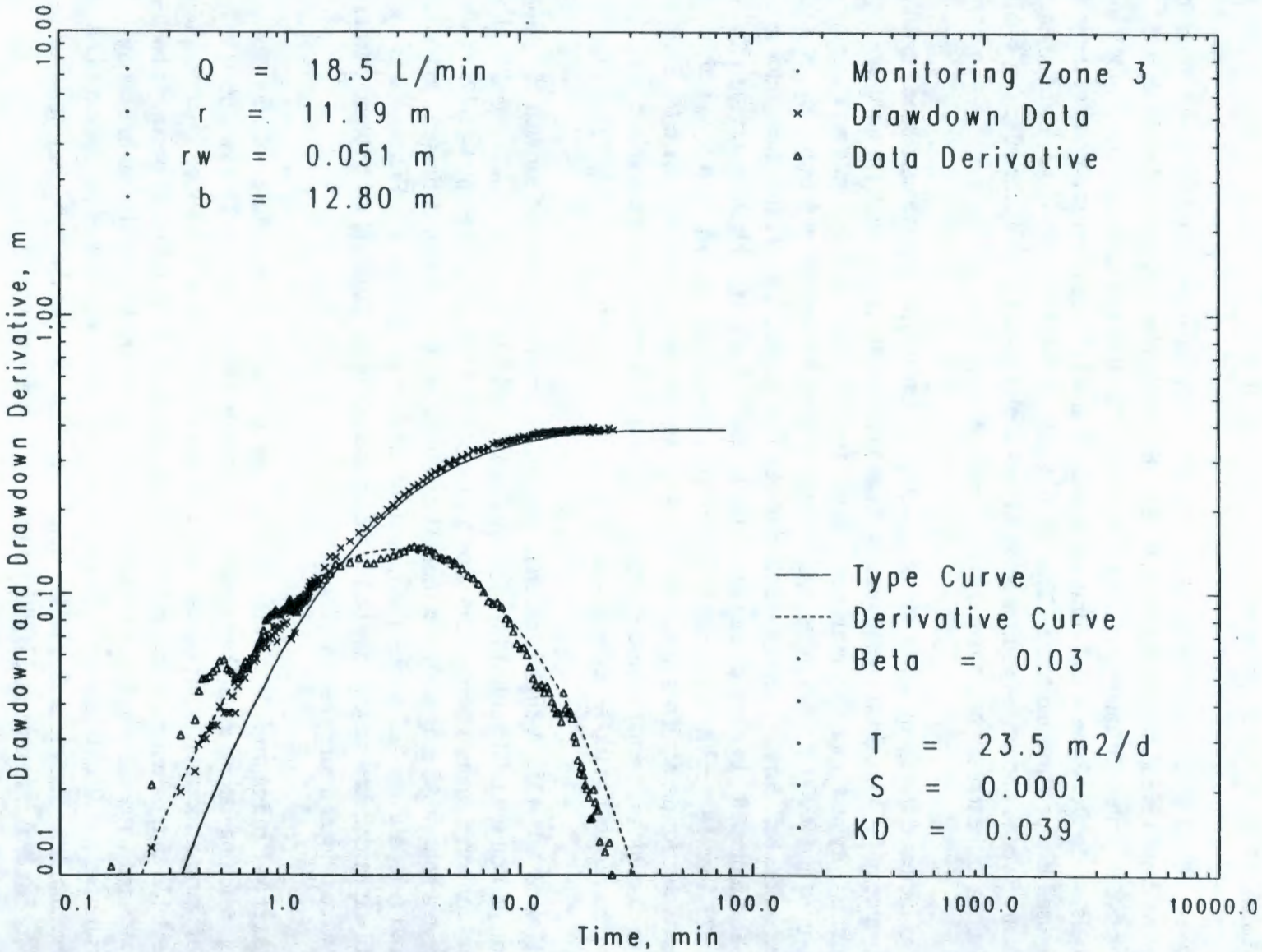

Figure A.8. Drawdown and Drawdown Derivative Type-Curve Analysis for Well 699-43-42K: Monitor Zone 3

(K_D) of 0.059, based on the beta curve value and the ratio of observation well distance to aquifer thickness, was also indicated.

Well 699-43-42K: Monitor Zone 3. The drawdown data and data derivative pattern for Monitor Zone 3 are shown in Figure A.8. The diagnostic plot of the drawdown data and derivative indicate a characteristic Type A unconfined aquifer test response. As for the analysis of Monitor Zone 4, only drawdown data obtained during the first 30 min of the test were used in type-curve matching. This test data set (i.e., 0 to 30 min) was selected to ensure that only Type A unconfined aquifer behavior was analyzed and to avoid the effects of small variations in the test discharge rate that occurred later in the test.

As indicated in Figure A.8, a wellbore storage affected Type A curve corresponding to a beta value of 0.03 provided a good drawdown and drawdown derivative curve match. Transmissivity and storativity estimates obtained from the type-curve analysis match points are 23.5 m^2/d and 0.0001, respectively. An estimated value for vertical anisotropy (K_D) of 0.039, based on the beta curve value and the ratio of observation well distance to aquifer thickness, was also indicated. In comparison to the Monitor Zone 4 results, a higher transmissivity value (i.e., 23.5 vs. 18.0 m^2/d) is indicated. The increased estimate for transmissivity yields a higher value for the aquifer's horizontal hydraulic conductivity (Zone 3 = 2.1 m/d; Zone 4 = 1.4 m/d), which is primarily responsible for the small difference in vertical anisotropy estimates (Zone 3 = 0.039; Zone 4 = 0.059).

Well 699-43-42J. A slightly different analysis procedure was utilized for well 699-43-42J in comparison to that described for Monitor Zones 3 and 4 at well 699-43-42K. Unlike the other monitored zones, observed drawdown and recovery patterns at well 699-43-42J exhibited divergent behavior during early test times (i.e., during the first 50 min of the test) and later in the test (i.e., after $\approx$ 200 min). The reason for the divergence shown in Figure A.9 is not readily apparent; however, it may be related to changes in instrumental drift characteristics that were evident during the pre-test period.

As shown in Figure A.5, well 699-43-42J does not exhibit an obvious association with barometric fluctuations as do the responses at Monitor Zones 3 and 4. This lack of atmospheric association is attributed to the fact that well 699-43-42J is screened across the water table and, therefore, would not display the imbalance in atmospheric pressures between the well and water table surface. Well 699-43-42J, however, does display an increasing pressure trend (5.2×10^{-6} m/min) during the pre-test period, which does not appear to be observed at the other monitor zone locations. This suggests that the trend may be attributed to non-formational responses and is likely a product of instrument drift.

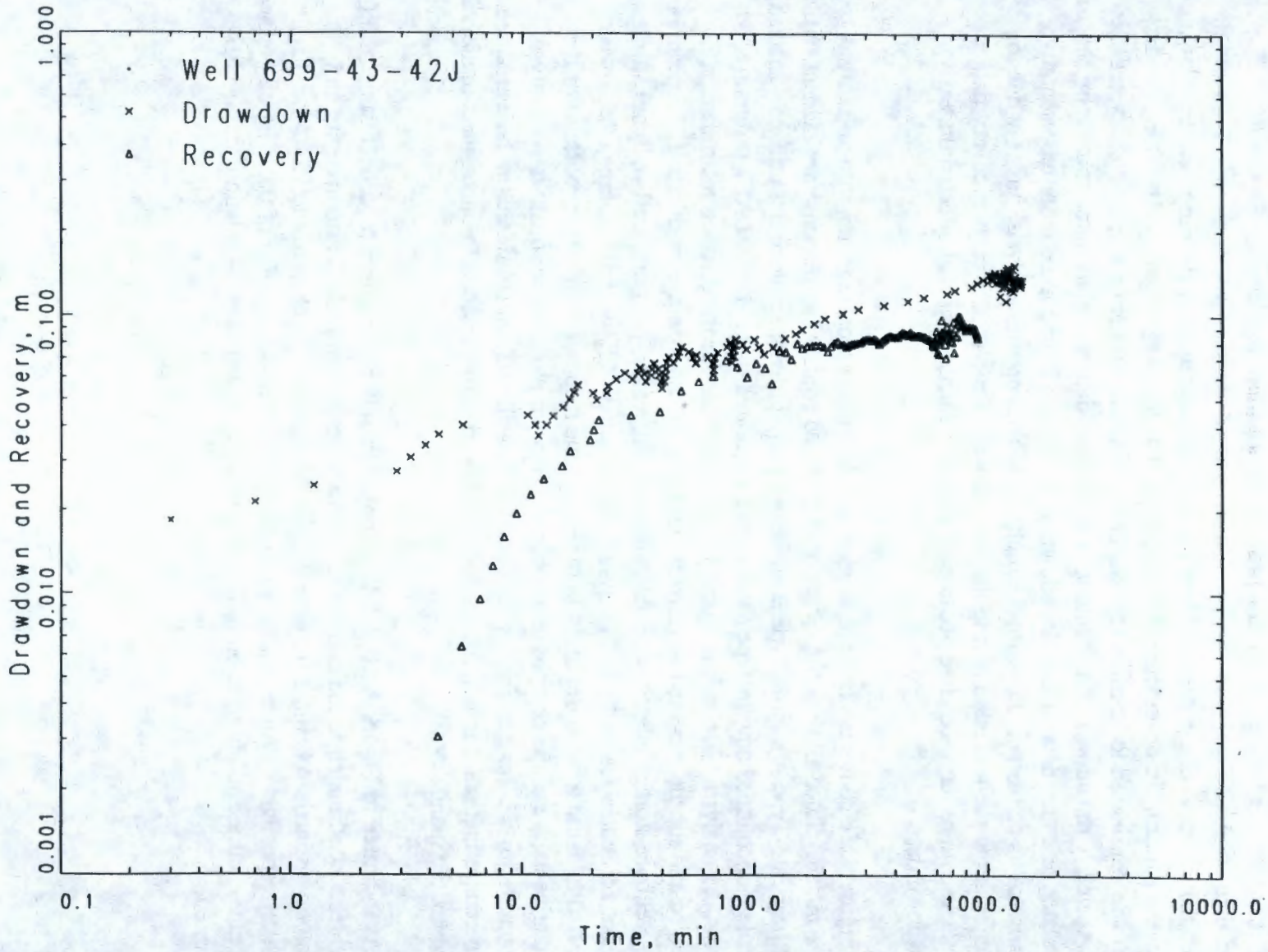

Figure A.9. Observed Drawdown and Recovery at Well 699-43-42J

In an attempt to analyze the test response observed at well 699-43-42J, the drawdown and recovery data were corrected for the pre-test trend pattern displayed in Figure A.5. The data were then combined and a composite recovery-drawdown plot was prepared. It should be noted that removal of the pre-test trend did not significantly alter the observed drawdown or recovery pattern. In developing the composite plot, the early recovery data (i.e., the first 70 min) was considered to be more representative of actual formation response characteristics than the early drawdown data, while later drawdown data was considered more representative than later recovery data. Later drawdown data was considered to be more representative, because of its consistent "fit" with the multiple-well composite analysis, possibly due to changes in the pre-test trend during the late recovery period. The early recovery data was considered more representative because of flow-rate fluctuations that affected the early drawdown data.

Figure A.10 shows the composite recovery-drawdown plot, together with an analysis type-curve match. Since all three segments of unconfined aquifer test response are evident in the plot, separate Type A and/or Type B curve matching procedures were not utilized. Instead, complete unconfined aquifer type curves were generated using the DELAY2 program, and used in the analysis. Preliminary analyses indicated that for the distance relationships involved and for the expected storativity range (i.e., elastic storage = 10^{-3} to 10^{-4}), pumping well wellbore storage effects were insignificant. Therefore, pumping well wellbore storage was not accounted for in the test analysis. Observation well wellbore storage effects were expected to cause a small deviation in the early-time response. However, because of the qualitative nature of the composite recovery-drawdown plot, a more quantitative analysis accounting for wellbore storage at the observation well was not considered to be warranted. A procedure that takes into account observation well storage effects in unconfined aquifers is presented in Spane (1993).

As indicated in Figure A.10, a full unconfined aquifer type curve for a beta value of 0.023 provides a good match to the composite recovery-drawdown plot. Transmissivity and storativity estimates obtained from the type-curve analysis match points are 24.4 m^2/d and 0.0002, respectively. An estimated value for vertical anisotropy (K_D) of 0.01, based on the beta curve value and observation well distance and aquifer thickness relationship, is also indicated.

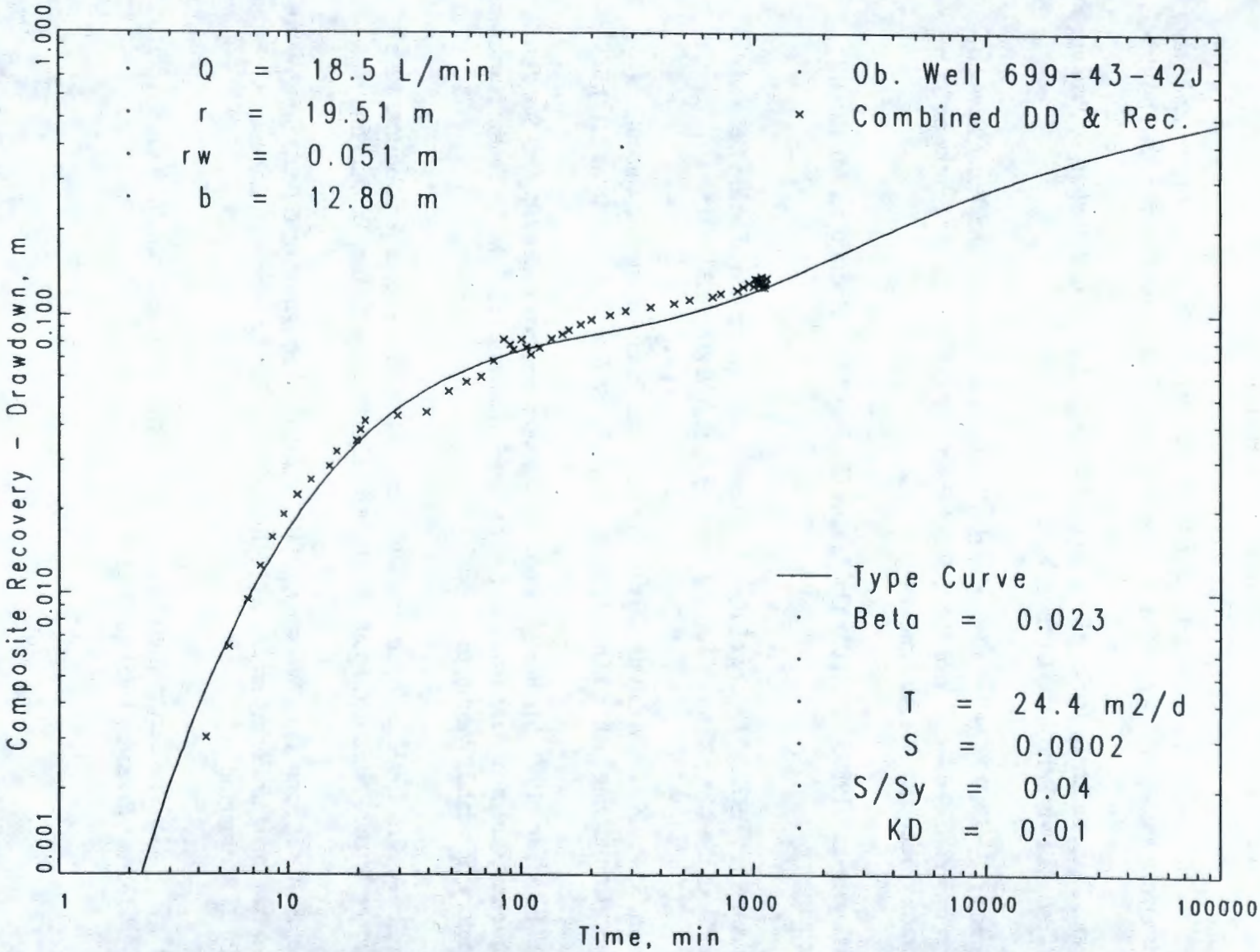

Figure A.10. Full Unconfined Type-Curve Analysis of Composite Recovery-Drawdown Plot at Well 699-43-42J

References

Clark, W. E. 1967. "Computing the Barometric Efficiency of a Well." In *Proceedings of the American Society of Civil Engineers, Journal of the Hydraulics Division* 43(HY4):93-98.

Dawson, K. J., and J. D. Istok. 1991. *Aquifer Testing - Design and Analysis of Pumping and Slug Tests*. Lewis Publishers, Chelsea, Michigan.

Gilmore, T. J. 1989. *The Installation of the Westbay Multiport Ground-Water Sampling System in Well 699-43-42K Near the 216-B-3 Pond*. PNL-6973, Pacific Northwest Laboratory, Richland, Washington.

Hydralogic, Inc. 1989. *ANIAQX - Operations Guide*, v2.50. Hydralogic, Missoula, Montana.

Neuman, S. P. 1972. "Theory of Flow in Unconfined Aquifers Considering Delayed Response of the Water Table." *Water Resources Research* 8(4):1031-1045.

Neuman, S. P. 1975. "Analysis of Pumping Test Data from Anisotropic Unconfined Aquifers Considering Delayed Gravity Response." *Water Resources Research* 11(2):329-342.

Spane, F. A., Jr. 1992. *Applicability of Slug Interference Tests under Hanford Site Test Conditions: Analytical Assessment and Field Test Evaluation*. PNL-8070, Pacific Northwest Laboratory, Richland, Washington.

Spane, F. A., Jr. 1993. *Selected Hydraulic Test Analysis Techniques for Constant-Rate Discharge Tests*. PNL-8539, Pacific Northwest Laboratory, Richland, Washington.

Spane, F. A., Jr., and S. K. Wurstner. 1992. *DERIV: A Program for Calculating Pressure Derivatives for Hydrologic Test Data*. PNL-SA-21569, Pacific Northwest Laboratory, Richland, Washington.

Weeks, E. P. 1979. "Barometric Fluctuations in Wells Tapping Deep Unconfined Aquifers." *Water Resources Research* 15(5):1167-1176.

Appendix B

Hydrologic Testing at Hanford Sitewide Monitoring Wells

THIS PAGE INTENTIONALLY
LEFT BLANK

Appendix B

Hydrologic Testing at Hanford Sitewide Monitoring Wells

To obtain hydrologic data in support of the Flow System Characterization Task of the Hanford Ground-Water Surveillance Program, constant-rate discharge tests were performed at several wells in the sitewide ground-water sampling network. The sitewide network currently provides the best spatial distribution of upper unconfined aquifer monitoring wells on the Hanford Site. Most monitoring wells in the network are equipped with a dedicated submersible sampling pump. These sampling pumps were used to perform constant-rate discharge tests at selected wells to provide estimates of hydraulic conductivity spatially distributed across the Hanford Site at a relatively low cost.

The sitewide monitoring wells tested during FY 1993 were constructed with either 6- or 8-in. diameter carbon steel casing and were screened or perforated over the upper portion of the aquifer (Table B.1). Observation well data were not available at any of the test sites. The monitoring wells are routinely sampled with dedicated 0.5-hp or 0.75-hp submersible pumps that produce, on average, 8 gpm. Because there were no check valves installed in the sampling pumps, some anomalies were observed in the early time drawdown data. The early time drawdown curve was relatively steep, corresponding to the pump column filling with water under low backpressure conditions. As water filled the pump column and backpressure on the pump increased, the drawdown curve deflected upward then followed the expected late time drawdown response. This anomalous response was observed within the first two minutes at several of the test wells. The lack of check valves in the sampling pump installations also caused recovery data to be masked as water in the pump column drained into the well after the pump was turned off. Therefore, recovery data obtained from the tests were not analyzable.

Tests Providing an Estimate of Hydraulic Conductivity

Four of the 15 tests resulted in a detectable drawdown response. Only these four tests provided a quantitative estimate of hydraulic conductivity for the tested intervals. Constant-rate discharge tests were run for a duration of 24 h at these wells, which included 699-15-15B, 699-29-4, 699-55-89, and 699-57-83A. Hydraulic test analysis methods for all of these constant-rate discharge tests were identical. Confined aquifer analysis (Cooper and Jacob 1946) was performed on test data sections that displayed radial flow conditions. The data

1946) was performed on test data sections that displayed radial flow conditions. The data sections displaying radial flow conditions were identified by plotting the drawdown and drawdown derivative as discussed in Spane (1993).

Prior to performing the confined aquifer analysis discussed above, drawdown data were corrected for barometric fluctuation effects and for the decrease in saturated thickness associated with drawdown in unconfined aquifers. Barometric fluctuation effects refer to the change in formation pressure associated with changes in atmospheric pressure. Drawdown data were corrected for the effects of barometric fluctuation using the method described by Clark (1967). In an unconfined aquifer, the saturated thickness of the aquifer decreases during a discharge test. When using confined-aquifer-based analysis methods, which assume a constant saturated thickness, the drawdown data must be corrected for dewatering. The correction was made using an equation presented by Jacob (1944).

It should be noted that the tested wells generally only partially penetrate the aquifer thickness and the analysis method does not account for the effects of partial penetration on the drawdown response. However, it was assumed that the unconfined aquifer is anisotropic with a relatively small vertical hydraulic conductivity. Therefore, flow is assumed to be nearly radial within the aquifer section penetrated by the pumping well and the vertical flow component within the aquifer is assumed to be negligible. Based on this assumption, calculated transmissivity values were assumed to pertain only to the tested interval thickness (screen length) and this thickness was used in calculating hydraulic conductivity values. Because the test interval is actually partially penetrating the unconfined aquifer, the transmissivity of the entire aquifer thickness is significantly underestimated; however, in calculating hydraulic conductivity, this error is offset by dividing the transmissivity result by the test interval length rather than the actual aquifer thickness. The actual hydraulic conductivity may be lower than the calculated value if vertical flow within the aquifer is significantly affecting the test response. Because of the many nonideal test conditions including partial penetration, unconfined aquifer conditions, anisotropy, a lack of observation wells, and a lack of recovery data; the test results should be regarded as order-of-magnitude estimates.

A diagnostic log-log plot of the corrected drawdown data and the associated drawdown derivative, calculated using the DERIV program described by Spane and Wurstner (1992), was generated for each monitoring well (Figures B.1, B.2, B.3, and B.4). Drawdown derivatives from all four tests indicated that radial flow conditions were achieved. Confined-aquifer, straight-line analysis techniques (Cooper and Jacob 1946) were utilized for analyzing this radial flow portion of the drawdown curve (Figures B.5, B.6, B.7, and B.8). The straight-line analyses resulted in hydraulic conductivity estimates shown in Table B.1.

Because no observation well data were available at the test sites, storativity and specific yield were not estimated.

Tests Providing a Lower Bound on Hydraulic Conductivity

Of the 15 monitoring wells tested during FY 1993, 11 showed no detectable drawdown. Data from these wells were not sufficient to estimate hydraulic conductivity. However, with knowledge of the pressure transducer resolution and applied stress level, a qualitative lower bound was estimated for transmissivity of the tested interval. Theoretical test responses were calculated for various transmissivities using the Theis (1935) solution and assuming the average discharge rate of 8 gpm (Figure B.9). Resolution of the strain gauge pressure transducer used in these tests was approximately 0.007 ft of water. However, turbulence created by the pump caused pressure fluctuations of as much as 0.05 ft of water in some wells; these pressure fluctuations limited the ability to resolve actual drawdown. Considering all of these factors, 2500 ft^2/d was identified as the highest transmissivity value that would produce a detectable drawdown response at the given stress level. This analysis is based on confined-aquifer methods that assume a fully penetrating well. At equal transmissivity, delayed yield effects caused by unconfined aquifer conditions are expected to reduce the magnitude of drawdown observed over a relatively short pumping period. Therefore, the lower bound of transmissivity was estimated at 1000 ft^2/d for the wells where no drawdown was detected. The actual transmissivity of the entire aquifer at these locations may be substantially higher, especially for partially penetrating wells. Because of uncertainty in the aquifer thickness and effects of partial penetration, no attempt was made to estimate hydraulic conductivity. For quantitative estimates of hydraulic conductivity, additional tests should be conducted at these wells using higher flow rates.

Table B.1. Results from Constant-Rate Tests of Sitewide Monitoring Wells

Hanford Well Number	Tested Interval (ft below ground surface)	Interval Length (ft)	Hydraulic Conductivity (ft/day)
699-S8-19	104 - 132	28	ND
699-S6-E4D	56 - 116	60	ND
699-S19-11	94 - 115	21	ND
699-4-E6	69 - 87	18	ND
699-8-17	122 - 158	36	ND
699-8-25	108 - 168	60	ND
699-15-15B	151 - 161	10	90
699-19-88	128 - 170	42	ND
699-20-E5A	95 - 100	5	ND
699-25-70	182 - 185	3	ND
699-29-4	102 - 112	10	130
699-29-78	185 - 300	115	ND
699-35-9	112 - 135	23	ND
699-55-89	160 - 210	50	22
699-57-83A	145 - 195	50	14

ND = No drawdown detected at average flow rate of 8 gpm; the transmissivity is assumed to be greater than 1000 ft^2/d.

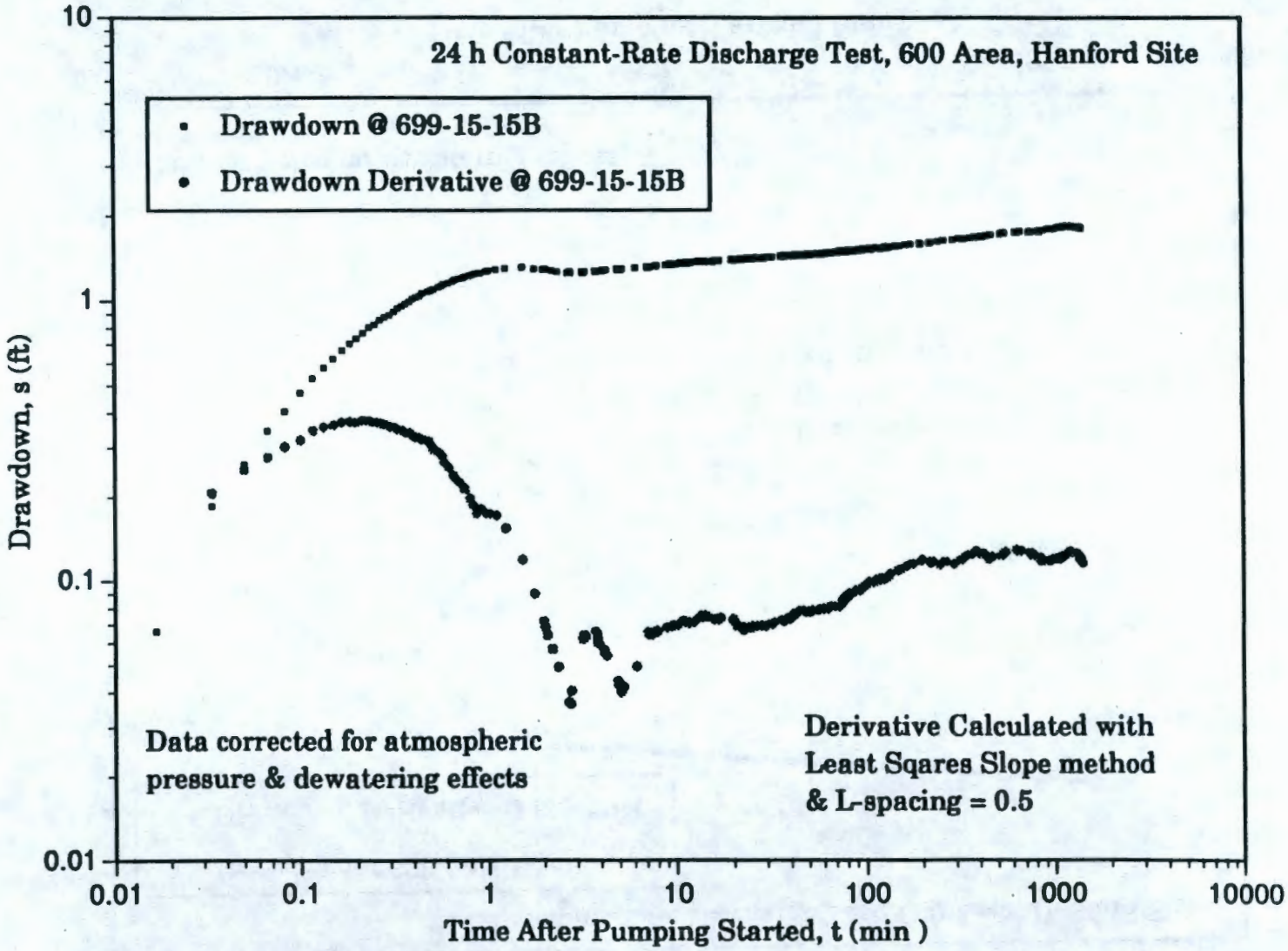

Figure B.1. Log-Log Diagnostic Plot of Drawdown and Drawdown Derivative at Well 699-15-15B

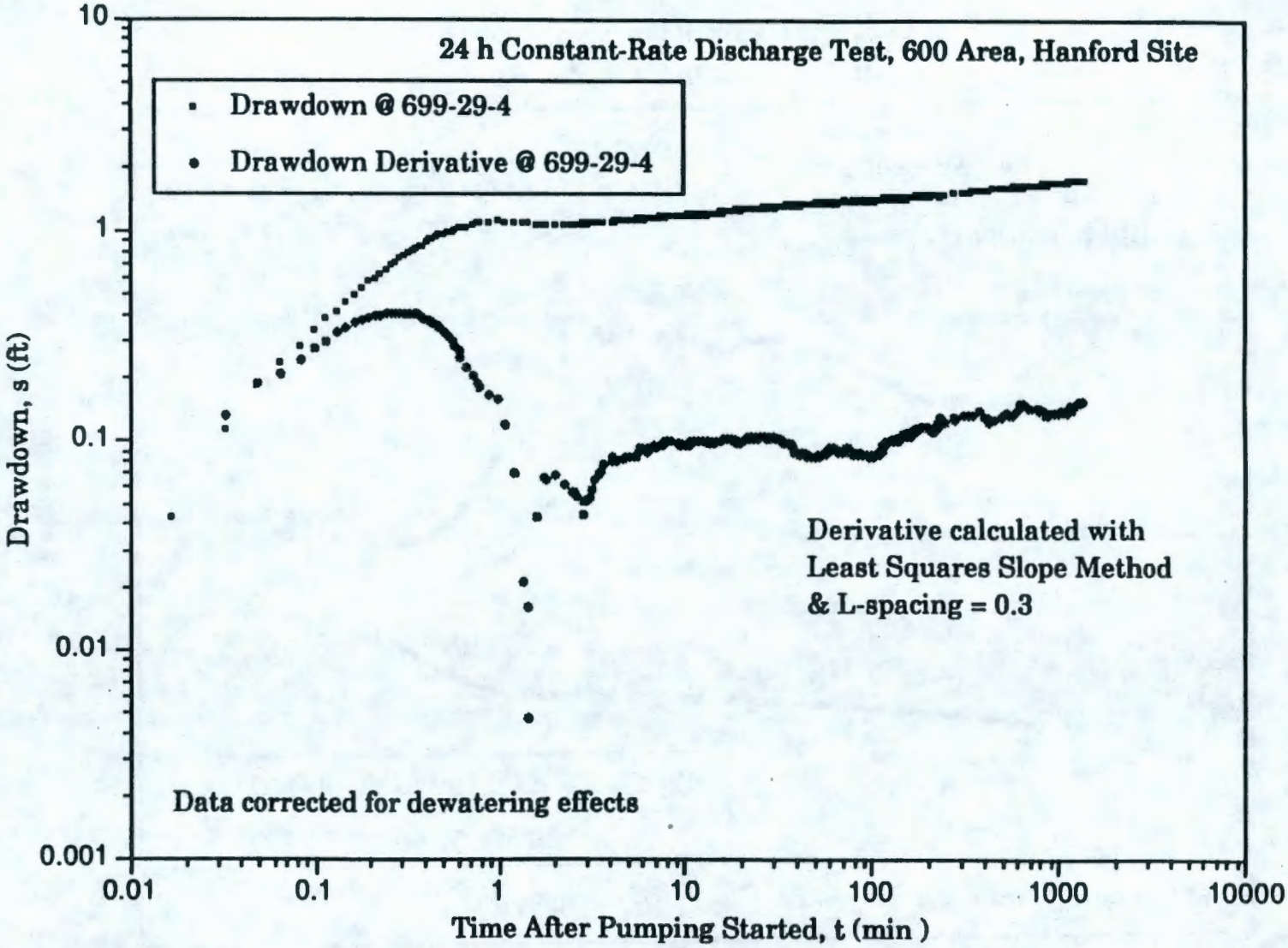

Figure B.2. Log-Log Diagnostic Plot of Drawdown and Drawdown Derivative at Well 699-29-4

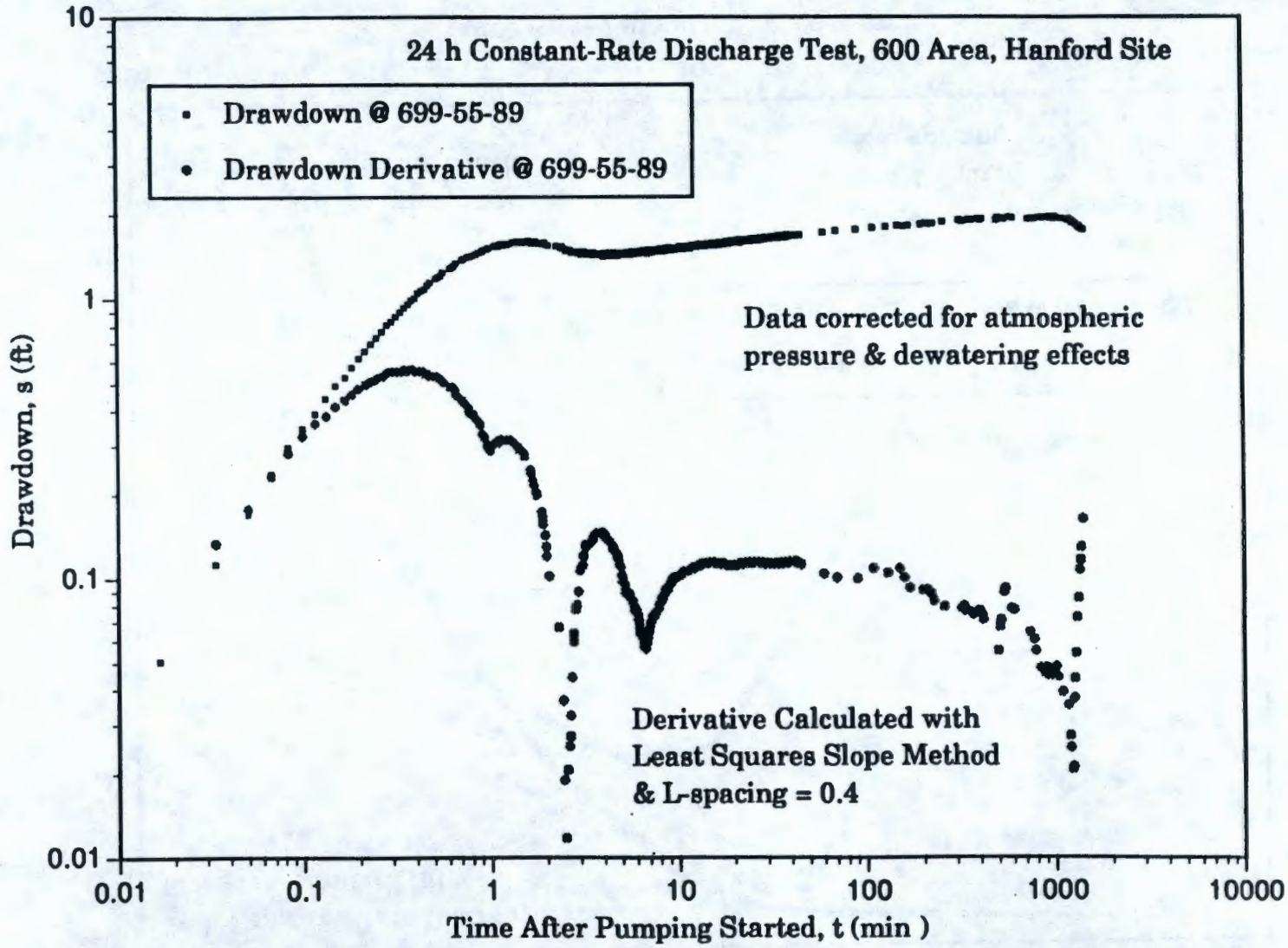

Figure B.3. Log-Log Diagnostic Plot of Drawdown and Drawdown Derivative at Well 699-55-89

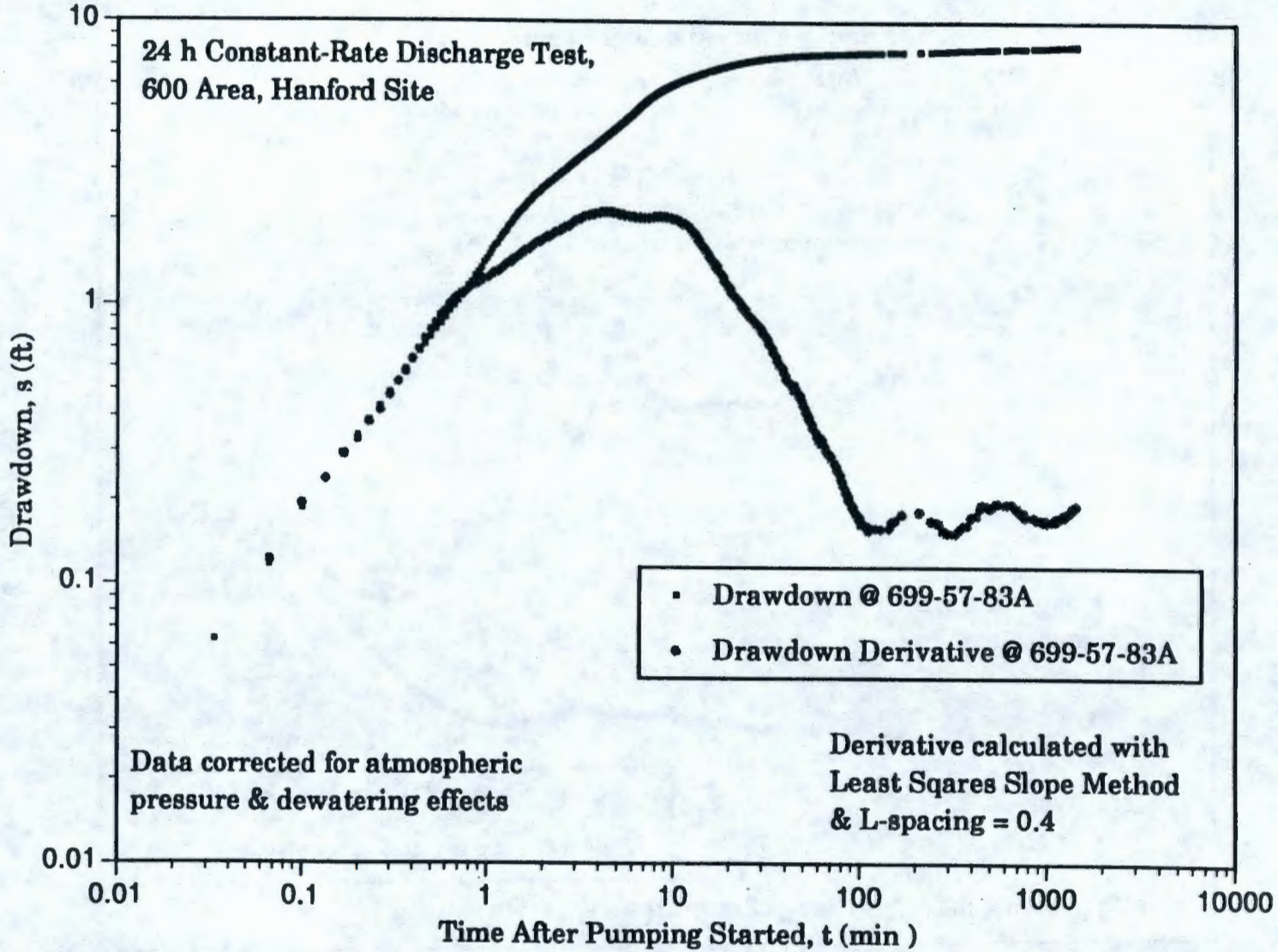

Figure B.4. Log-Log Diagnostic Plot of Drawdown and Drawdown Derivative at Well 699-57-83A

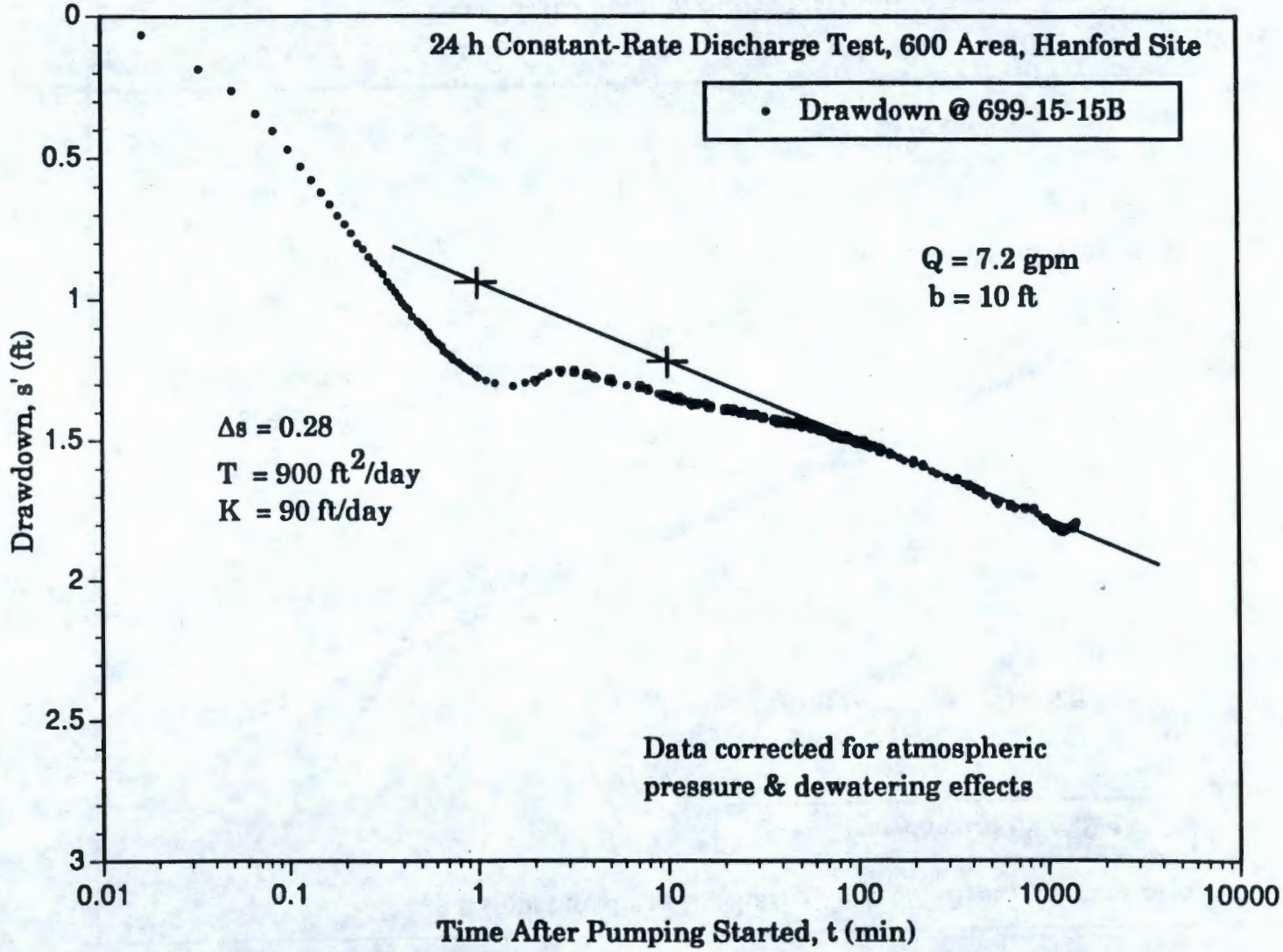

Figure B.5. Cooper and Jacob Straight Line Analysis for Well 699-15-15B

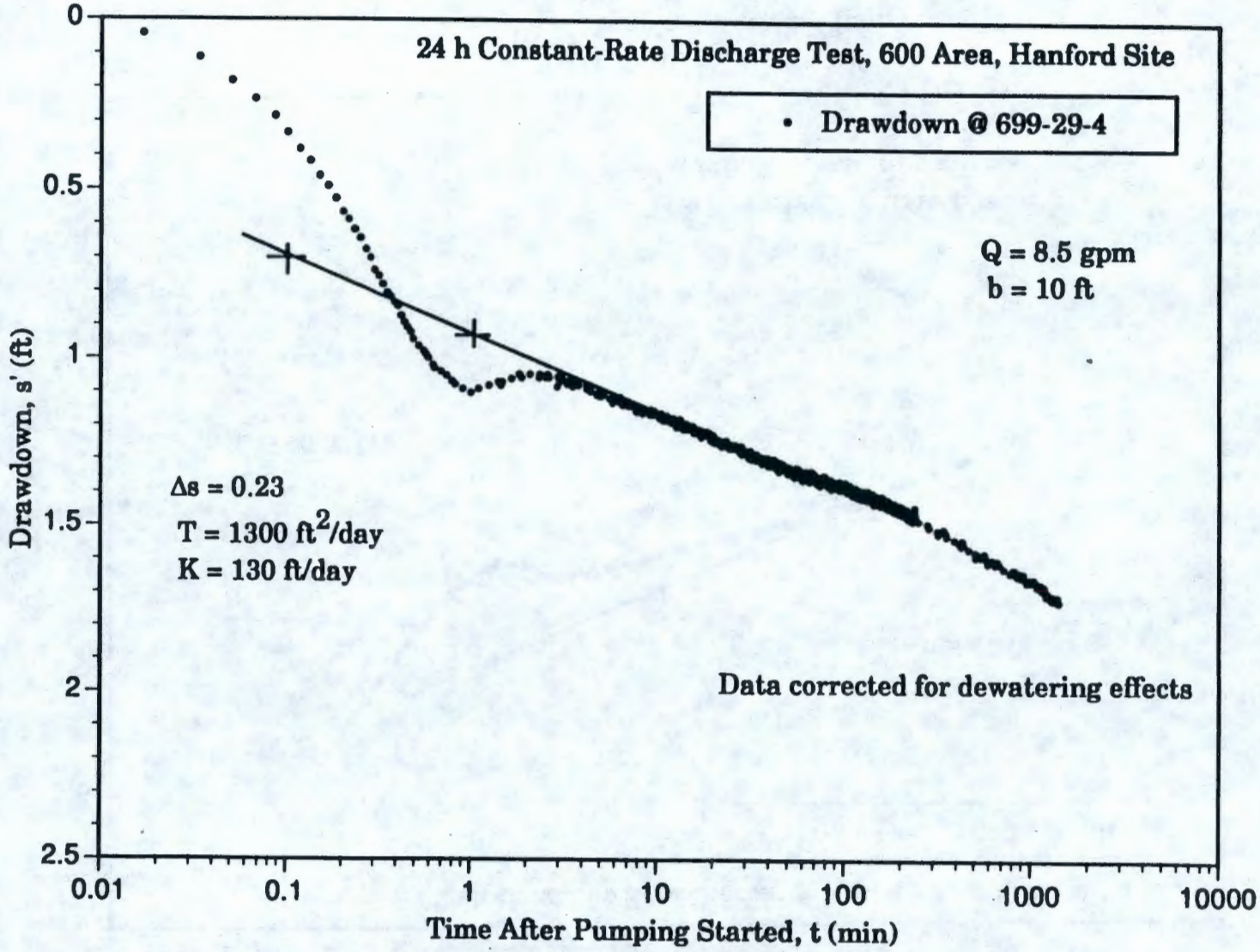

Figure B.6. Cooper and Jacob Straight Line Analysis for Well 699-29-4

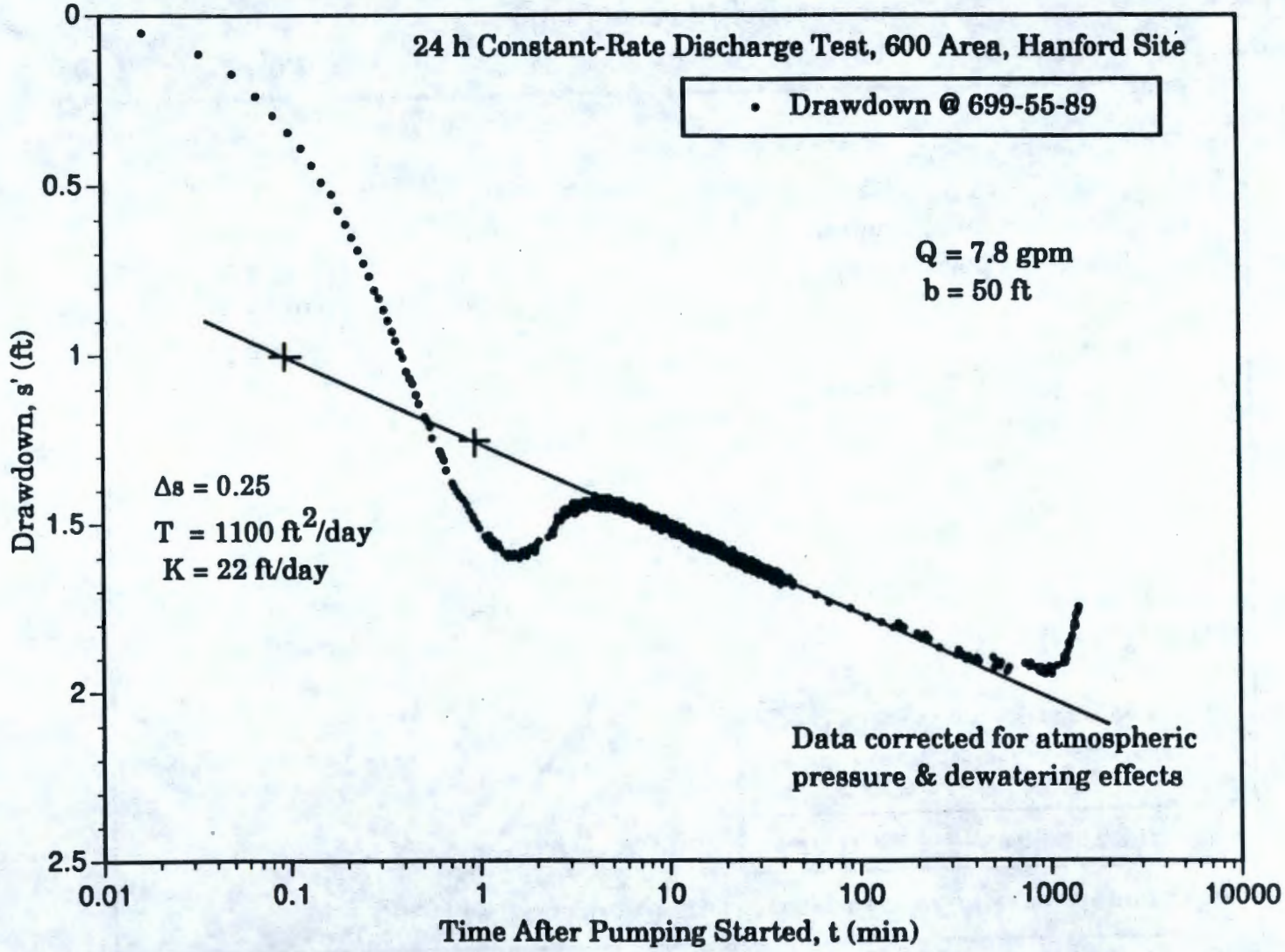

Figure B.7. Cooper and Jacob Straight Line Analysis for Well 699-55-89

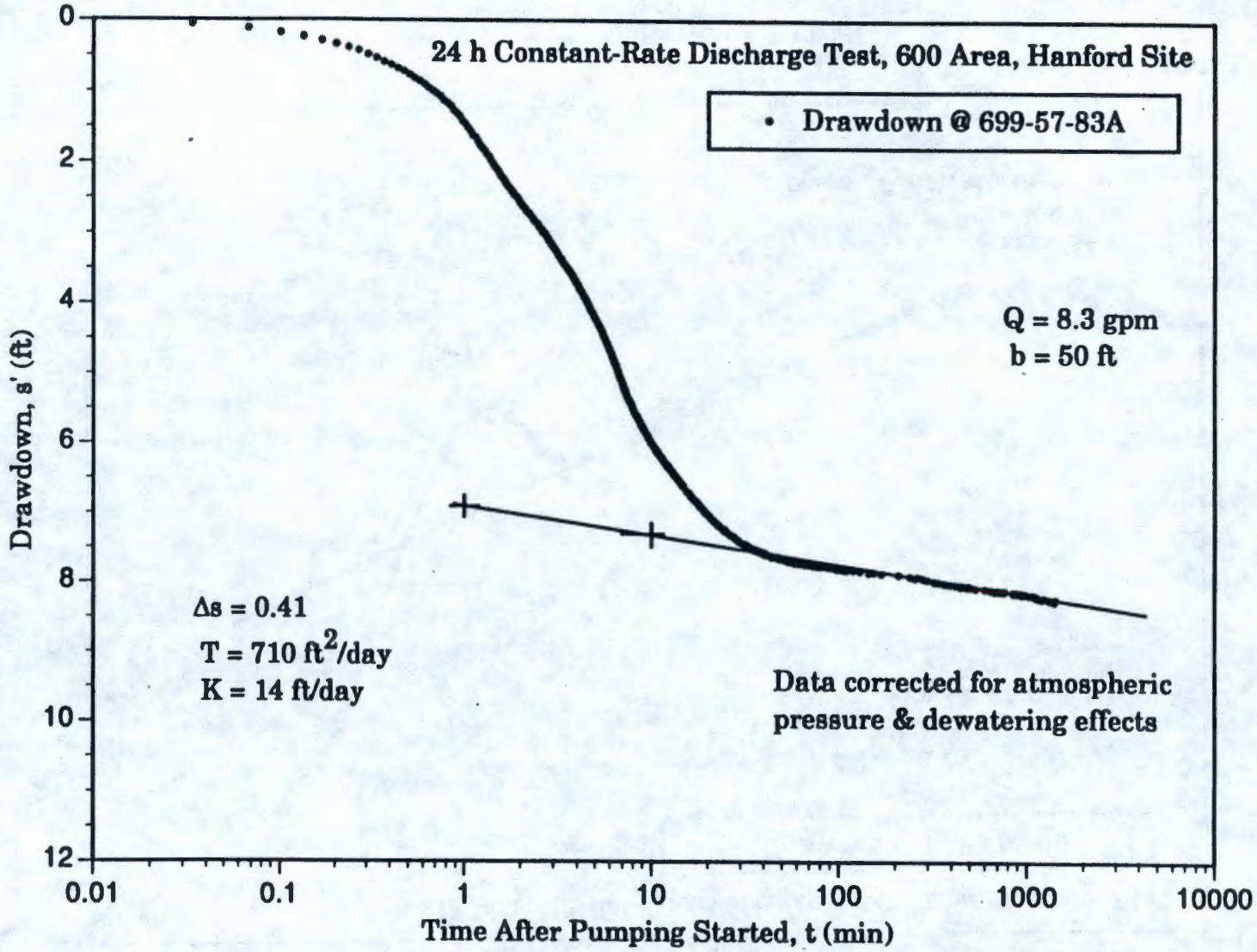

Figure B.8. Cooper and Jacob Straight Line Analysis for Well 699-57-83A

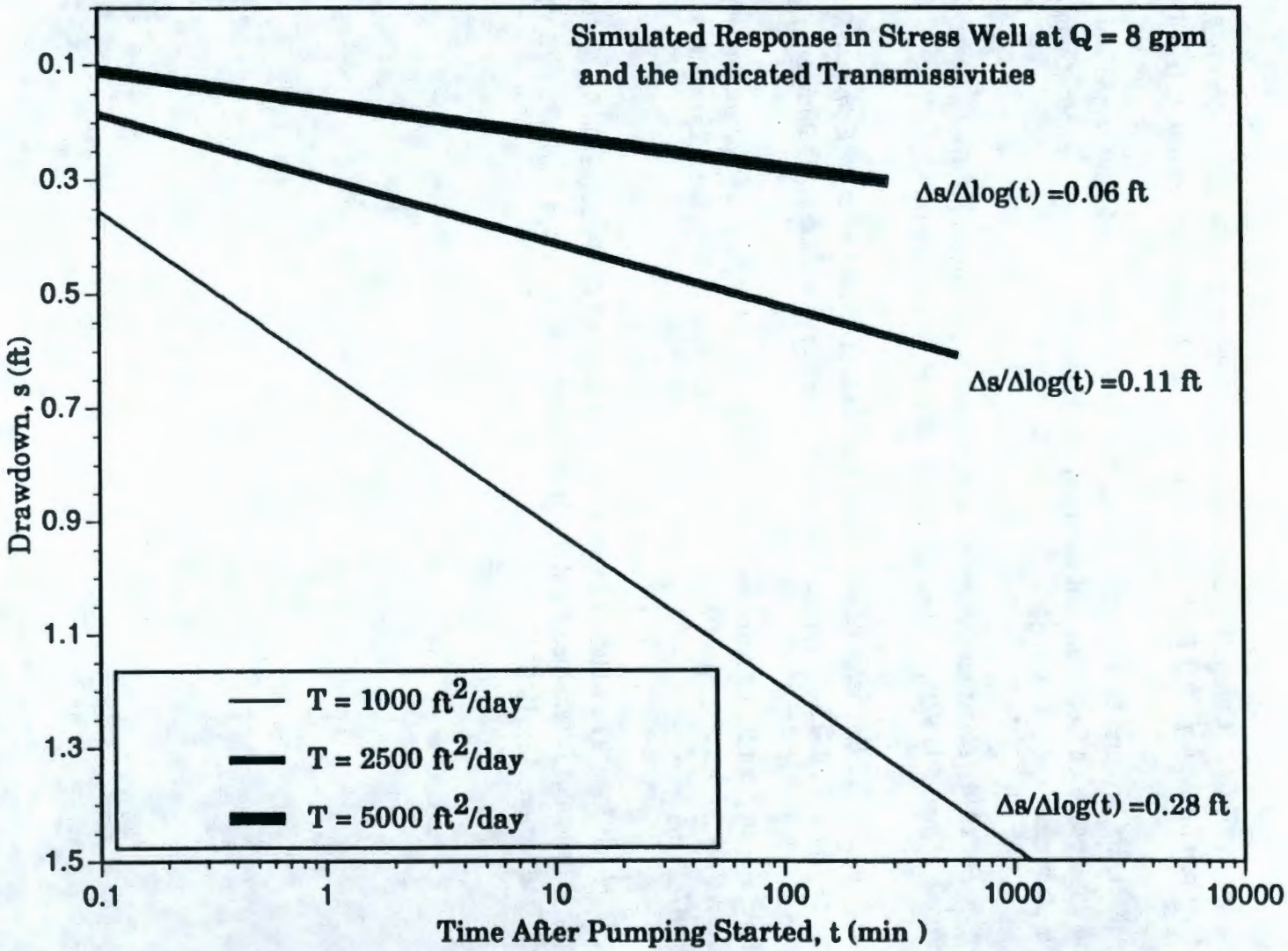

Figure B.9. Simulated Theis Response at Average Discharge Rate of 8 gpm and Indicated Transmissivity

References

Clark, W. E. 1967. "Computing the Barometric Efficiency of a Well." In *Proceedings of the American Society of Civil Engineers, Journal of the Hydraulics Division* 43(HY4):93-98.

Cooper, H. H., Jr., and C. E. Jacob. 1946. "A Generalized Graphical Method For Evaluating Formation Constants and Summarizing Well-Field History." *Amer. Geophysical Union, Transactions* 27(4):526-534.

Jacob, C. E. 1944. *Notes on Determining Permeability by Pumping Tests Under Water-Table Conditions*. Open File Report, U.S. Geological Survey, Washington D.C.

Spane, F. A., Jr. 1993. *Selected Hydraulic Test Analysis Techniques for Constant-Rate Discharge Tests*. PNL-8539, Pacific Northwest Laboratory, Richland, Washington.

Spane, F. A., Jr., and S. K. Wurstner. 1992. *DERIV: A Program for Calculating Pressure Derivatives for Hydrologic Test Data*. PNL-SA-21569, Pacific Northwest Laboratory, Richland, Washington.

Theis, C. V. 1935. "The Relation Between the Lowering of the Piezometric Surface and the Rate and Duration of Discharge of a Well Using Groundwater Storage." *Amer. Geophysical Union, Transactions* 16:519-524.

Appendix C

Reconfiguration of "Golder" Wells

THIS PAGE INTENTIONALLY
LEFT BLANK

Appendix C

Reconfiguration of "Golder" Wells

More than 100 wells were drilled on the Hanford Site during 1979 to 1982 as part of the site investigations for a proposed Skagit-Hanford Nuclear Power Plant. These wells are commonly known as "Golder" wells because Golder Associates, Inc., supervised the well installation. Many of the wells were drilled to basalt, and a few were drilled through the upper basalt flows to the Rattlesnake Ridge interbed or other units within the confined aquifer system. The Golder wells provide valuable information on subsurface geologic structure and some of the wells are potentially useful for hydrologic characterization. However, reconfiguration of the wells is required to gain access to hydrostratigraphic intervals that are of interest. Two Golder wells were reconfigured during the past year to support three-dimensional characterization of the unconfined aquifer system. Information on the reconfiguration of these wells is provided in this appendix.

Most of the Golder wells were drilled with a combination of air-rotary and mud-rotary techniques. Steel casing (usually 6-in. diameter) was placed to the depth where the air-rotary drilling method was terminated. The bottom of the steel casing is usually at some point below the water table. Following open-hole, mud-rotary drilling, a 4-in.-diameter polyvinyl chloride (PVC) liner was placed from the surface to the bottom of the borehole. The PVC liner pieces are generally connected by external-upset slip-joints. There is some evidence that the PVC joints were connected using solvent primer, but no glue. Many of the wells were used for seismic tests and several have been damaged by explosive charges used in testing. The wells have no surface seals.

Four wells (699-18-21, 699-19-23, 699-31-11, and 699-31-17) were identified in locations where information is needed on hydraulic properties, hydraulic head, and contaminant concentrations within deeper permeable zones in the unconfined aquifer system. The current condition of these wells was ascertained by examining the original well construction logs, by site inspection, and by running borehole television and magnetic logs. The television logs allowed inspection of the inside of the PVC liner for damage, and the magnetic logs provided information on depth of the bottom of the steel casing. Wells 699-18-21 (Golder S-12) and 699-31-11 (Golder 50) were then selected for the initial reconfiguration trial. Well 699-19-23 (Golder S-5) was eliminated from consideration because it was originally drilled to the

Rattlesnake Ridge interbed and may provide a future opportunity for monitoring this unit. Figures C.1 and C.2 show the as-found well conditions and the final configuration of the wells after remediation for the two reconfigured wells.

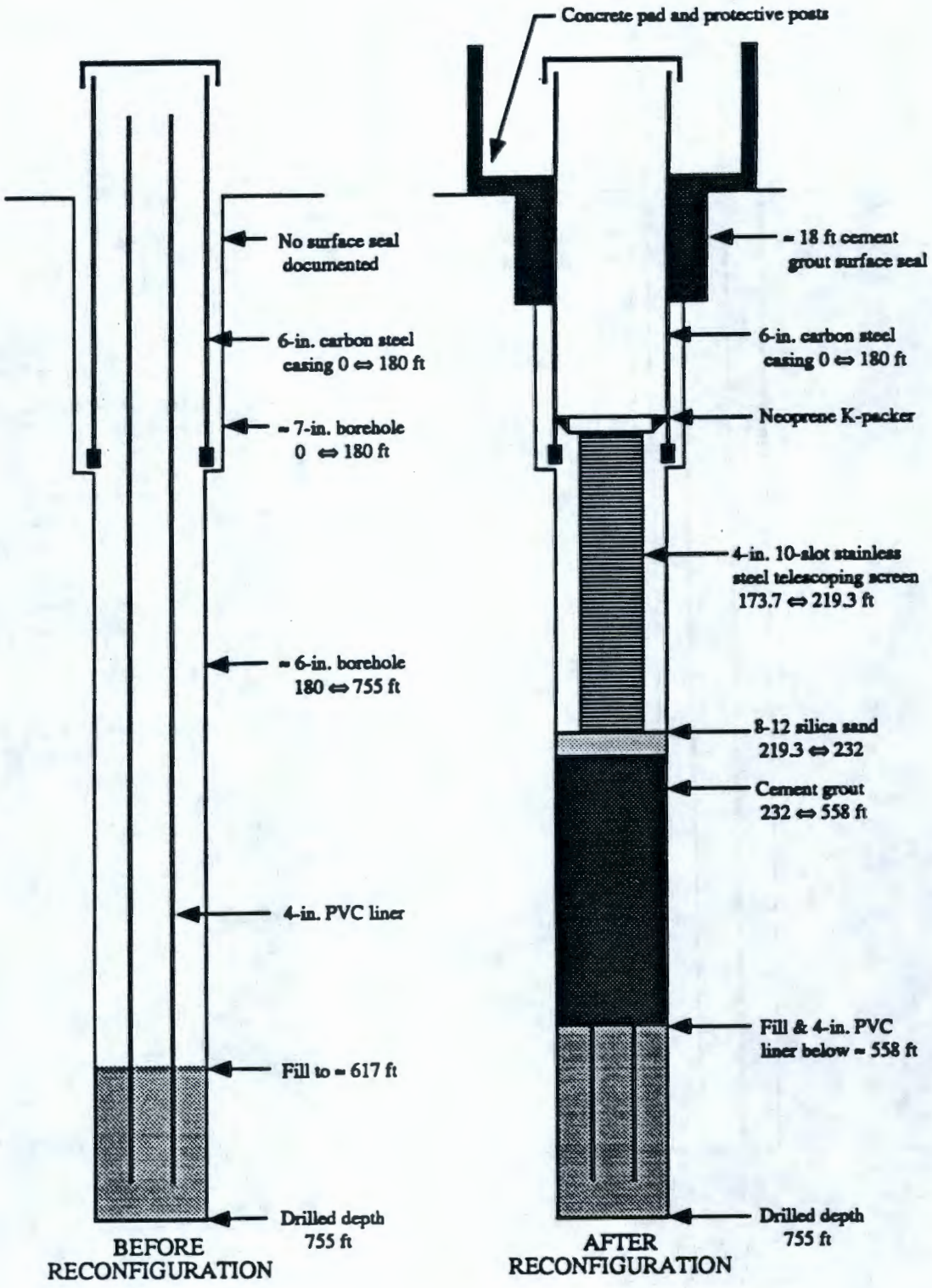

Figure C.1. As-Built Diagrams for Well 699-18-21 (Golder S-12) Before and After Reconfiguration

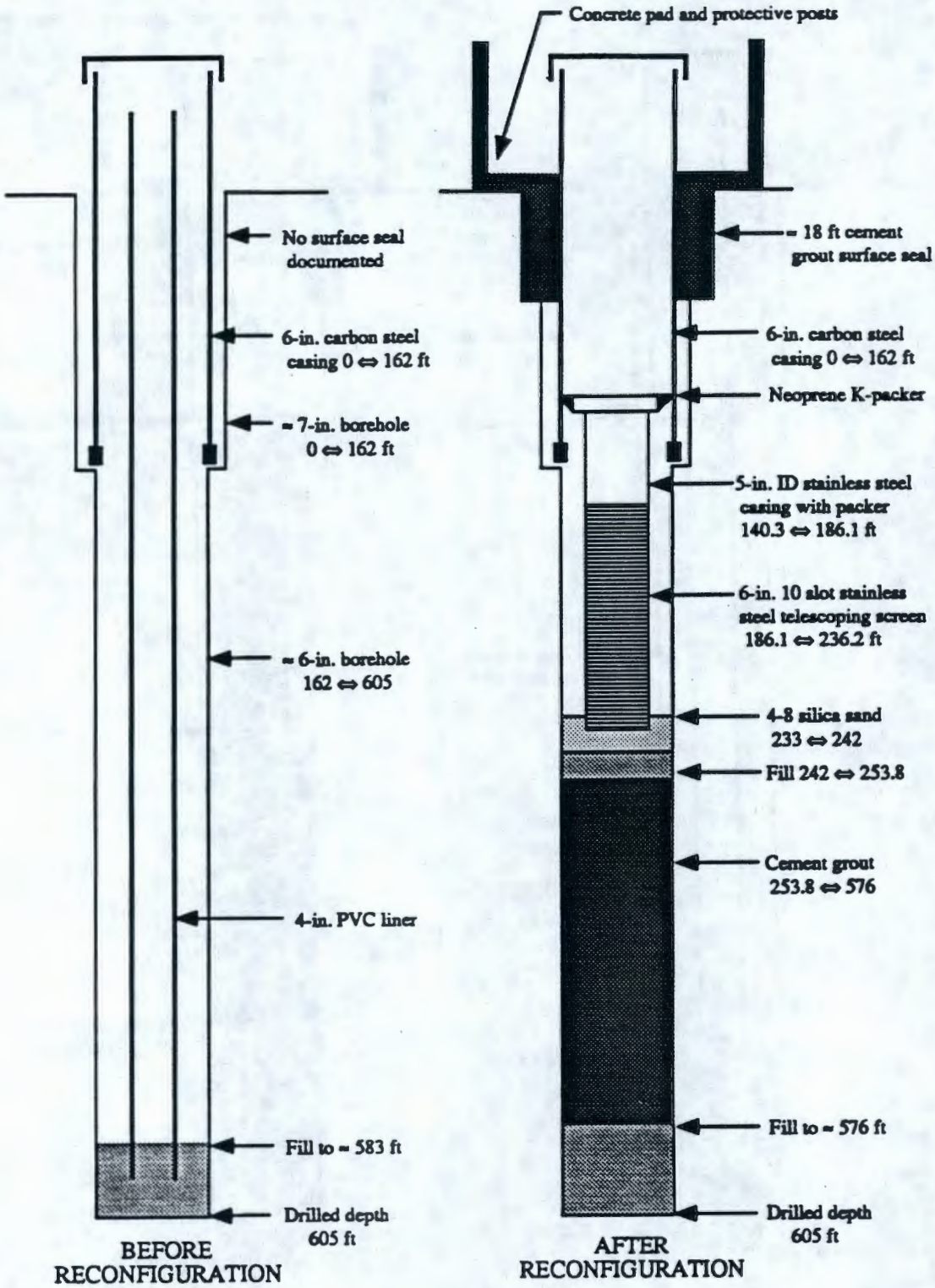

Figure C.2. As-Built Diagrams for Well 699-31-11 (Golder 50) Before and After Reconfiguration

Distribution

No. of Copies

OFFSITE

12 DOE/Office of Scientific and Technical Information

B. Blake
133 1st Avenue North
Minneapolis, MN 55401

A. Danielson
Washington State Department of Health
1801 South 66th Avenue
Yakima, WA 98808

T. Gilmore
Confederated Tribes of the Umatilla Indian Reservation
Department of Natural Resources
Hanford Projects
P.O. Box 638
Pendleton, OR 97801

3 D. Nilander
Washington State Department of Ecology
7601 W. Clearwater Avenue, Suite 102
Kennewick, WA 99336

R. Patt
Oregon State Department of Water Resources
3850 Portland Road
Salem, OR 97310

No. of Copies

2 U.S. Geological Survey
Water Resources Division
1201 Pacific Avenue, Suite 600
Tacoma, WA 98402
ATTN: B. W. Drost
W. Lumm

3 Washington State Department of Ecology
99 South Sound Center
M.S. 7600
Olympia, WA 98504-7600
ATTN: D. Jansen
C. Cline
K. Kowalic

2 Washington State Department of Health
Division of Radiation Protection
Airdustrial Center
Building 5, M.S. L-13
Olympia, WA 98503
ATTN: J. Erickson
G. Robertson

ONSITE

22 DOE Richland Operations Office

G. M. Bell	A5-52
J. K. Erickson	A5-19
M. J. Furman	R3-80
E. D. Goller	A5-19

No. of Copies		
	J. D. Goodenough	A5-19
	A. C. Harris	A5-19
	R. D. Hildebrand (10)	A5-55
	R. G. Holt	A5-15
	R. G. McLeod	A5-19
	P. M. Pak	A5-19
	R. K. Stewart	A5-19
	K. M. Thompson	A5-15
	M. W. Tiernan	A5-55
2	U.S. Army Corps of Engineers	
	W. Greenwald	A5-20
	M. P. Johansen	A5-19
3	U.S. Environmental Protection Agency	
	P. T. Day	B5-01
	D. R. Sherwood (2)	B5-01
23	Westinghouse Hanford Company	
	M. R. Adams	H6-01
	S. W. Clark	H6-01
	L. B. Collard	H6-01
	M. P. Connelly	H6-06
	K. R. Fecht	H6-06
	L. C. Hulstrom	H6-03
	R. L. Jackson	H6-06
	A. J. Knepp	H6-06
	N. K. Lane	H6-01
	M. J. Lauterbach	H6-01
	A. G. Law	H6-06
	K. A. Lindsey	H6-06
	S. M. McKinney	T1-30
	W. J. McMahon	H6-06
	R. E. Peterson	H6-06
	S. P. Reidel	H6-06
	J. W. Roberts	H6-02
	J. A. Serkowski	H6-06
	K. R. Simpson	H6-06
	L. C. Swanson	H6-06
	S. J. Trent	H6-06
	S. E. Vukelich	H6-02
	Public Reading Room	
49	Pacific Northwest Laboratory	
	M. P. Bergeron	K6-77
	B. N. Bjornstad	K6-96
	J. V. Borghese	K6-96
	R. W. Bryce	K6-96
	M. A. Chamness	K6-96
	C. R. Cole	K6-77
	J. L. Devary	K6-77
	P. E. Dresel	K6-96
	M. D. Freshley	K6-77
	G. W. Gee	K6-77
	R. E. Gephart	K1-22
	T. J. Gilmore	K6-96
	R. H. Gray	K1-33
	S. H. Hall	K6-96
	M. S. Hanson	K1-51
	R. E. Jaquish	K1-30
	G. V. Last	K6-96
	T. L. Liikala	K6-96
	P. E. Long	K6-84
	S. P. Luttrell	K6-96
	J. P. McDonald	K6-96
	P. D. Meyer	K6-77
	D. R. Newcomer	K6-96
	K. B. Olsen	K6-81
	J. T. Rieger	K6-96
	M. L. Rockhold	K6-77
	R. Schalla	K6-96
	F. A. Spane, Jr.	K6-96
	S. S. Teel	K6-96
	P. D. Thorne (10)	K6-96
	V. R. Vermeul	K6-96
	W. D. Webber	K6-96
	S. K. Wurstner	K6-77
	Publishing Coordination	K1-06
	Technical Report Files (5)	

Routing

R. M. Ecker	SE-UI
M. J. Graham	K6-78
P. M. Irving	K6-98
C. S. Sloane	K6-04
P. C. Hays (last)	K6-86

THIS PAGE INTENTIONALLY
LEFT BLANK